TECHNICAL UNIVERSITY OF LIBEREC
Faculty of Textile Engineering

MECHANICAL AND THERMO-ACOUSTIC CHARACTERIZATION OF BARKCLOTH AND ITS POLYMER REINFORCED COMPOSITES

PhD Thesis

Study programme: P3106 – Textile Engineering
Study branch: 3106V007 – Textile and Material Engineering
Author: **Ing. Samson Rwawiire**
Supervisor: Ing. Blanka Tomkova, PhD.

Liberec, 2016

DECLARATION

I hereby declare that the material in this thesis, herewith I now submit for assessment for PhD defense is entirely my own work, that I have taken precautionary measures to ensure that the work is original and does not to the best of my knowledge breach any copyright law, and hasn't been extracted from the work of others save and to the extent that such work has been cited and acknowledged within the text of this work.

The core theme of the thesis is **MECHANICAL AND THERMO-ACOUSTIC CHARACTERIZATION OF BARKCLOTH AND ITS POLYMER COMPOSITES** and contains 10 original papers published in peer reviewed journals. The ideas, development and writing up of all the papers in the report were the principal responsibility of me, the candidate working within the Department of Material Engineering, under the supervision of Ing. Blanka Tomkova, PhD and Prof. Ing. Jiri Militky, CSc., EURING.

Name: Ing. Samson Rwawiire

Signature:

Student Number: T12000364

Date: April 2016

TABLE OF CONTENTS

ACKNOWLEDGMENTS

Completing this thesis has been a long journey that had mountains and valleys; the God on the mountain is still the same God in the valley! May the name of the Lord God in Heaven be praised for His infinite wisdom that has enabled me and my wider family for completing this work.

First and foremost, thank you Prof. Ing. Jiri Militky, CSc., EURING for allowing this novel topic to be researched in your department, and also my supervisor Ing. Blanka Tomkova, PhD. If it wasn't for the trust you two put in me to embark on this project of revealing the properties of barkcloth to the scientific world, then it wouldn't have been possible. In the absence of financial support, this research wouldn't have been possible; I, therefore, thank the Deans and Vice Deans of the Faculty of Textile Engineering, Ing. Jana Drasarova, Ph.D; Ing. Pavla Tesinova, PhD., Ing. Gabriela Krupincova for approving PhD studies in English Language, Conference attendance and Journal publication funds where necessary such that this work may be done and progresses to another level.

In the same vein, I would like also to thank Busitema University for believing in me. I extend my gratitude to the Association of African Universities for having provided a Thesis and Dissertation grant to enable me to complete this research.

Thank you, Ing. Petr Prucha, PhD, the Research and Development Director of L.A. Composite s.r.o who by the way supervised my Master's Thesis but still was of help whereby he allowed me to use the state of art Resin Transfer Molding equipment and consumables at L.A. Composite s.r.o, Prague.
For surface functional groups characterization, there was need of Fourier Infra-Red Transform (FTIR); this is where Ing. Jana Mullerova, Ph.D., of the Institute for Nanomaterials, Advanced Technologies and Innovation, TUL, for providing the FT-IR spectra. I also thank Ing. Vijay Bajeti, PhD for the initial training he gave me in using the TGA, DSC and DMA machines whereas Ing. Martina Novotna was pivotal in guidance while carrying out bending tests on the TiraTest 2300 machine.
Most of the times, I had to travel to and from Uganda so as to obtain the materials to use, therefore, the Vice Chancellor Mary J. N. Okwakol was pivotal in encouraging me in this research; the Academic Registrar Mr. Elisha Obella; the University Bursar were individuals who supported me through thick and thin.

I would like to say a big thank you to my work colleagues in the department especially Bandu Majumdar Kale, Abdul Jabbar and Masqood Shahzad who we always shared the perils of doctoral research.

Last but not least, I wouldn't be where I am today without the support from my family. You have been an inspiration. My wife Etro Lisa Mirembe and daughter Elioenai Sharai Rwahwire, you always inspired me to move on.

My Late father Samson Rwahwire was an inspiration before his passing and the advice he left me with has always pushed me ahead. He taught me to trust in the Lord and lean not on my own understanding and ever since, I have seen the Lord's hand at work. My mother, Janet Namaganda is unwavering prayer warrior who in the wee hours of the night gets up every day to lift us in prayer, whenever I would be away, she would be in prayer, thank you so much, mom, your son now is to become a Doctor of Engineering. To my siblings, thank you so much, Isaac, Esther, Alice, Janet, and Ida. To my nieces, nephews and grandkids, thank you for the prayers.

Who are we without the body of believers? The church has been another family and still is; thank you Pastors Balaam Kirya, Rogers Kaggwa, Josiah Usaba for the un-relentless efforts and prayers. Thank you, Elder Maseruka for the prayers and trust you put in me.

In God I Trust

Samson Rwawiire Jr.

ABSTRACT

Natural fiber reinforced composites have attracted interest due to their numerous advantages such as biodegradability and comparable mechanical strength. The desire to mitigate climate change due to greenhouse gas emissions has led to the utilization and development of sustainable and environmentally friendly raw materials. Plant fibers and biodegradable resins are explored as the alternative material selection for composite materials apart from their synthetic counterparts which are non-renewable. In this thesis, barkcloth, a naturally occurring non-woven fabric and its reinforced epoxy polymer composites are characterized for possible automotive applications. Since there have been no tangible scientific studies that have been made elsewhere on barkcloth except those published by the author, the thesis gives an in-depth analysis of the mechanical and thermo-acoustic properties of barkcloth and its polymer composites.

The fabric microstructure and morphology were investigated using Scanning Electron Microscopy (SEM) whereas the Chemical constituent analysis and Surface functional group characterization was done using FTIR. To further understand the behavior of the fabric after surface modification, X-Ray Diffraction (XRD) characterization was done on alkaline treated fabrics. Surface modification of the fabric was done using the enzyme, plasma, and alkali treatment. The design of the composites utilized fabrics which were surface modified and used for reinforcement of synthetic and green epoxy polymer resins.

In order to produce composites with required thickness as per the tensile testing standards (ASTM D3033), four barkcloth fabric layers were sufficient for the fabrication of composites. A hierarchal fabric architecture based on the micro-fiber angles was utilized in order to find out the best fabric layer design. Vacuum Assisted Resin Transfer Moulding (VARTM) and hand layup were utilized in the production of the synthetic epoxy and green epoxy composites respectively. The composites produced as the effect of the hierarchal architecture were evaluated and the best set of composite layup was utilized to design green epoxy polymer composites utilizing green epoxy resin. The ply stacking sequence 90^o, 0^o, -45^o, 45^o had the best mechanical properties and, therefore, was the stacking sequence investigated for the production of biocomposites. Static and thermal mechanical analyses were done on the set of composites.

In this investigation, for the first time, the thermo-acoustic properties of barkcloth and its polymer reinforced composites were investigated in order to study the potential of barkcloth as a sound absorption material. Theoretical empirical sound absorption models were employed to predict the behavior of the fabrics and the results were compared with commercially available products in automotive applications.

Keywords: Barkcloth, Composites, Thermo-acoustics, Sound Absorption, Modeling

ABSTRAKT

Kompozity vyztužené přírodními vlákny dnes přitahují pozornost díky mnoha svým výhodám – jsou biologicky odbouratelné a mechanicky odolné. Potřeba zmírnit klimatické změny způsobené emisemi skleníkových plynůvedek vývoji udržitelných a environmentálně šetrných surovin. Rostlinná vlákna a biologicky odbouratelné pryskyřice jsou zkoumányjako alternativa pro kompozitní materiály, které jsou na rozdíl od svých syntetických protějšků recyklovatelné.

V této práci je zkoumána netkaná textilie získaná z kůry (barkcloth) stromů z čeledi morušovníkovitých rostoucí přirozenou cestou a tedy bez potřeby tovární výroby, která je použita jako výztuž epoxidových polymerů.. Tato textilie se jeví jakovhodná výztuž pro aplikace v automobilovém průmyslu. Protože dosud nebyly publikovány studie, které by se tímto typem materiálu zabývaly, krom těch, které publikoval autor, je součástí této práce podrobnáanalýzamechanických a tepelně-akustických vlastností studovaného materiálu a z něj vyrobených polymerových kompozitů.

Mikrostruktura a morfologie materiálu byly zkoumány s využitím rastrovacího elektronového mikroskopu (SEM), analýza chemického složení a charakteru funkčních skupin na povrchu proběhla s využitím FTIR. K hlubšímu porozumění chování materiálu po modifikaci povrchu byla využita rentgenová difrakce (XDR) na alkalicky ošetřeném povrchu. Modifikace povrchu byly provedeny enzymaticky,plazmaticky a vybranými alkalickými činidly. V navržených kompozitech byl použit povrchově upravený materiál, kterým byly vyztuženy jak syntetickétak biodegradabilní pryskyřice.

Testovací vzorky kompozitůbyly vyrobeny tak, aby jejichtloušťka odpovídala standardům používaným při zkoušce tahem (ASTM D3033). Pro jejich vyztužení byly použity čtyři vrstvy netkané textiliez kůry. Hierarchická architektura materiálu založená na rozloženímikrovláken byla využita při návrhu orientace jednotlivých vrstev. Při výrobě kompozitů ze syntetické i bio- pryskyřice byly použity technologie VARTM a technologie ručního kladení . Nejprve byl analyzován vliv rozložení jednotlivých vrstev na vlastnosti kompozitu ze syntetické pryskyřice a následně bylo vybráno nejvhodnější rozložení vyztužujících vrstev. Takto rozložené vrstvy byly využity pro přípravu kompozitu z biologicky odbouratelnou pryskyřicí. Jako nejlepší se ukázalo následující kladení vrstev: 90º, 0°, -45º, 45°, které vykazovalo nejlepší mechanické vlastnosti, a proto byly pro další výzkum připravovány biokompozity s takto rozloženou výztuží. Statické a tepelně-mechanické analýzy byly dále provedeny pro tento soubor kompozitů.

V provedeném výzkumubyly poprvé prozkoumány také tepelně-akustické vlastnosti textilie z kůry a z nich vyrobených kompozitů. Cílem studie bylo prozkoumat potenciál textiliez kůry jako zvukově izolačního materiálu, zejména pro interiéry automobilů. Teoreticko-empirické modely zvukové izolace byly užity při predikci chování materiálu a výsledky byly srovnány s komerčně dostupnými produkty v automobilovém průmyslu.

Klíčová slova:barkcloth, kompozity, termo-akustika, zvuková izolace, modelování.

LIST OF ORIGINAL PUBLICATIONS

1. **RWAWIIRE, S.,** Tomkova, B., Militky, J., Jabbar, A., & Kale, B. M. (2015). Development of a biocomposite based on green epoxy polymer and natural cellulose fabric (barkcloth) for automotive instrument panel applications. *Composites Part B: Engineering*, 81, 149-157.
   (Impact Factor: 2.983).
2. **RWAWIIRE, S.**, & Tomkova, B. (2015). Thermal, static, and dynamic mechanical properties of barkcloth (ficus brachypoda) laminar epoxy composites. *Polymer Composites*
   (Impact Factor: 1.632).
3. **RWAWIIRE, S.,** & Tomkova, B., Militky J., Kale, B. M., Prucha, P. (2015). Effect of layering pattern on the mechanical properties of barkcloth (Ficus natalensis) epoxy composites, *International Journal of Polymer Analysis and Characterization*, 20 (2), 160-171.
   (Impact Factor: 1.264).
4. **RWAWIIRE, S.,** & Tomkova, B. (2015). Static and Dynamic mechanical properties of barkcloth epoxy laminar composites, *Journal of Natural Fibers*, 13 (2),137 - 145
   (Impact Factor: 0.460).
5. **RWAWIIRE, S**., Tomkova, B., Gliscinska, E., Krucinska, I., Michalak, M., Militky, J., & Jabbar, A. (2015). Investigation Of Sound Absorption Properties Of Bark Cloth Nonwoven Fabric And Composites. *Autex Research Journal*, 15(3), 173-180.
   (Impact Factor: 0.220).
6. **RWAWIIRE, S.,** Tomkova, B., Weiner, J., & Militky, J. (2015). Effect of enzyme and plasma treatments of barkcloth from Ficus natalensis: morphology and thermal behavior. *The Journal of The Textile Institute*, 107 (5), 663-671.
   (Impact Factor: 0.722).
7. **RWAWIIRE, S.,** & Tomkova, B. (2014). Thermo-physiological and comfort properties of Ugandan barkcloth from Ficus natalensis. *The Journal of The Textile Institute*, 105(6), 648-653
   (Impact Factor: 0.722)
8. **RWAWIIRE, S.,** Tomkova, B., Militky, J., Jabbar, A., & Kale, B. M. (2015). Preparation and Characterization of Epoxy Polymer Composites Reinforced with Enzyme and Plasma Treated Natural Cellulose Fabric (*Under Review*)
   (Impact Factor: 1.438).
9. **RWAWIIRE, S**., G. W. Luggya and B. Tomkova.2013. Morphology, Thermal, and Mechanical Characterization of Barkcloth from Ficus natalensis. *ISRN Textiles*, 2013

10. **RWAWIIRE, S**., Tomkova, B., Militky, J., Hes, L., Bandu, M. Empirical Modeling of Sound Absorption Properties of Natural Nonwoven Fabric (Antiaris toxicaria Barkcloth). *Accepted Materials Science Forum*

Conference proceedings

1. **Rwawiire, S**., & Tomkova, B. 2014. Comparative evaluation of the thermal conductivity of barkcloth epoxy composites. *In: Proceedings of the Fiber Society Conference, Liberec, 21-23 May 2014*

Scopus indexed

2. **Rwawiire, S**., Wandera, J. 2012. Natural Fibers: A Blue Print for Ecofriendly Textiles and Biocomposites. *In: Proceedings of XVth International Scientific and Practical Workshop: Physics of Fibrous Materials, pp 67-73, ISBN 978-5-88954-374-9.*
3. **Rwawiire, S**., & Tomkova, B. 2014. Comparative evaluation of the dynamic mechanical properties of barkcloth epoxy laminar composites. *In: Proceedings of the Workshop for PhD students of the faculty of textile engineering and faculty of mechanical engineering, pp 112-116, ISBN 978-80-7494-100-9*
4. **Rwawiire**, S., & Tomkova, B. 2015. Barkcloth (Ficus natalensis) reinforced epoxy composites: Effect of enzyme and plasma treatments on morphology, thermal, static and dynamic mechanical properties. *In: 5th International Conference on Innovative Natural Fiber Composites for Industrial Applications, Rome, 15-16 October 2015*
5. **Rwawiire, S**., Tomkova, B., Militky, J., Hes, L., Bandu, M. Empirical Modeling of Sound Absorption Properties of Natural Nonwoven Fabric (Antiaris toxicaria Barkcloth). *In: Proceedings of First International Conference on Civil Engineering and Materials Science Singapore, 1st to 3rd May 2016*

LIST OF TABLES

LIST OF FIGURES

List of Symbols

ASTM	American Standard Testing Methods
AT	Antiaris toxicaria
BFRP	Barkcloth Fabric Reinforced Plastic Composites
DMA	Dynamic Mechanical Analysis
DP	Degree of Polymerization
DSC	Differential Scanning Calorimetry
DTG	Differential Thermogravimetric
EU	European Union
FAO	Food and Agricultural Organization
FAO	Food and Agricultural Organization
FT	Fourier Transform
FTIR	Fourier Transform Infra-Red Spectroscopy
GRPC	Glass Fiber Reinforced Plastic Composites
GWP	Global Warming Potential

HT	Hough Transform
Hz	Hertz
IEC	International Environmental Product Declaration Consortium
IPCC	Intergovernmental Panel on Climate Change
ISO	International Standard Organization
NFC	Natural Fiber Composites
NFRC	Natural Fiber Reinforced Composites
NFRP	Natural Fiber Reinforced Plastics
NRE	Non Renewable Energy
OH	Hydroxyl
PE	Polyethylene
PHA	Poly(hydroxyalcanoate)
PHB	Poly(hydroxybutyrate)
PLA	Poly lactic Acid
PP	Polypropylene
PVC	Poly (Vinyl Chloride)
ROM	Rule of Mixtures
SEM	Scanning Electron Microscopy
TGA	Thermogravimetric Analysis
UN	United Nations
US	United States
UNESCO	United Nations Educational, Scientific and Cultural Organization
VARTM	Vacuum Assisted Resin Transfer Moulding
WHO	World Health Organization
XRD	X-Ray Diffraction

Symbol	**Nomenclature**	**Unit Used**
α-Cellulose	Alpha Cellulose	%
λ	Thermal conductivity coefficient	W/m.K
ρc	Thermal Capacity of The Fabric	J/m^3
α	Thermal Absorptivity Of Fabrics	$Ws^{1/2}/m^2K$
a	Thermal Diffusivity	m^2s^{-1}
E’	Storage Modulus	MPa
E’’	Loss Modulus	MPa

tan δ	Mechanical damping factor	-
E_f	Fiber Modulus	GPa
E_m	Matrix Modulus	GPa
v_f	Fiber Volume Fraction	-
v_m	Matrix Volume Fraction	-
η_l	Fiber Length Distribution Factor	-
η_o	Fiber Orientation Factor	-
Φ	Volume fraction of the composite	-
k_f	Thermal conductivity of the reinforcing fiber preform	W/m.K
k_m	Thermal conductivity of matrix	W/m.K
ρ_O	Density Of Air	kg/m^3
c_o	Speed Of Sound In Air	ms^{-1}
Z_c	Characteristic Impedance	$Pa{\cdot}s/m^3$
Z_s	Surface Impedance	
k	Propagation Constant	-
f	Frequency	Hz
ω	Angular Frequency	Rad
σ	Airflow Resistivity	Ns/m^4
d	Thickness	mm
P_r	Prandtl's number	-
P	Load at Failure	N
L	Span Length	mm
b	Width of Specimen	mm
ΔP	Pressure difference	Pa
U	Airflow Velocity	ms^{-1}
t	Temperature between human skin and the textile	K
t_1	Unsteady temperature between the human skin and fabric	K
t_2	Initial temperature	K
B	Bending Stiffness	N
E	Young's Modulus	MPa
I	Moment of Inertia	m^4
I'	Moment of Inertia per unit	m^2

f_c	Critical frequency	Hz
m	Material surface density	kgm^{-2}
ρ	Density	Kgm^{-3}

CHAPTER 1

Introduction

1.0. PROLOGUE

This chapter gives the evolution of natural fibers and the respective reinforced composites and their applications in industry. It goes further by revealing the statement of the problem; aim of the research and specific objectives.

1.1. BACKGROUND

Worldwide, researchers are embroiled in a race for niche products whereby industries can boost production processes as well as putting into consideration sustainability. The quest for structural materials which are environmentally friendly, to mitigate global warming effects is on the agenda of industrialized nations and recommendations are put forward for production of recyclable, biodegradable products or materials with zero emissions [1].

Transition to a more sustainable biobased economy, as a political consequence of the Kyoto protocol on global climate change, includes a shift from petrochemical to renewable sources [2].

The ecological "green" image of cellulosic fibers is the leading argument for innovation and development of products which are biodegradable and can be applied to the automotive industries [3], building and construction [4], geotextiles and agricultural products [5,6].

Plant based fibers like flax, hemp; nettle and kenaf which were previously used for fiber in the western world have attracted renewed interest in textile and industrial composite applications [7–9].

Natural fibrous materials were used by early civilizations from biblical times; Egyptians reinforced mud bricks with straw. However, the turn of the 20th century, new fibers, largely from petrochemical sources and with exceptional strength impeded the use and production of natural fibers.

Ever since the discovery of synthetic fibers, their contribution towards fuel economy in automotive and aerospace industries is unparalleled. The unique structural properties of composites have seen their application in construction beside the traditional automotive and aerospace sectors (Figure 1.1). Table 1.1 shows synthetic fibers whose feedstock are fossil fuels with negative effects such as environmental degradation due to the toxicity of the fumes emitted, demanding energy for production and non-biodegradability; whereas natural fibers have advantages such as biodegradability, low cost, non-toxicity, acoustical properties etc. [10].

1.1.1. Drivers for Change

The Intergovernmental Panel on Climate Change (IPCC) most recent report recommends cutting of greenhouse gas emissions by 70% and an increase of the use of clean green energy by 2050 respectively. Effective strategies such as utilization of sustainable biodegradable materials instead of synthetic materials can contribute to lowering greenhouse gas emissions thus combating climate change [11].

In reference to European Union (EU) guideline 2000/53/EG [12] issued by the European Commission, 95% of the weight of a vehicle have to be recyclable by 2015. This has led to a surge of utilization of natural fiber reinforced composites among the European automotive industry by designing and production renewable biodegradable composites based on natural fibers [3,13–22]. Furthermore, the EU Landfill Directive 1999/31/EC whose main goal is to reduce on the quantity of biodegradable municipal waste that ends up in landfill has sparked research in sustainable and biodegradable materials that can be reused [23].

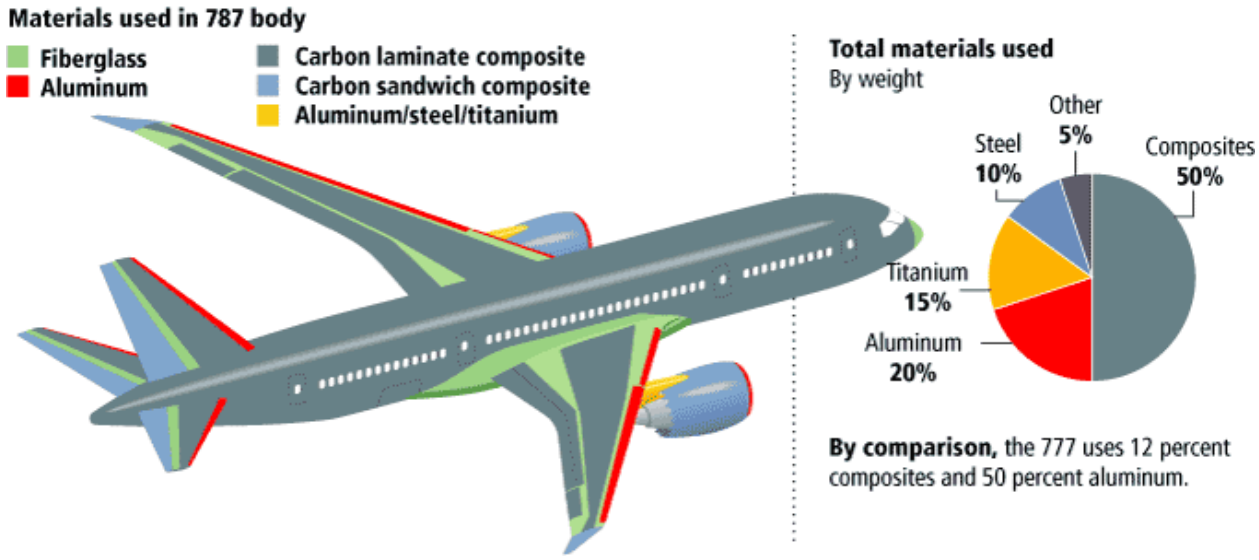

Figure 1.1. Boeing B787 Structural Materials

Image Source: http://modernairliners.com/boeing-787-dreamliner/boeing-787-dreamliner-specs

The increasing costs of oil vis-à-vis the diminishing oil reserves world over and environmental concerns has led to the reigniting of the natural fiber spark. Production of chemicals and materials from bio-based feedstock is expected to increase from today's 5% level to approximately 12% in 2010, 18% in 2020 and 25% in 2030 [24].

The need for a lightness of materials with superb performance characteristics has sparked interest in lightweight composite materials. With the dwindling petroleum resources, coupled with high prices, fiber

from lignocellulosic materials will play a major role in the transition from synthetic to environmentally friendly, biodegradable green composites whose feedstock is from wood and plants [24,25]. Numerous researches elsewhere have documented on the use of novel plants for production of fiber, such as Sansevieria [26–28], Piassava [29], Okra [30], Oil palm [31], carnauba [32], barkcloth [33], banana etc.

Table 1.1. Fibrous Materials Comparison [24,34]

	Properties	**Unit**	**Plant Fibers**	**Glass Fibers**	**Carbon Fibers**
Economy	Annual global production	Tonnes	31,000,00	4,000,000	55,000
	Distribution for FRPs in EU	Tonnes	Moderate (~60,000)	Wide (600,000)	Low (15,000)
	Cost of raw fiber	Euros	Low	High	High
TECHNICAL	Density	gcm^{-3}	Low (~1.35-1.55)	High (2.50-2.70)	Average (~1.70-2.20)
	Tensile Modulus	GPa	Moderate (~30-80)	Moderate (70-85)	High (150-500)
	Tensile Strength	GPa	Low (~0.4-1.5)	Moderate (2.0-3.7)	High (1.3-6.3)
	Percentage Elongation	%	Low (~4-3.2)	High (2.5-5.3)	Low (0.3-2.2)
	Tribological resistance		No	Yes	Yes
	Energy requirements	MJ/kg	Low (4-15)	Moderate(30-50)	High (>130)
Ecological	Renewability		Yes	No	No
	Recyclable		Yes	Partially	Partially
	Biodegradable		Yes	No	No
	Dermal and inhalation toxicity during processing		No	Yes	Yes

Figure 1.2. Helmet, Car body and other natural fiber composite products by INVENT GmbH

Application of natural fiber reinforced composites in the EU is on the increase with various researchers and industries taking the lead in the application of bio fibers for polymer reinforcement (Figure 1.2). According to the report on Global Natural Fiber Composites Market 2014-2019: Trends, Forecast and

Opportunity Analysis [35], by 2016 the natural fiber composites market is expected to be worth US $531.2 million with an expected annual growth rate of 11% for the next five years. Currently, natural fibers account to over 14% share of reinforcement materials; however, the share is projected to rise to 28% by 2020 amounting to about 830,000 tons of natural fibers [36].

Table 1.2. Vehicle Manufacturers and use of natural fiber composites [37].

Automotive Manufacturer	Model	Model Applications
Audi	A2, A3, A4 (and Avant), A6, A8.	Roadster, coupe, seat backs, side and back door panels, boot lining, hat rack, spare tyre lining
BMW	3,5,7 Series	Door panels, headliner panel, boot lining, seat backs, noise insulation panels, moulded foot well linings
Citroen	C5	Interior door paneling
Daimler-Chrysler	A,C,E and S-Class; EvoBus (exterior)	Door panels, windshield, dashboard, business table, pillar cover panel
Ford	Mondeo CD 162, Focus	Door panels, B-pillar, boot liner
Lotus	Eco Elise	Body panels, spoiler, seats, interior carpets
Mercedes-Benz	Trucks	Internal engine cover, engine insulation, sun visor, interior insulation, bumper, wheelbox, roof cover
Peugeot	406	Seat backs, parcel shelf
Renault	Clio, Twingo	Rear parcel shelf
Rover	2000 and Others	Insulation, rear storage shelf/panel
Toyota	Brevis, Harrier, Celsior, Raum	Door panels, seat backs, Spare tyre cover
Vauxhall	Corsa, Astra, Vectra, Zafira	Headliner panel, Interior door panels, pillar cover panel, instrument panel
Volkswagen	Golf, Passat, Bora	Door panel, seat back, boot lid finish panel, boot liner
Volvo	C70, V70	Seat padding, natural foams, cargo floor tray

1.2. RESEARCH PROBLEM

With increasing level of technology and research, new fibers have been developed. The shift from overdependence on synthetic fibers with fossil fuels as raw material sources and the need for reduction of adverse effects of man-made fibers which contribute to the carbon footprint is realized worldwide. The quest for sustainable materials from renewable sources is being fronted as one of the ways of becoming resilient to climate change and to provide for a reduction in emissions. Plant based fibers haven't been fully characterized and their respective processing and pretreatment technologies for the production of industrial composites are still under development.

Barkcloth has been in existence as far back as the 13th century, however, the fabric had not been characterized and there was limited scientific published information on the naturally occurring non woven felt. This report, therefore, presents the findings of the investigation of the microstructural, mechanical and sound absorption properties of barkcloth and its reinforced epoxy polymer composites for possible automotive applications.

1.3. AIM AND OBJECTIVES OF THE STUDY

The overall aim of this study was the investigation of the mechanical and thermo-acoustic properties of barkcloth and its polymer reinforced composites for automotive applications.

The specific objectives are investigation of:

1. Morphology, Chemical and Thermo-physiological properties of Barkcloth.
2. Mechanical and Thermal Analysis of Barkcloth Laminar Epoxy Polymer Composites.
3. Thermo-acoustic Properties and Sound Absorption Models of barkcloth.

1.4. RESEARCH DESIGN

The present work was simplified into a flowchart illustrated in Figure 1.3. Furthermore, in reference to the present research and available literature, there are three novel/original concepts found:

1. There has been limited laboratory work done on barkcloth fabrics except for the work which is now documented in the publications arising from this work.
2. This work is the first to study the morphological and chemical characterization of barkcloth nonwoven fabrics.
3. The utilization of barkcloth fabrics as a promising sound absorption material is the first of its kind and the fabric showed exceptional properties.

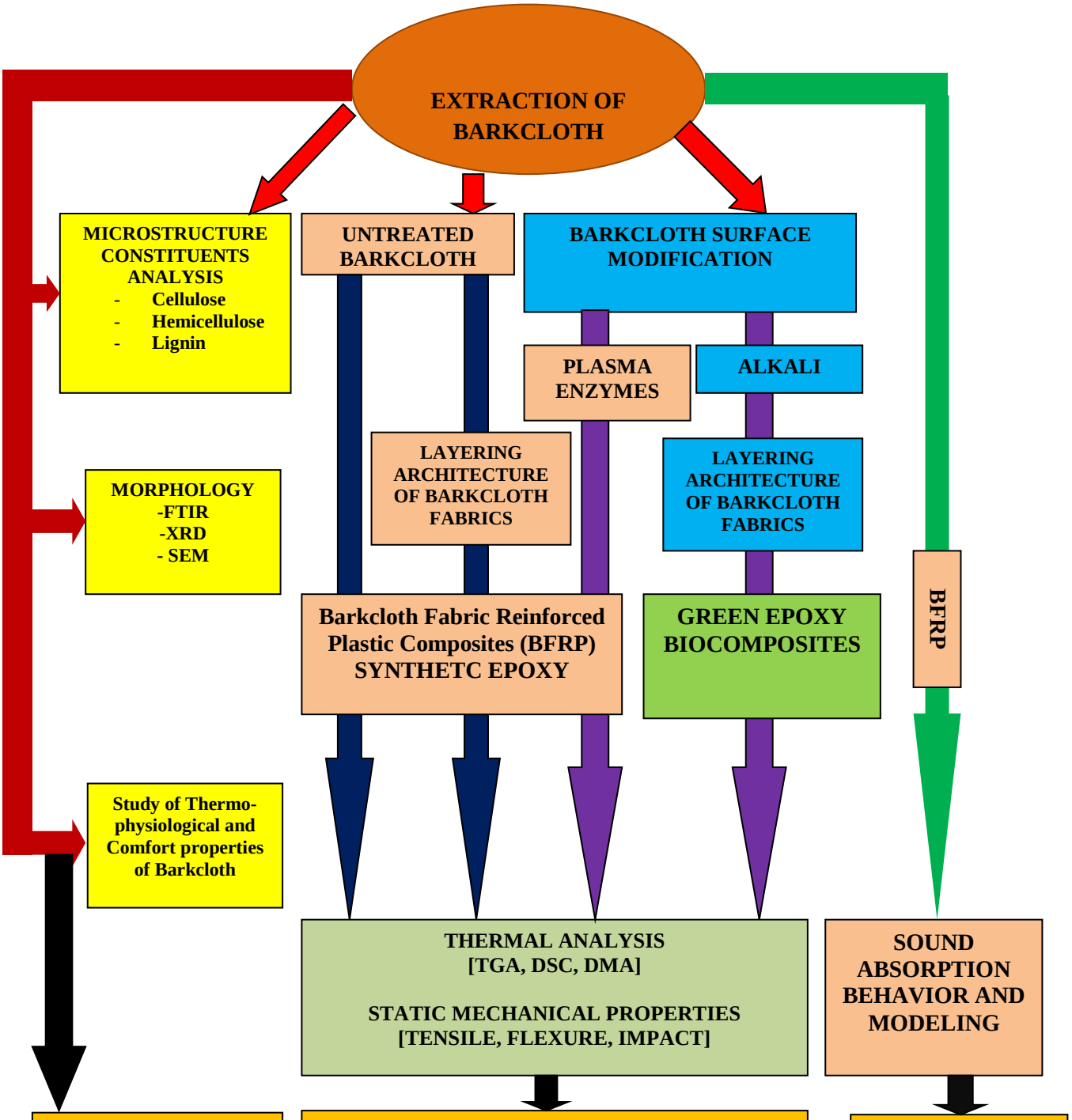
EXTRACTION OF BARKCLOTH
MICROSTRUCTURE CONSTITUENTS ANALYSIS
- Cellulose
- Hemicellulose
- Lignin
UNTREATED BARKCLOTH
BARKCLOTH SURFACE MODIFICATION
PLASMA ENZYMES
ALKALI
LAYERING ARCHITECTURE OF BARKCLOTH FABRICS
LAYERING ARCHITECTURE OF BARKCLOTH FABRICS
MORPHOLOGY
-FTIR
-XRD
- SEM
Barkcloth Fabric Reinforced Plastic Composites (BFRP) SYNTHETC EPOXY
GREEN EPOXY BIOCOMPOSITES
BFRP
Study of Thermo-physiological and Comfort properties of Barkcloth
THERMAL ANALYSIS [TGA, DSC, DMA]
STATIC MECHANICAL PROPERTIES [TENSILE, FLEXURE, IMPACT]
SOUND ABSORPTION BEHAVIOR AND MODELING
Discussion of the fabric microstructural composition and morphology
The thermo-physiological behavior of the fabric
-Discussion of the static and dynamical mechanical properties of the Barkcloth Composites
- Discussion of the Effect of Surface Modification on the static and dynamic mechanical properties of the fabric.
- Discussion of the effect of barkcloth fabric and the optimization of the fabric layering to ASTM thickness standards.
- Discussion of the effect of layering on the mechanical properties.
- The development of green composites based on the tested and optimized layering architecture.
Discussion of thermo-acoustic behavior of the fabrics with various layers.
Discussion of sound absorption behavior of composites.
Sound absorption modeling.

1.5. SUMMARY OF THESIS

Chapter 1: Introduction

A general overview of the natural fibers and composites are presented. The thesis builds on the background and presents a research problem, aim, and objectives of the study.

Chapter 2: Literature Review

The detailed background to the research is presented. The microstructure and properties of natural fibers, challenges and limitations are discussed. A transition from the reinforcing materials to natural fiber reinforced composites is examined putting consideration to the polymers, manufacturing processes and finally challenges and limitations.

An overview of sustainable natural fibrous sound absorption materials is presented. Theoretical empirical absorption materials used to predict the sound absorption of materials are also presented.

Chapter 3: Raw Material Analysis

A detailed description of the new materials is described giving emphasis to microstructure analysis of barkcloth and overview of the physical and chemical properties. Green epoxy polymer is also characterized.

Chapter 4: Design of Composites

The underlying fundamentals of design of laminar composites is introduced and the criteria utilized for the production of Barkcloth Fabric Reinforced Plastic Composites (BFRP).

Chapter 5: Experimental

An overview of the methods used for the investigation of the research is presented.

Chapter 6: Results and Discussion

The material properties of the fabric; the fabric surface functional groups characterization are discussed. The results from the utilization of the fabric for epoxy laminar composites from both synthetic and green epoxy are presented. The utilization of the fabric for sound absorption and modeling the behavior of the fabric is discussed.

Chapter 7: Conclusion

The conclusion of the whole thesis and a summary of the new knowledge generated by this work is presented.

Chapter 8: Industrial Applications and Future Work

Possible applications of barkcloth in the industry are highlighted based on the industry standards.

CHAPTER 2

Literature Review

2.0 PROLOGUE

This chapter gives a broad overview of the field of research, background, underlying theories and up-to-date research that has been made in the field. The reader will familiarize him/herself to the experimental procedures which follow in the next section.

2.1 NATURAL FIBERS

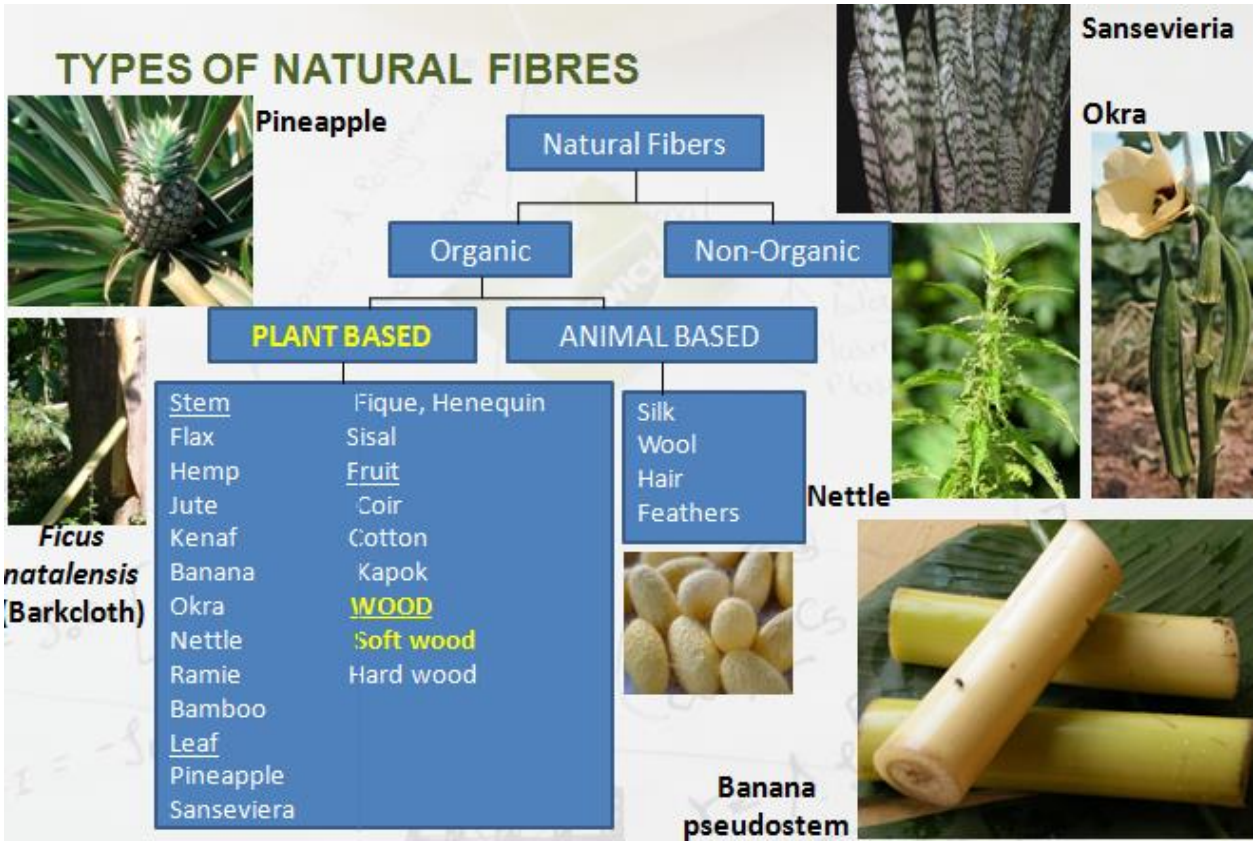

Figure 2.1. Classification of Natural Fibers

Synthetic fibers whose feedstock are fossil fuel are the leading causes of environmental degradation due to the toxicity of the fumes emitted, demanding energy for production and non-biodegradability whereas natural fibers have advantages such as biodegradability, low cost, non-toxicity, sound absorption properties etc. [10]. Furthermore, the IPCC most recent report recommends cutting of greenhouse gas emissions by 70% and an addition of the usage of clean green energy by 2050 respectively. Effective

strategies such as usage of sustainable biodegradable materials instead of synthetic materials can lead to lowering greenhouse gas emissions thus combating climate change.

Plainly put, bio-based originate from agricultural and forestry feedstock including wood, grass, shrubs and plant fibers. Vegetable fibers exhibit several advantages, including low density, acceptable to good specific strength properties, good sound abatement capability, low abrasivity, high biodegradability and the existence of vast resources [38].

Natural fibers also known as vegetable fibers are usually classified as shown in Figure 2.1 depending on the source:

- Leaf fibers, these are usually extracted from the leaves of plants. The fibers usually are the medium of transportation of various plant nutrients.
- Fruit fibers, these are usually extracted from the fruit of the plant. There are in most cases, soft and hairy and can be easily carried off by the wind whereas others are coarse.
- Bast fibers, these are extracted from the stem of the plant, they are usually long and have robust mechanical strength.

2.1.1. Structure

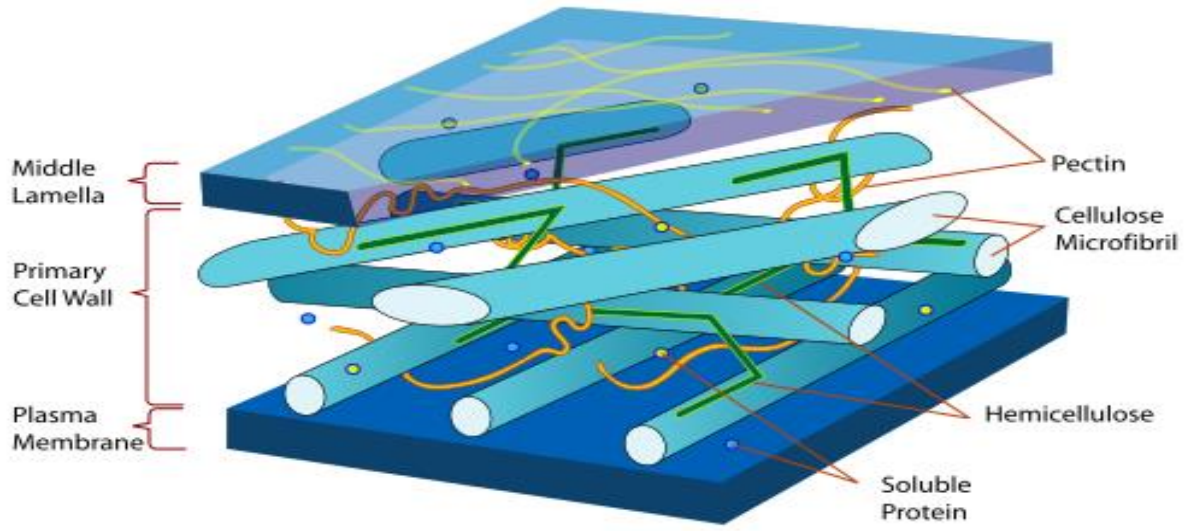

Figure 2.11. Microstrutural constituents of a plant cell wall (Image Source: www.nature.com)

A plant cell wall is arranged in three major layers (Figure 2.11): the primary cell wall, the middle lamella, and the secondary cell wall and the microstructure constituents are made up of cellulose microfibrils which act as reinforcement and hemicelluloses, pectin, lignin, and soluble proteins act as a matrix.

Cellulose makes up the highest constituent of all vegetable fibers and is responsible for the fiber properties [39,40].

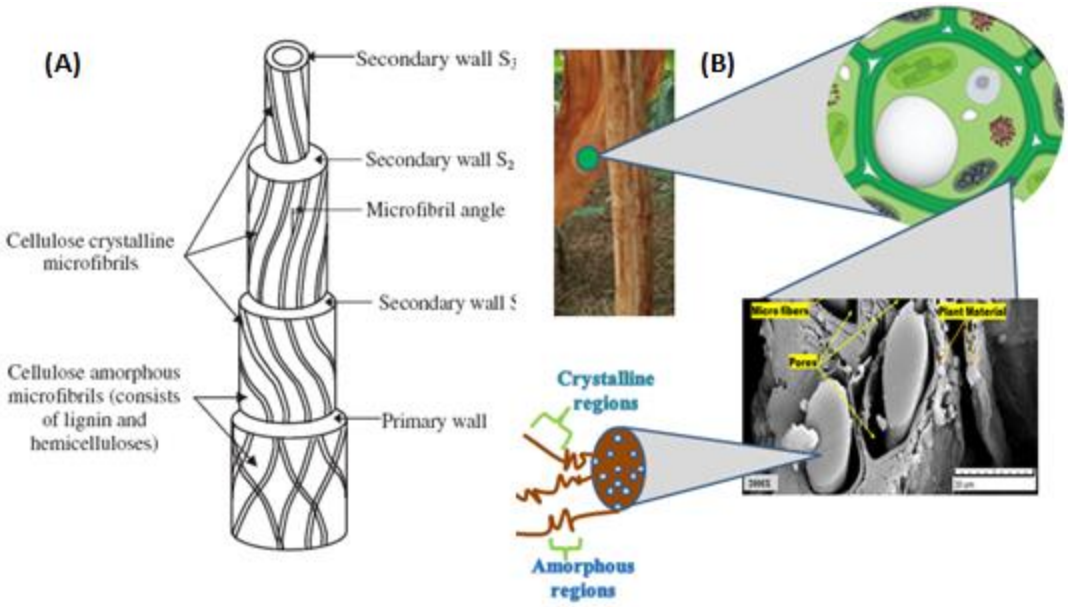

Figure 2.12. Scheme of arrangement of amorphous and crystalline fibrils in the cell wall

The fibers are composed of layered membranes of the primary and secondary walls (Figure 2.12A). The primary wall is composed of amorphous cellulose microfibrils which are in a composite matrix of lignin and hemicelluloses. The secondary wall is composed of three layers which have helically wound cellulose, microcrystalline microfibrils; It's these microfibers that determine the mechanical strength of the fiber, the angle between the fiber axis and the microfibril is determined as the microfibril angle [41,42].

The fibrils in primary and secondary walls are essentially similar but they are arranged differently. In primary walls, they are comparatively poorly oriented. Noncellulosic constituents such as pectin, lignin, and hemicellulose may occupy the spaces between the fibrils in both primary and secondary walls. Removal of these noncellulosic components of the cell walls seems not to disturb the remaining cellulose fibrils. The structure of wood or natural fiber consists of a thin primary wall and three secondary layers (S1, S2, and S3) [43]. Each layer is composed of cellulose fibers, a bio polymer, mainly crystalline, surrounded by an amorphous matrix of hemicellulose and lignin [39].

2.1.1.1. Cellulose

Cellulose is the most abundant polymer on Earth, [44] which makes it also the most common organic compound. According to the United Nation's Food and Agriculture Organization (FAO), there is $3.27x10^9m^3$of cellulose on Earth and yet only 1% is utilized. Cellulose is a tough water insoluble substance that can be obtained from trees, plants and is also biosynthesized by bacteria [45].

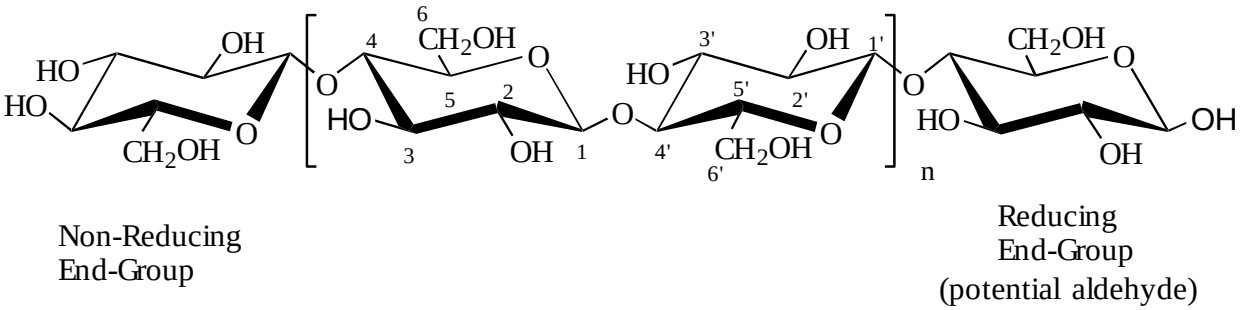

Figure 2.13. Chemical Structure of Cellulose

Cellulose is a linear and fairly rigid homopolymer consisting of D-anhydroglucopyranose units (AGU). These units are linked together by β (1→ 4) glycosidic bonds formed between C-1 and C-4 of adjacent glucose moieties (Figure 2.13) [45].

In the solid state, AGU units are rotated by 180° with respect to each other due to the constraints of β-linkage. Each of the AGU units has three hydroxyl (OH) groups at C-2, C-3 and C-6 positions. According to Sjoström [46], native cellulose in wood has a degree of polymerization (DP) of approximately 10,000 glucopyranose units and it is around 15,000 for native cellulose in cotton. The DP in cellulose depends on the source and part of the plant [47].

$$DP = \frac{\text{Molecular weight of cellulose}}{\text{molecular weight of one glucose unit}} \quad (1)$$

Terminal groups at the either end of the cellulose molecule are quite different in nature from each other. The C1 OH at one end of the molecule is an aldehyde group with reducing activity. Aldehyde groups form a pyranose ring through an intramolecular hemiacetal form. In contrast, the C4 OH on the other end of the chain is an alcohol borne OH constituent and thus is called the non-reducing end.

Annual cellulose synthesis by plants is close to 1012 tons. Plants contain approximately 33% cellulose whereas wood contains around 50 per cent and cotton contains 90%. Currently, most of the cellulose is utilized as a raw material in paper production. This equates to approximately 108 tons of pulp produced annually. Cellulose usually exists as cellulose I (in most plants) and rarely as cellulose II (in several algae

and some bacteria) allomorphs, in which are the glucan chains oriented parallel and anti-parallel respectively.

Table 2.1. Degree of polymerization of some cellulosic materials [48].

Material	Degree of polymerization
Cotton (unopened)	15,300
Cotton (opened)	8,100
Cotton linters (bleached)	1,000-5,000
Textile flax	8,800
Jack pine (Hard wood)	7,900
Bacteria	5,000
Sulphate pulp, bleached	1,255
Kraft pulp	975
Rayon	305

Fibers with high cellulose content are suitable for composite reinforcement because of the strength provided by cellulose whereas fibers with high hemicelluloses content are suitable for the production of ethanol because the sugars in hemicelluloses can be easily hydrolyzed [49].

2.1.1.2. Hemicellulose

Hemicelluloses exist in all vegetation and give plant fibers their strength through interaction with cellulose and in cell walls with Lignin [50]. Structurally, hemicelluloses are co-polymers of two or more sugars and sugar acids glucose, mannose, galactose, xylose, arabinose and 4-O-methylglucuronic acid [8]. They are of low DP 120 - 200 with short branching chains, making them amorphous heteropolysaccharides.

Hemicelluloses are commonly isolated from halocellulose through extraction with aqueous alkaline solutions Potassium, Sodium and Lithium hydroxides.

2.1.1.2. Lignin

Lignin is the most abundant polymer behind cellulose. It’s composed of different functional groups such as phenolics, methoxyls, aliphatic alcohols, aldehydes, ketones and ethers [51].

2.1.2. Properties

2.1.2.1. Mechanical Properties

The mechanical properties of vegetable fibers are generally dictated by the structure which is dominated by cellulose, lignin, pectins and waxes [52]. Table 2.2 shows the mechanical properties of selected vegetable fibers. It's observed that bast fibers generally have better mechanical properties compared to leaf and fruit fibers. The fiber percentage elongation is generally lower with bast fibers and higher with leaf fibers.

2.1.2.2. Thermal Stability

The thermo-gravimetric behavior is directly proportional to the chemical constituents of the fibers [53]. The thermal decomposition of cellulose in vegetable fibers is usually plotted on the TG/DTG curve.
A first stage, up to about 200^{o}C corresponding to about 10% loss is followed by a second stage with about 70wt% loss with temperature up to 500^{o}C which is a limit for organic materials. The final third stage extends to the usual ending test and corresponds to about 20 wt% and a final temperature of about 800^{o}C. The DTG peaks also show thermal decomposition peaks as well as shoulder and tail peaks that are ascribed to the fiber's constituents [53].

Thermal decomposition of wood was indicated to occur at 210-260^{o}C by dehydration subsequently followed by the major endothermic reaction of depolymerization. Differential Thermogravimetric (DTG) peaks that vary from 310-450^{o}C; Hemicellulose generally decomposes at a maximum temperature of 290^{o}C whereas lignin decomposition is observed from 280-520^{o}C.

The thermal decomposition rate of vegetable fibers is affected by the TGA atmospheres. It's observed that the tests were done in an inert environment (Helium and Nitrogen) have higher decomposition temperatures compared to tests done in an oxidative environment (Air and Oxygen). This phenomenon is attributed to the fact that the oxidative environment leads to reactions with cellulose thus having the main DTG peak shifted to the left [53].

Table 2.2. Mechanical Properties of Selected Natural Fibers [4,25,54,55]

Technical Fibers	**Density** (g/cm^3)	**Tensile Strength** (MPa)	**Young's Modulus** (GPa)	**Percentage Elongation (%)**
Ramie	1.5	400-938	61.4-128	2
PALF	1.44	413-1627	34.5-82.5	1.6
Flax	1.5-3	450-1100	27.6	1.2-1.6
Jute	1.3-1.45	393-773	13-26.5	1.8
Hemp	1.48	400-800	17-70	1.6
Sisal	1.45	468-640	9.4-22.0	2-3
Cotton	1.5-1.6	287-800	5.5-12.6	3-10
Coir	1.15	131-175	4-6	15-25
Kenaf	1.5-1.6	930	53	1.5
Nettle	1.51	560-1600	24.5-87	2.1-2.5
Abaca	1.5	430-760	72	10-12
Oil palm	0.7-1.55	248	25	3.2
Pineapple	1.44	170-1627	60-82	2.4
Banana	1.35	529-914	27-32	3
Alfa	0.89	35	22	5.8
Bagasse	1.25	222-290	17-27.1	1.1
Bamboo	0.6-1.1	140-800	11-32	2.5-3.7
Curaua	1.4	87-1150	11.8-96	1.3-4.9
Henequen	1.2	430-570	10.1-16.3	3.7-5.9
Isora	1.2-1.3	500-600		5-6
Piassava	1.4	134-143	1.07-4.59	7.8-21.9
Luffa cylindrica		385	12.2	2.65
Ferula communis		475.6	52.7	4.2
Wool		25-35	120-174	2.3-3.4
Spider Silk		17-18	875-972	11-13
B.mori silk	1.33	19.55	208.45	6.10
E-glass	2.5	2000-3500	70	2.5
S-glass	2.5	4570	86	2.8
Aramid	1.4	3000-3150	63	3.3-3.7
Carbon	1.7	4000	230-240	1.4-1.8

2.1.3. Challenges and Limitations

2.1.3.1. Thermal decomposition temperature

During processing of natural fiber composites, the thermal decomposition of natural fibers produces volatile gasses at temperatures above 200^{o}C, this leads to porous polymer composites with inferior mechanical properties. Improving the thermal stability of the fibers is of utmost importance if the fibers

are to be used as reinforcement for the production of natural fibrous composites with a wide sphere of applications [56].

The vegetable fiber thermal decomposition temperature of 200^{o}C renders them not suitable for higher processing temperatures, especially if they are to be used for reinforcement with thermoplastic matrices.

2.1.3.2. Moisture Absorption

Vegetable fibers are hydrophilic in nature due to the structure of cellulose which is the major microstructure constituent. Water absorption, therefore, takes place because of the possibility of hydrogen bonding with the free hydroxyl groups or through diffusion through the matrix materials. The high affinity to water renders natural fibers not suitable for marine application, however, this limitation is usually counteracted by utilization of treatments such as chemical and plasma treatments as a means of increasing hydrophobicity; using coupling agents, hybridization, compatibilizers as means of increasing fiber-to-matrix bonding [57].

2.2. BARKCLOTH

Barkcloth utilization has been confirmed with archeologists discovering grooved stones in Xiantouling site of Shenzhen similar to grooved hammers used today [58]. It is considered that the extraction of barkcloth in ancient China spread to Taiwan, Philippines, Africa, Central America, and Oceania. Barkcloth produced from Polynesia is derived from the bast of mulberry, whereas in Uganda the felt is derived from Ficus trees all being from Moraceae family.

According to United Nations Educational, Scientific and Cultural Organization (UNESCO) [59], Barkcloth, a non-woven fabric has been in production in Uganda for over six centuries; however, there's limited study of the non-woven felt which is produced through a series of pummeling processes. That notwithstanding, in 2005 UNESCO proclaimed it as a "Masterpiece of the Oral and Intangible Heritage of Humanity".

In terms of green credentials and sustainability, the trees grow naturally in Central Uganda and don't need fertilizers [60]. For a material to be sustainable, the supply should be continuous and should be available for the future generations.

2.3. NATURAL FIBER REINFORCED COMPOSITES

Natural fibrous materials were used by early civilizations from biblical times; Egyptians early in the 20th century reinforced mud bricks with straw. However, on the turn of the 20th century, new fibers, largely from petrochemical sources and with exceptional strength dented the use and production of natural fibers. Ever since their discovery, synthetic fibers' contribution towards fuel economy in automotive and aerospace industries is unparalleled. The unique structural properties of composites have seen their application in construction beside the traditional automotive and aerospace sectors.

With the implementation of EU directives [12] on waste and end of life disposal strategies, there has been a surge of activity driven by the European automotive industry to introduce Natural Fiber Composites (NFC) as a substitute to Glass Fiber Reinforced Plastic Composites (GRPC), where appropriate. The production of these non-woven and plied single layer laminates has significantly escalated within the last 5 years due to demand from the automotive industry and the need for industries to develop by-products from their waste materials in response to directives to further reduce the accumulation of waste in landfill sites.

Figure 2.3. Flax/polypropylene underbody components have replaced glass fiber reinforced plastic components in vehicles such as the Mercedes Benz A-Class [61]

The increasing costs of oil vis-à-vis the diminishing oil reserves world over and environmental concerns has led to the reigniting of the natural fiber spark. Production of chemicals and materials from bio-based feedstock is expected to increase to 18% in 2020 and 25% in 2030 [24].

Estimations show that two-thirds of the $1.4 trillion global chemical industry will eventually be based on renewable resources such as renewable resins PolyLactic Acid (PLA) from corn, biodiesel from jatropha etc. Petroleum transitioned from a single product (kerosene in the early 1900's) to a multiproduct industry (petrol, jet fuel, diesel fuel, asphalt and polymeric materials) between the late 19th and the middle of the 20th Century. Research conducted from the 1990's to the present has led to many new bio-based products [62–65].

Several of the world's largest chemical companies, including DuPont, Monsanto and Cargill have announced a major shift in their base science and technology from traditional petrochemical processing to life sciences. DuPont has invested $12.5 billion to acquire expertise in agricultural biotechnology [66].

It's a known fact that synthetic fibers such as carbon and glass are facing problems of recyclability. Landfills can't solve the problem because other problems attached to their production such as emissions of toxic chemicals still stand. The alternative to synthetic fibers is natural fibers. The front seat drivers for this technology are exceptional specific strength closely comparable to synthetics.

Sustainable, eco-friendly plant fibers are now anticipated to be economically viable and would lead to various industrial applications. Due to the increased demand of eco-friendly materials, there is a growing interest in bio-based or "green composites", also referred to as "ecocomposites", "biocomposites", "Natural Fiber Reinforced Composite (NFRC)" or "Natural Fiber Reinforced Plastics (NFRP)".

The industrial use of NFRCs in automotive applications was inspired by automotive entrepreneur Henry Ford in the 1930s, when he produced a hemp body vehicle. To-date various car makers (Table 1.2) are now utilizing NFRCs in various parts of automotive components (Figure 2.2)

2.3.1. Polymer Matrices

Polymer matrices serve a purpose of holding the reinforcing fibers in place and they are usually of lower strength compared to the reinforcing fibers. The polymer matrix should be strong enough to withstand the load but good enough to transfer the load to the reinforcing fibers.

There are majorly two classes of polymer matrices: Thermoplastic and Thermoset matrices.

Thermoset resins vis-à-vis thermoplastic resins exhibit the following thermomechcanical behavior: [23]

- Brittle behavior over a wide range of temperatures.
- Inability to deform viscoelastically.
- No rubbery behavior.

- Non-crystalline structure in the form of a cross-linked network.
- Polymer degrades, or burn rather than melt
- Cannot be recycled by melting and reforming.

2.3.1.1. Thermoset

Thermoset matrices are liquid monomers or pre-polymers which are processed into final products through catalysts commonly known as hardeners. Thermoset polymers are composed of covalent bonds, which are pivotal against sliding thus giving thermoset polymers exceptional strength and creep resistance [56]. Epoxies, vinyl esters and polyesters account for the majority of thermoset resins used in industry. The physical and mechanical properties are shown in Table 2.3.

Table 2.3. Thermoset Polymer Properties [67].

Property	Polyester resin	Vinylester resin	Epoxy
Density [g/cm^3]	1.2-1.5	1.2-1.4	1.1-1.4
Elastic Modulus [GPa]	2-4.5	3.1-3.8	3-6
Tensile Strength [MPa]	40-90	69-83	35-100
Compressive Strength [MPa]	90-250	100	100-200
Elongation[%]	2	4-7	1-6
Cure shrinkage [%]	4-8	-	1-2
Water Absorption [24hours @20^{o}C]	0.1-0.3	0.1	0.1-0.4
Izod Impact Notched [J/cm]	0.15-3.2	2.5	0.3

Epoxies are petroleum based low molecular weight prepolymers majorly produced through the combination of epichlorohydrin and bisphenol A. Epoxy hasn't widely been utilized in natural fiber composites; this could be due to the fact that the cost is high however considerable research elsewhere has documented the effect of process parameters such as fiber treatment on the mechanical properties of jute [68,69], sisal [70,71], flax [70], sugar palm fiber [72], banana [73], jute [74,75], bamboo[76], kenaf [77] epoxy composites.

Polyester resins are synthetic based resins which are produced by the reaction of dibasic organic acids and polyhydric alcohols. Polyester is the most widely used natural fiber composite resins due to the fact that they are cheaper than epoxies [78–80].

2.3.1.2. Thermoplast

Thermoplastic materials that currently dominate as matrices for natural fibers are polypropylene (PP), polyethylene (PE), and poly (vinyl chloride) (PVC) [81]. Table 2.4 shows the properties of the most common thermoplastic polymers used with natural fiber reinforced composites.

Unlike thermoset resins which require fiber chemical treatment to clean the fiber surface which leaves a rough, grooved surface, thereby enhancing the fiber-to-matrix adhesion, Thermoplastic polymers are hydrophobic, therefore, to enhance the fiber-to-matrix adhesion, compatibilizers such as Maleic anhydride grafted polymer (PE/PP), copolymers are utilized in order to strengthen the natural fiber-to-grafted polymer bond [82].

Table 2.4. Physical and Thermo-Mechanical properties of thermoplast polymers [67].

Property	**PP (Isotactic)**	**LDPE**	**HDPE**
Density [g/cm^3]	0.899-0.920	0.910-0.925	0.94-0.96
Water Absorption [-24 hours/ %]	0.01-0.02	<0.015	0.01-0.2
T_g [^{o}C]	-10 to -23	-125	-133 to -100
T_m [^{o}C]	160-176	105-116	120-140
Tensile Strength [MPa]	26-41.4	40-78	14.5-38
Elastic Modulus [GPa]	0.95-1.77	0.044-0.38	0.4-1.5
Elongation [%]	15-700	90-800	2.0-130
Izod Impact Strength [J/m]	21.4-267	>854	26.7-1068

2.3.1.3. Biodegradable Polymer Matrices

Biodegradable polymers are types of polymers which are obtained through environmentally friendly renewable sources and designed to degrade naturally through the action of microorganisms. There's an ambiguity in the definition of biodegradable or green and biobased polymers. Most of the biodegradable epoxy polymers are not completely biobased that notwithstanding, there has been the development of oxidized green polymers from natural oils.

The US Department of Agriculture and the US Department of Energy have set goals of having at least 10% of all basic chemical building blocks be created from renewable, plant-based sources in 2020, increasing to 50% by 2050 [4].

There are several biodegradable, naturally derived polymers in existence (Table 2.5), such as polysaccharides (starch, chitin, collagen, gelatines, etc.), Proteins (casein, albumin, silk, elastin, etc.), Polyesters (e.g. Poly (hydroxyalcanoate) (PHA), poly (hydroxybutyrate) (PHB), polylactic acid (PLA), lignin, lipids, natural rubber, some polyamides, polyvinyl alcohols, polyvinyl acetates, and polycaprolactone [9]. Biodegradable polymers are classified according to their source: agropolymers (starch), microbial derived (PHA) and chemically synthesized from agrobased monomers (PLA) or conventional monomers (synthetic polyesters) [9].

PLA, Cashew Nut Shell Liquid (CNSL) and Soy based resins are the most commonly used biodegradable polymers for the production of biocomposites. Starch based polymer resins have serious concerns such as their affinity to moisture; however compatibilizer agents have shown to reverse the hydrophilicity of starch resins [83]. Commercially, various companies have also introduced green epoxies, but not fully based from plant sources.

Table 2.5. Properties of Natural polymers [3].

Polymer	Density [g/cm^3]	T_m [^{o}C]	Tensile Strength [MPa]	Young Modulus [GPa]	Elongation at break [%]
Starch	1-1.39	110-115	5-6	0.125-0.85	31-44
PLA	1.21-1.25	150-162	21-60	0.35-3.5	2.5-6
PHB	1.18-1.26	168-182	24-40	3.5-4	5-8

2.3.2. Manufacturing Processes

The processing of composites depends on the selection of the matrices and the envisaged end product. Compression Moulding, Injection Moulding and Extrusion are utilized for production of components with thermoplastic resins whereas Sheet Moulding Compound and Resin Transfer Moulding is utilized for production of components utilizing thermoset resins [54].

2.3.2.1. Injection Moulding

The molten polymer is mixed with the short fiber with critical length to form pellets. The pellets are therefore fed through the hopper into a heated compression barrel with rotation screws; the viscous liquid is therefore led to the mould cavities and after cooling the part is ejected from the mould cavity.

2.3.2.2. Compression Moulding

This process includes two processes: Hot press and autoclave technology. For hot press, the fiber and the matrix material are arranged in layers. Two hot plates melt the matrix polymer and this aides with matrix impregnation into the fiber network.

The viscosity of the polymer matrix should be low enough so as to effectively impregnate into the fiber network and as well as high enough so as to prevent spurting out [54].

2.3.2.3. Resin Transfer Moulding

For thermoset composites, the most commonly used fabrication procedures are the Vacuum Assisted Resin Transfer Moulding (VARTM) in which case the resin is infused into the fiber preform by use of pressure. This is usually the preferred method for production, however, it has challenges of voids which can be minimized by varying the pressure at which the resin is infused.

2.3.2.4. Hand lay-up

The ‘‘hand lay-up’’ technique, is the oldest composite manufacturing method. It’s utilized in such a way, the fiber preform is infused with resin by hand through pouring the resin on top, using rollers, the resin is infused into the fiber network; thereafter the composite structure is cured at room temperature or in an autoclave for better bonding and hence a mechanically robust product is produced. Hand lay-up has challenges with thickness; the ability to produce good parts goes down to workmanship skill [84].

2.3.3. Mechanical Properties

The mechanical properties of NFRC are influenced by the fiber-to-matrix adhesion, fiber orientation, and structure. This aids smooth, stress transfer from the matrix to the fillers.

2.3.4. Empirical Mechanical Models

2.3.4.1. Rule of Mixtures

The Rule of Mixtures (ROM) is the empirical predictive model used in material science to predict properties of composites when the load applied is along the direction of the fiber (longitudinal) or transverse.

$$E = E_f v_f + (1 - v_f) E_m \tag{2}$$

Equation (2) shows the longitudinal ROM which is based on the Voigt Model for prediction of the modulus of the composite in axial direction [85].

2.3.4.2. Inverse Rule of Mixtures

When the loading is perpendicular to the fiber, direction, the inverse rule of mixtures [86] is usually used.

$$E = \frac{E_f E_m}{v_m E_f + v_f E_m} \tag{3}$$

2.3.4.3. Thermal Conductivity Models

Various models have been formulated to study and predict the effective thermal conductivity (k_e) of heterogeneous materials. The models presented here take the heterogeneous material as macroscopically heterogenic [87].

The effective thermal conductivity models are based on measurable quantities such as thermal conductivity of matrix (k_m); thermal conductivity of the reinforcing fiber preform (k_f) and corresponding fiber volume fraction in the composite (v_f)

Series Model

$$k_e = \frac{k_m k_f}{v_f k_m + (1 - v_f) k_f} \tag{4}$$

Heat flow in the series model is assumed to flow perpendicular to the layers and therefore gives the minimum value of thermal conductivity [88].

Parallel Model

$$k_e = v_f k_f + (1 - v_f) k_m \tag{5}$$

The parallel model assumes the layers are arranged parallel and gives the maximum thermal conductivity of the composite since heat flows proportionally through the layers. [89].

Geometric Mean Model

$$k_e = k_f^{v_f} k_m^{(1 - v_f)} \tag{6}$$

Maxwell Model

$$k_e = k_m \frac{k_f + 2k_m + 2v_f(k_f - k_m)}{k_f + 2k_m - 2v_f(k_f - k_m)} \tag{7}$$

Maxwell postulated the effective thermal conductivity of randomly distributed spheres in a matrix [90]. The Maxwell model is based on the assumption that the volume fraction of the composite is less than 25%.

Cheng and Vachon Model

$$k_e = -\left[\frac{2}{\sqrt{C.(k_f-k_m)(k_m+B)(k_f-k_m)}} tan^{-1}\left[\frac{B}{2}\sqrt{\frac{C.(k_f-k_m)}{k_m+B(k_f-k_m)}}\right] + \frac{1-B}{k_m}\right]^{-1} \quad (8)$$

$$B = \sqrt{\frac{3v_f}{2}} \; and \; C = -4\sqrt{\frac{2}{3v_f}}$$

The Cheng and Vachon model endeavors to solve the effective thermal conductivity of a two phase solid mixture using distribution functions [91].

2.3.5. Challenges and Limitations

Natural fibers are composed of cellulose, hemicelluloses, lignin, pectins which are highly polar molar molecules composed of hydroxyl groups whereas the matrices are hydrophobic, therefore there's a challenge of fiber-to-matrix adhesion which is usually addressed through fiber treatments [40,84,92].

Natural fibers and biodegradable polymers such as PLA degrade at temperatures above 200^{o}C. Regulation of the processing temperatures especially with extrusion and compression moulding is done to avoid processing at the critical temperature.

2.4. INTRODUCTION TO SOUND ABSORPTION

The increase in the industrialization and growth of the metropolis world over is a serious concern in terms of noise pollution from various sources. According to a new World Health Organization report, traffic related noise accounts for over one million healthy years of life lost annually to ill health, disability, or early death in western Europe. Among environmental factors contributing to disease in Europe, environmental noise leads to a disease burden that is only second in magnitude to that from air pollution. Noise pollution causes or contributes to not only annoyance and sleep disturbance, but also heart attacks, learning disabilities, and tinnitus [93]. The use of acoustic absorbing materials is the most effective means used in buildings, automotive, aerospace and other transport vehicles to abate noise and vibrations this is achieved through the absorption of the acoustic energy of the acoustic wave as it propagates through the sound absorber [94]. Synthetic materials such as polymer foams, glass fiber, polyester, mineral wool are the leading sound absorption or noise reduction materials used. However, the biggest drawback is that most of the raw materials sources are from fossil fuels. In order to create a new class of materials, sustainable, renewable material sources are being explored as a consequence of the Kyoto protocol on global climate change [95].

The ecological "green" image of cellulosic fibers and considerable mechanical properties fit for secondary structures coupled with low health risk is the leading argument for innovation and development of products which are biodegradable and can be applied to automotive industries, building and construction [3–5]. Plant based fibers like flax, hemp; nettle and kenaf which were once used to provide textile fiber in the western world have attracted renewed interest this time for industrial composite applications [8,9,96].

According to the report on Global Natural Fiber Composites Market 2014-2019: Trends, Forecast and Opportunity Analysis, showed that by 2016, the natural fiber composites market is expected to be worth US $531.2 million with an expected annual growth rate of 11% for the next five years [97]. Currently, natural fibers account to over 14% share of reinforcement materials; however, the share is projected to rise to 28% by 2020 amounting to about 830,000 tons of natural fibers [36]. A comparison based on the Ecoinvent database between the environmental impacts of some traditional and natural sound insulation materials from cradle to gate is shown in Figure 2.4 [98].

2.4.1. Factors influencing sound absorption

For a material to work as a sound absorber, it has to be porous, and the level of porosity varies from one material to another. Sound absorbing materials absorb the sound energy hitting them whereas they reflect a small amount (Figure 2.31).

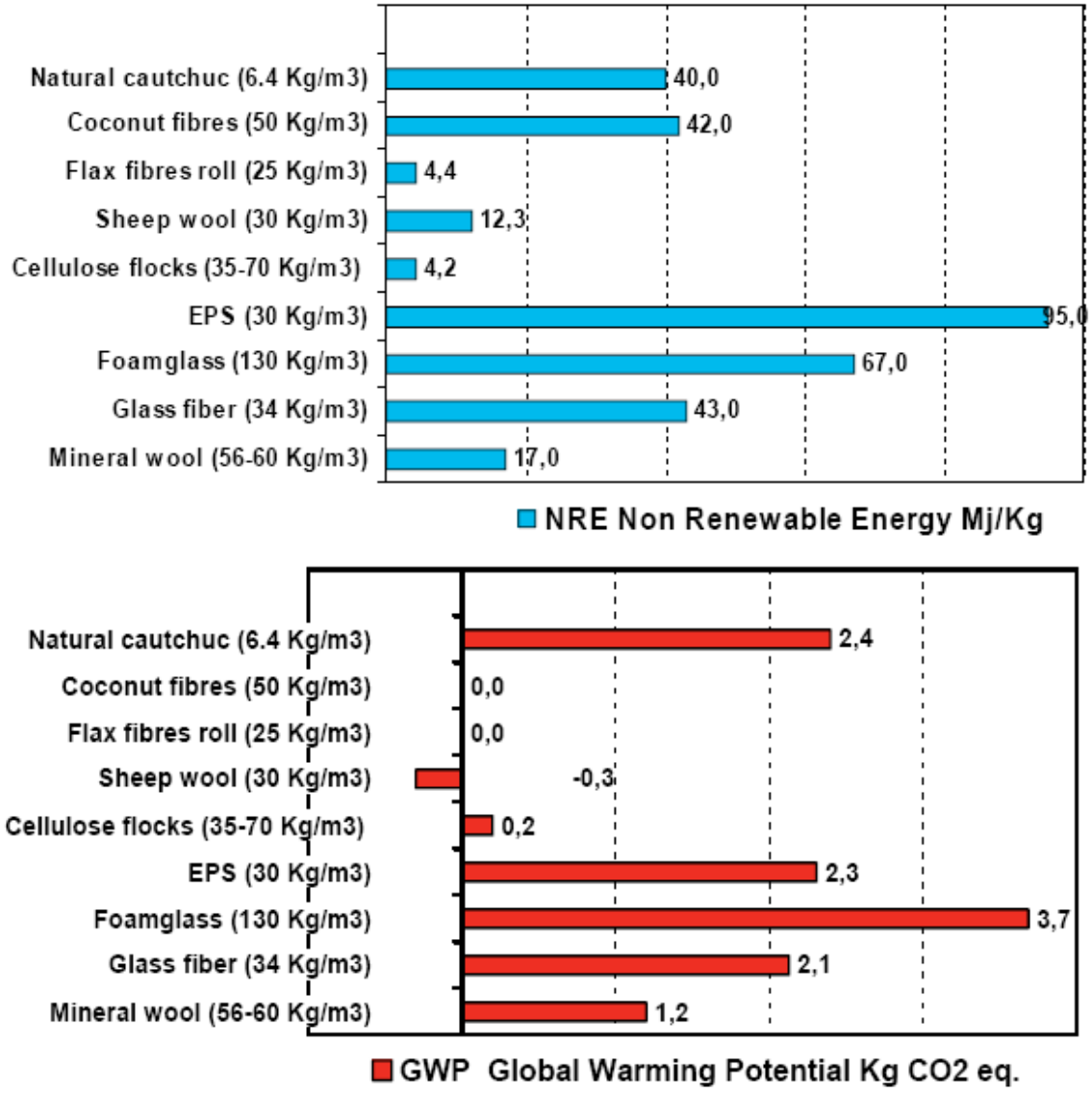

Figure 2.4. Ecoinvent. Comparison of environmental impacts of traditional and natural materials [98].

Figure 2.42 shows a schematic representation of porous structures. The structure is characterized by closed pores which influence macroscopic properties such as bulk density, mechanical strength, and thermal conductivity, however, they are inactive in a fluid flow or absorption of the gaseous medium [99]. These kind of closed pores are typical of most vegetable fibers which have hollow lumens such as banana fibers (Figure 2.42).

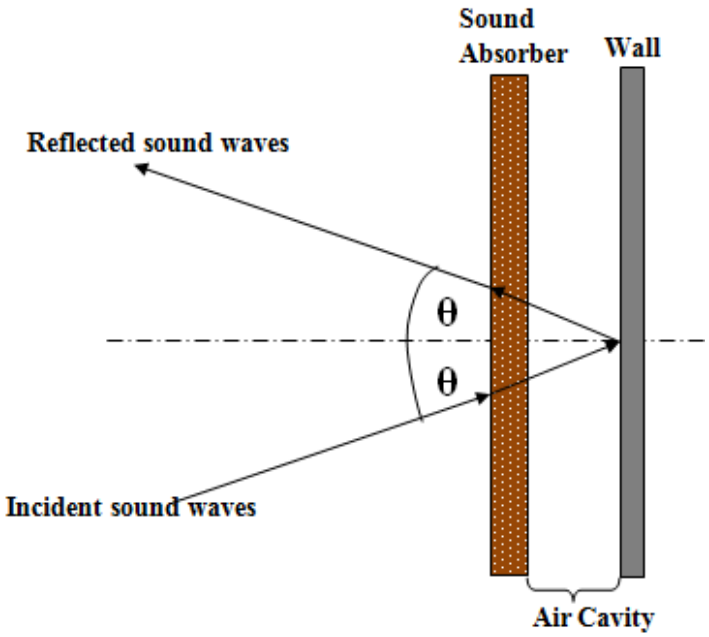

Figure 2.41. Illustration of a sound absorbent set up.

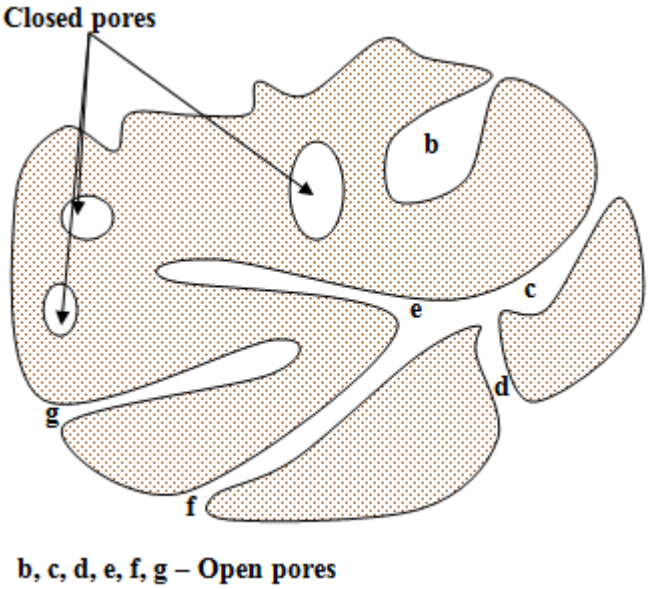

Figure 2.42. Scheme of porous material.

On the other hand, a porous structure can also be characterized by open pores, these have interaction with the fluid medium. The open pores can either be closed having a dead end such as b and g (Figure 2.32). For the purpose of this chapter, only natural fibrous sound absorption materials will be reviewed. Because sound absorbing materials are porous in nature, the sound absorption coefficient is proportional to their thickness and inversely proportional to the resistance of air through them.

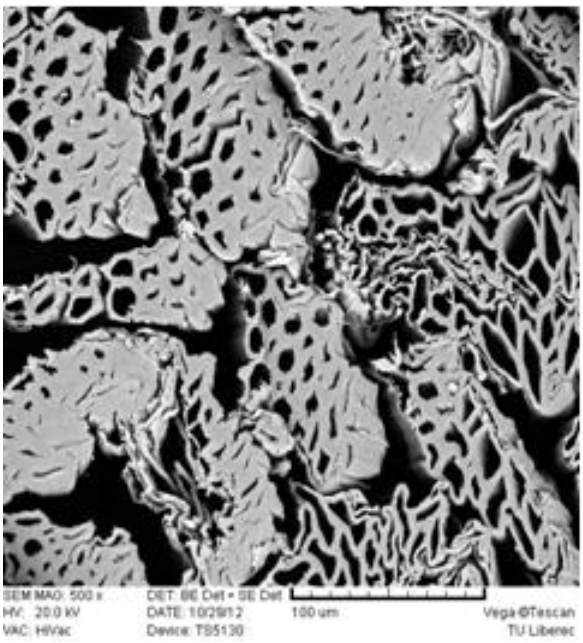

Figure 2.43. Morphology of banana fiber showing the pore structures.

2.4.2. Natural Fibrous Materials for Sound Absorption

2.4.2.1. Wood

There are not many wood-based materials used as sound absorbers due to the challenges of low sound absorption. It has been shown that soft fiber boards have an airflow resistivity in the range of 5000000Rayls/m whereas wood-wood has an airflow resistivity of 1000Rayls/m [100]. The empirical models show that the airflow resistivity dictates the suitability of a material as a sound absorber, it is evident that a very high or too low airflow resistivity makes it unsuitable as a sound absorber. The Optimum value of airflow resistivity for sound absorbers is in the range of 10^3 to 10^5 Rayls/m. The wood based sound absorbers are slabs made of wood strands or chips and perforated fiber boards relying on the Helmhotz resonance mechanism [100]. Liu et al. [101] utilized wood fiber and rice straw for the development of thermal and acoustic insulation panels with the thickness ranging from 50-150mm. The sound absorption coefficient of the developed biocomposites was above 0.8 for a wide frequency range 250-7000Hz.

Mohammed et al.[102] studied the sound absorption coefficient of 100 types of Malaysian woods. He showed that the sound absorption coefficient of Malaysian wood is low and at a higher frequency (>500 Hz), the sound absorption coefficient was high. Moreover, at higher frequency, with higher density value, the sound absorption coefficient of one species is lower compared to other species with a lower density. Jianying et al. [103] investigated the sound absorption coefficients of low-density kenaf binderless particleboard with densities ranging from 0.10 to 0.25gcm^{-3} and thickness of 12mm. The sound

absorption property of kenaf binderless particleboard at a density of 0.15g/cm^3 was almost equal to that of the insulation board.

An analysis of sound insulation properties of three types of composite panels by Zhao et al. [104] showed that the wood-waste tyre rubber composite panel possesses better soundproof effect than that of commercial wood particleboard and composite floorboard. The sound insulation property was improved with increasing rubber crumb content and polymeric methylene diphenyl diisocyanate adhesive level in the composite panel.

Jiang et al. [105] showed that the sound absorption coefficients of the five eucalyptus wood species did not change evidently below 1000Hz, but above 1000Hz their sound absorption coefficients increased with the increasing frequency. The sound absorption property of eucalyptus wood of 0.5cm thickness was much better than that of 1.0cm thickness. It was concluded that wood sound absorption properties of eucalyptus are affected by their board thickness and the type of sawn timber within the testing frequency.

2.4.2.2. Bast Fibers: Jute, Flax, Kenaf and Ramie

The acoustic properties of jute felt and rubber composites were investigated by Fatima and Mohanty [106]. Addition of rubber was found to reduce the noise reduction coefficient whereas treatment with alkali had no significant change on the sound absorption coefficient. Youngjoo and Gilsoo [107] investigated the sound absorption and viscoelastic property of automotive nonwovens and their plasma treatment. It was observed that jute nonwoven of 5.62mm thickness used in car headliner felts had good sound absorption at a higher frequency; plasma treatment reduced the sound absorption property of jute nonwovens. A blend of jute-polypropylene non-woven performed well as a sound absorber and was found to be suitable materials for car flow coverings [108,109]. Yang and Li [110] showed the exceptional sound absorption performance of Jute, Ramie and Flax nonwovens of 40mm thickness compared to the synthetic fibers. Arenga pinnata bast fiber was studied for the sound absorption, the results for 2000 Hz to 5000 Hz were within the range of 0.75 – 0.90. The optimum sound absorption coefficient was obtained from the thickness of 40mm [111].

2.4.2.3. Fruit Fibers: Coir, Cotton, kapok

Zulkifh et al. [112] studied the acoustic properties of multilayer coir fibers, and found out that the developed panels had a sound absorption coefficient of 0.70 – 0.80 in the frequency range of 1000-1800Hz. Fouladi et al. [113] showed that fresh coir fiber has an average absorption coefficient of 0.8 at a frequency greater than 1360 Hz and 20 mm thickness. Increasing the thickness improved the sound

absorption at lower frequencies, having the same average at frequencies greater than the 578Hz and 45mm thickness. The addition of recycled tyre rubber to coir reinforced polyurethane resin composites produced a positive effect of the composite boards under investigation [114]. Xiang et al. [115] showed that the kapok fiber has excellent acoustical damping performance due to its natural hollow structure, and the sound absorption coefficients of kapok fibrous assemblies were significantly affected by the bulk density, thickness and arrangement of kapok fibers but less dependent on the fiber length. Compared with assemblies of commercial glass wool and degreasing cotton fibers, the kapok fiber assemblies with the same thickness but much smaller bulk density may have the similar sound absorption coefficients.

2.4.2.4. Agricultural Waste: Rice straw, Sawdust, Sugarcane bagasse, Tea Leaf

The acoustic properties in the rage of 500-8000Hz of rice straw-wood particle composite boards and found that the sound absorption coefficient was higher than wood based materials [116]. Generally, because agricultural waste such as rice straw and saw dust have low porosity after compaction with binders, the sound absorption properties are lower compared to nonwovens [117]. Doost-hoseini et al. [118] investigated the sound absorption coefficients, of 12mm insulating boards made of bagasse. Urea–formaldehyde and melamine–urea–formaldehyde were used to produce homogeneous as well as three-layered insulating boards with three densities of 0.3, 0.4, and 0.5 g/cm^3. The obtained results indicated that resin-type affected the sound absorption coefficients. The maximum absorption coefficient was found at 2000Hz of frequency (in multi-layered board of 0.50 g/cm3 of density, produced with urea–formaldehyde resin), and the minimum was observed at 500Hz (homogeneous board of 0.50 g/cm3 produced with urea–formaldehyde resin).

Ersoy and Küçük [119] showed that tea leaf fiber can be used as a sound absorption material, the results showed high beyond average absorption coefficient with backings of cotton.

2.4.2.5. Barkcloth

According to United Nations Educational, Scientific and Cultural Organization (UNESCO), Barkcloth, a non-woven fabric has been in production in Uganda for over six centuries; however, there's limited study of the non-woven felt which is produced through a series of pummeling processes. That notwithstanding, in 2005, UNESCO proclaimed it as a "Masterpiece of the Oral and Intangible Heritage of Humanity".

Non-woven felts have been investigated as sound absorption materials by various researchers Therefore, in this report, an exploratory investigation of the sound absorption properties of the non-woven fabric from the inner bark of mutuba trees (*Ficus natalensis*) and *Antiaris toxicaria* are presented. In terms of

green credentials and sustainability, the trees grow naturally in Central Uganda and don't need fertilizers. The fabric layers were studied and their performance in sound absorption was evaluated. Epoxy polymer was used as a binder of the barkcloth plies and the developed composites were also studied for their sound absorption properties. For a material to be sustainable, the supply should be continuous and should be available for the future generations.

2.4.2. Theoretical Sound Absorption models

The sound absorption theoretical models utilize physically measurable material parameters to estimate the sound absorption parameters.

2.4.2.1. Delany and Bazley Model

In 1970, Delany and Bazley introduced the first empirical model for determining the bulk acoustic properties of porous substrates. The Delany and Bazley model [120] is only applicable if and only if the frequency is higher than 250Hz [121].

$$Z_c = \rho_o c_o [1 + 0.057X^{-0.754} - j0.087X^{-0.732}] \quad (9)$$

$$k = {}^{\omega}/_{c_o} [1 + 0.0978X^{-0.700} - j0.189X^{-0.595}](\quad (10)$$

$$X = \frac{\rho_O f}{\sigma} \quad (11)$$

$$\alpha = 1 - |R|^2 \quad (12)$$

$$R = \frac{Z_s - \rho_o c_o}{Z_s + \rho_o c_o} \quad (13)$$

$$Z_s = -jZ_c cot(kd) \quad (14)$$

Where:

ρ_O is density of air; $c_o$is Speed of sound in air; Z_c is characteristic impedance; k is propagation constant; f is frequency; ω is angular frequency; σ is airflow resistivity; $j = \sqrt{-1}$; R is sound pressure reflection coefficient; Z_s is the surface impedance; d is the thickness

2.4.2.2. Miki Model

Miki [122] proposed a new model based on the Delany – Bazley equations that would address the negative real part of the surface impedance at low frequencies for multi-layer membranes:

$$Z_c = \rho_o c_o \left[1 + 5.50\left(10^3 \frac{f}{\sigma}\right)^{-0.622} - j8.43\left(10^3 \frac{f}{\sigma}\right)^{-0.632}\right] \quad (15)$$

$$k = {}^{\omega}/_{c_o} \left[1 + 7.81\left(10^3 \frac{f}{\sigma}\right)^{-0.618} - j11.41\left(10^3 \frac{f}{\sigma}\right)^{-0.618}\right] \quad (16)$$

2.4.2.3. Mechel Model

Mechel [123] proposed a theoretical model for low frequencies as follows:

$$\Gamma = i\frac{\omega}{c_0}\sqrt{1 - i\frac{\gamma}{2\pi X}} \tag{17}$$

$$Z_k = -i\frac{c_o^2\rho_0}{\omega\gamma\phi} \tag{18}$$

Where $\gamma = 1.4$ is the adiabatic constant of air; ϕ is the porosity

For the mid and high frequencies, Mechel proposed the following formulas:

$$Z_c = \rho_o c_o[1 + 0.06082X^{-0.717} - j0.1323X^{-0.6601}] \tag{19}$$

$$k = {}^{\omega}/_{c_o}\,[0.2082X^{-0.6193} - j0.1087X^{-0.67311}] \tag{20}$$

2.4.2.4. Allard and Champoux Model

Allard and Champoux [124] postulated a model that is based on the assumption that the thermal effects are dependent on frequency.

$$\rho(\omega) = \rho_o\left[1 - i\left(\frac{\sigma}{\rho_o\omega}\right)G_1\left(\frac{\rho_o\omega}{\sigma}\right)\right] \tag{21}$$

$$K(\omega) = \gamma P_o\left(\gamma - \frac{\gamma - 1}{1 - \left(\frac{i}{4P_r}\right)\left(\frac{\sigma}{\rho_o\omega}\right)G_2\left(\frac{\rho_o\omega}{\sigma}\right)}\right)^{-1} \tag{22}$$

Where: P_r is the Prandtl's number

$$G_1\left(\frac{\rho_o\omega}{\sigma}\right) = \sqrt{1 + \frac{i}{2}\left(\frac{\rho_o\omega}{\sigma}\right)} \tag{23}$$

$$G_2\left(\frac{\rho_o\omega}{\sigma}\right) = G_1\left(\frac{\rho_o\omega}{\sigma}\right)\left[4P_r\left(\frac{\rho_o\omega}{\sigma}\right)\right] \tag{24}$$

Where $\rho(\omega)$ is the effective density and $K(\omega)$ is the bulk modulus.

2.4.4. Mechanical and Acoustic Property Relations

Bies and Hansen[125] and Harrison[126] showed that propagation of sound waves through panels is dependent on the mechanical properties (Young's Modulus; Poison's ration) and the thickness of the panels. Sound vibration in panels may propagate in the form of compression, torsion or shear waves whereas for thin layers vibration may propagate through compression and shear leading to the deflection of the panel as a result of the bending forces.

The Bending stiffness is described as:

$$B = EI \tag{25}$$

Where E is the Young's Modulus [MPa] and I is the moment of inertia [m^4]. For plates of thickness h, the moment of inertia per unit with I' is used.

$$I' = \frac{h^3}{12} \tag{26}$$

Therefore the bending stiffness of the plate will be:

$$B' = \frac{I'E}{1-\mu^2} \tag{27}$$

Where μ is the Poisson's ratio.

Bies and Harrison in their formulations established a mechanical property dependence whereby the critical frequency at which the flexural/bending wavelength in the panel equals to the sound wavelength in the air by:

$$f_c = \frac{c^2}{2\pi}\sqrt{\frac{m}{B}} \tag{28}$$

Where c is the speed of sound in air [ms^{-1}] and m is the material's surface density [kgm^{-2}]

CHAPTER 3

RAW MATERIAL ANALYSIS

3.0. PROLOGUE

This chapter is aimed at introducing the raw materials and their analysis. Since this is the first report in the scientific world investigating barkcloth, it is important to first introduce a detailed study of the material as a background to the proceeding chapters.

3.1. BARKCLOTH

Barkcloth utilized in this study was from two species *Ficus natalensis* and *Antiaris toxicaria*. Both species were obtained from Uganda and were extracted using the method described by Rwawiire and Tomkova, 2014 [127].

3.1.1. Barkcloth Extraction

Figure 3.1. Extraction of Barkcloth non-woven natural fabric: (a) Scrapping of tree outer layer. (b) Use of local wedged tool to peel off the bark. (c) Peeling of the bark. (d) Covering of the tree stem for environmental sustainability. (e) Pummeling under the shade.
(f) Sun drying of the non-woven fabric. [127]

Figure 3.1 shows the detailed process of production of barkcloth. The extraction of the naturally occurring non-woven starts with scraping off the surface layer of the trunk to expose the fresh raw bark using a sharp blade. The blade is held at an angle such that only the surface layer is removed and also avoids

damaging the tree and fresh bark as shown in Fig. 3.1a. A ring is then cut with a knife on both ends of the scrapped stem that reflected the length of barkcloth that is to be produced. At the same time, a vertical slit is made from the top of the stem to the bottom. With the help of a wedged tool locally known as *ekiteteme*, carved out of the innermost part of a banana stem, the bark is easily peeled off starting from the base slowly moving upwards (Fig. 3.1b and c). For environmental sustainability, the debarked stem is wrapped with banana leaves, (Fig. 3.1d) which act as bandages to prevent dehydration; these are usually removed after a week, giving way to growth of fresh bark. The extracted bark is then subjected to heat as a means of softening prior to pummeling process which utilizes different well designed wooden grooved hammers. Pummeling is usually done under a shade to prevent direct sunrays from creating creases in the barkcloth (Fig. 3.1e). After pummeling, the barkcloth is sun-dried for 3h every day for 6days giving it a rich deep terracotta color and then re-pounded to smoothen the cloth surfaces. Drying involves stretching the wet fresh barkcloth using heavy loads at its perimeter to retain its dimensions on drying (Fig. 3.1f).

3.1.2. Barkcloth Microstructural Analysis

The utilization of SEM for fabric morphology is advantageous due to the fact that more fibers in the fabric are in focus and included in the image compared with other methods [128,129].

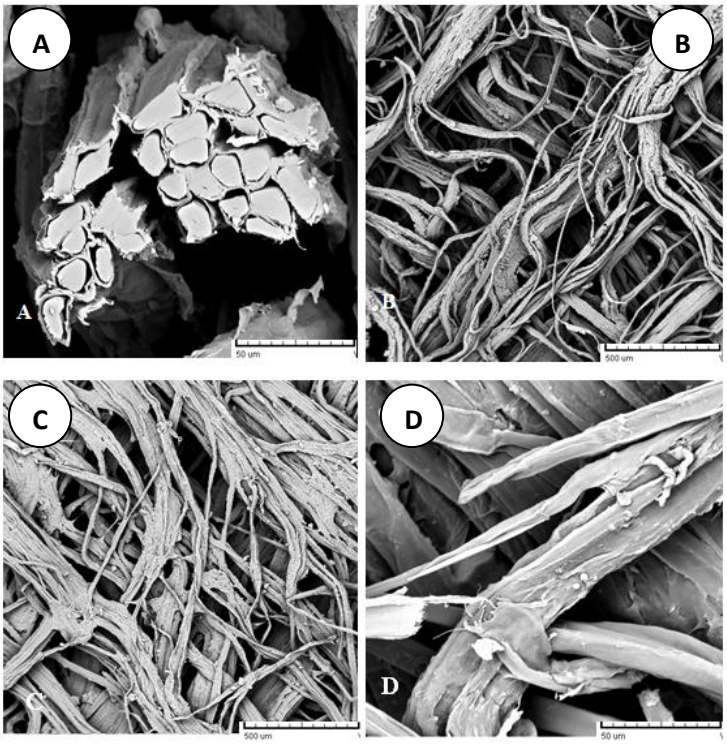

Figure 3.11. SEM morphology of treated barkcloth at magnifications (A) 50X, (B) and (C) 100X and (D) 500X

In order to show a representative image of the fabric, the magnification was optimized by using magnifications of 50, 100, 500, 1000 and 2000 (Figure 3.11). Several images were taken in order to show a representative microstructure of the fabric and to pinpoint the fiber orientations in barkcloth. The fabric morphology is made up of a dense network of naturally bonded microfibers that are oval in shape with diameters 10-20µm. The microfiber bundles appear to be aligned at angles, (Figure 3.12a). The inter-fiber bond structure gives the strength of the load bearing microfibers and damage is initiated through separation of the individual microfiber bundles through the failure of the inter-fiber bond and thence fracture [33]. The transverse section of the fabric is characterized by air cavities and microfibers surrounded by plant material, (Figure 3.12b). The air cavities are responsible for the thermal insulation and sound absorption properties of the fabric [130,131].

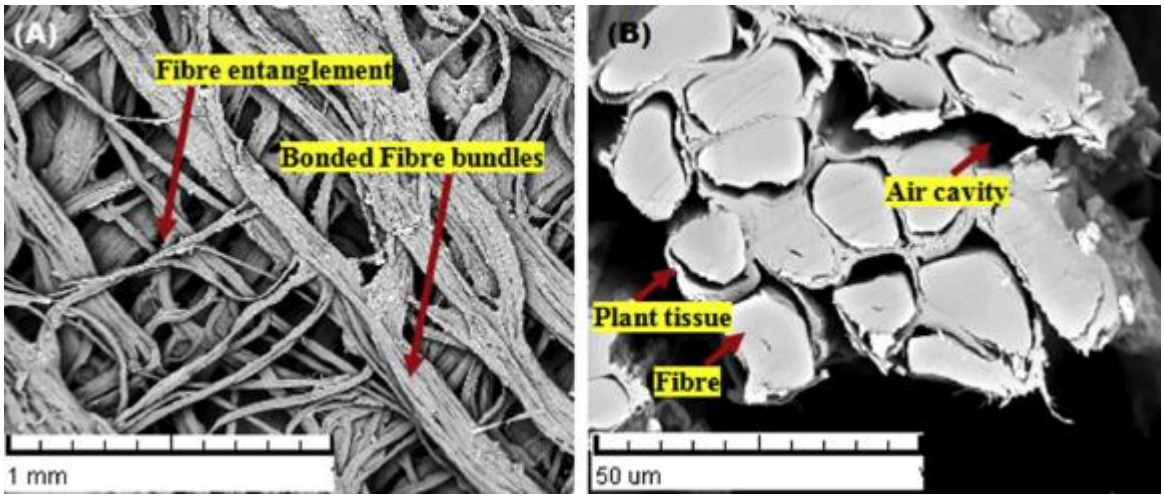

Figure 3.12. Barkcloth morphology

3.1.3. Fiber Orientation Distribution in Barkcloth

Image processing techniques are used in the microstructure investigation of nonwoven fabrics so as to understand fiber orientation distribution and fiber diameter. The Fourier Transform (FT), Hough Transform (HT) and Direct Tracking are the methods used in the estimation of the fiber orientation distribution in nonwoven materials[132]. Unlike other methods, the HT method obtains the fiber distribution in the nonwoven directly and the actual orientation of the straight lines is plotted on the image with minimal computational power.

Using a digital camera image as shown in Figure 3.13 it's observed that the bonded barkcloth microfiber bundles are nearly aligned at an angle of $\pm 45^{o}$ to the horizontal. These fiber bundles are held together through fiber entanglement. That notwithstanding, a robust technique utilizing the HT was further used to investigate the microfiber bundle orientation distribution (Figure 3.14). The matlab HT codes utilized are shown in the *Appendix A* of this thesis. While using the HT, the image magnification affects the results obtained, elsewhere Ghassemieh [128] showed that a magnification of 30X and 50X produced the best

representative image of the nonwoven; consequently, the results were favorable compared to higher magnifications.

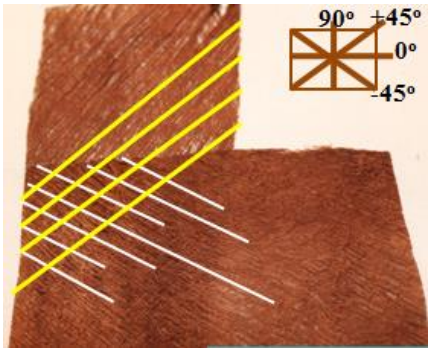

Figure 3.13. The backcloth ply representation.

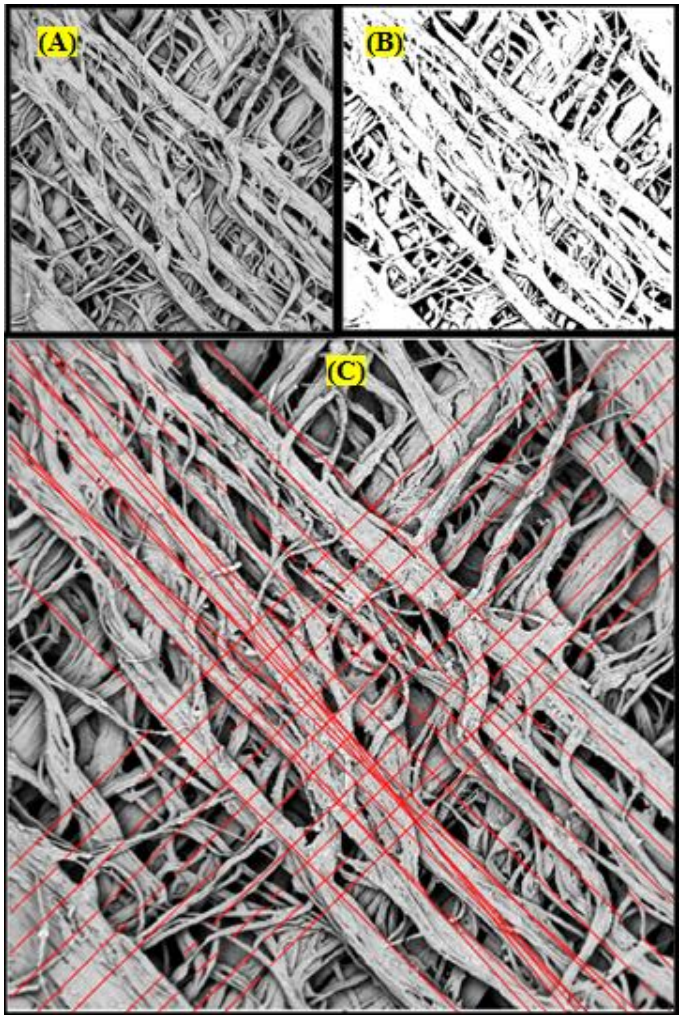

Figure 3.14. Image Processing: Scanning Electron Microscope image at 50X magnification (A); Binarized image (B); Hough Transform Lines showing Fiber Orientation in the image (C)

The 50X SEM image magnification was therefore utilized for image processing in matlab (Figure 3.14A). In order for the HT to function optimally, the image is binarized (Figure 3.14B); therefore the HT algorithm identifies points in the image which fall on to the straight lines. The lines are thereafter plotted on the original image. Figure 3.14C shows the orientation of the most microfiber bundles in the barkcloth. The application of the HT further justifies the barkcloth microfiber bundle orientation of ±45°

3.2. BARKCLOTH MATERIAL PROPERTIES

Table 3.2. Overview of Barkcloth Material Properties

Property	Unit	Value
Physical and Mechanical Properties		
Areal Weight (Alkali Treated)	g/m^2	142
Areal Weight (Untreated)	g/m^2	327
Average Thickness	mm	1.12
Fabric Strength		
Microfiber bundle Direction (Figure 3.15)	N	101.7
Transverse	N	23.5
Chemical Composition		
α-Cellulose	%	68.69
Hemicellulose	%	15.07
Lignin	%	15.24
Thermo-physiological properties		
Thermal conductivity coefficient	W/m.K	0.0357
Thermal absorptivity	$Ws^{1/2}/m^2K$	0.197
Thermal Resistance	m^2K/W	81.4
Thermal Diffusivity	m^2s^{-1}	0.034
Peak heat flow density	$[Wm^2]\ x10^{-3}$	0.234
Relative Water Vapor Permeability	%	66
Evaporation resistance	$Pa.m^2$	4.4

The mean fabric thickness was computed as 1.084mm from ten samples of readings at different positions of the fabric. The mean strength of the fabric was 101.7N and 23.5N in the direction of the most microfiber bundle arrangement and transverse section respectively. Since barkcloth microfiber bundles are aligned at angles as shown in Figure 3.13 and Figure 3.14, the fabric samples were cut in such a way that the tests are applied in the longitudinal (microfiber bundles direction) and transverse directions (perpendicular) as shown in Figure 3.15.

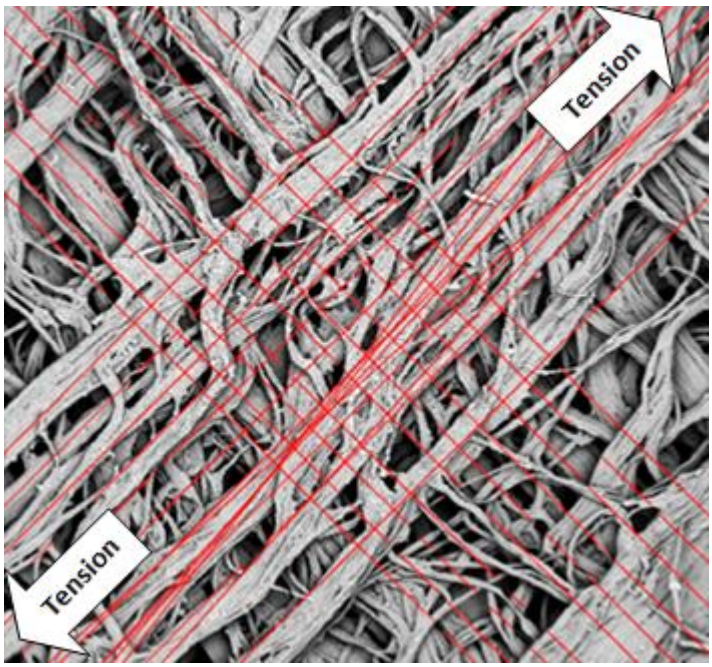

Figure 3.15. Representation of fabric strength tests with respect to microfiber bundle direction

The barkcloth microstructure chemical analysis showed that the fabric is majorly made up cellulose. Alpha cellulose is the type of cellulose found in wood. Since barkcloth is extracted from the bark of a tree, the cellulose microfibers are responsible for the strength of the fabric (Table 3.2). In comparison to other naturally occurring fabrics such as that from *Manicaria saccifera* palm [133], the chemical microstructure analysis showed that barkcloth had a low hemicelluloses and lignin content.

Thermal conductivity is the amount of heat, transmitted through a unit area of material having the unit thickness within a second due to a unit temperature gradient. Metals have the highest thermal conductivity, whereas polymers have low thermal conductivity ranging from 0.2 to 0.4W/m.K; textile structures, 0.033- 0.01W/m.K; steady air at 20°C is 0.026 W/m.K. Thermal conductivity of water is 0.6W/m.K, which is 25times more than that of air, therefore, presence of water in textile materials is uncomfortable. The thermal conductivity of barkcloth was 0.0357 W/m.K. This low level of thermal conductivity is attributed to the fabric structure being a natural nonwoven material with some pores

arising from the fabric handling and rigorous manual production processes; the high porosity is a haven for entrapped air leading to a low thermal conductivity of the fabric thereby having a positive effect on the sound absorption properties.

Thermal absorptivity is the phenomenon that characterizes thermal feeling (heat flow level) during short contact of human skin with the fabric surface. Provided that the time of heat contact, t, between the human skin and the textile is shorter than several seconds, the measured fabric can be simplified into the semi-infinite homogeneous mass with certain thermal capacity ρc [J/m^3] and initial temperature t_2. Unsteady temperature field between the human skin (with constant temperature t_1) and fabric with respect to boundary conditions offers a relationship, which enables us to determine the heat flow q [W/m^2] through the fabric:

$$\boldsymbol{q} = \frac{\boldsymbol{\alpha}\,(\boldsymbol{t_1} - \boldsymbol{t_2})}{(\boldsymbol{\pi t})^{1/2}} \tag{29}$$

$$\boldsymbol{b} = (\boldsymbol{k\rho c})^{1/2} \tag{30}$$

where ρc [J/m^3] is the thermal capacity of the fabric and the term α represents thermal absorptivity of fabrics. The higher the thermal absorptivity of the fabric, the cooler is its feeling upon contact with the skin. In textile applications, thermal absorptivity ranges from 20Ws$^{1/2}$/m^{2}K for fine nonwoven webs to 600 Ws$^{1/2}$/m^{2}K for heavy wet fabrics. Barkcloth had a thermal absorptivity of 81.4 Ws$^{1/2}$/m^{2}K which was lower than the values of reported elsewhere for cotton by Demiryurek [134]; Oglakcioglu [135] and Chidambaram [136]. This gives a warm feel of barkcloth fabric when in contact with the skin.

Thermal resistance is the measure of a material's resistance to the flow of heat. It depends on the fabric thickness h and thermal conductivity,k: $\boldsymbol{R} = \boldsymbol{h/k}$ Therefore the fabric thickness influences the thermal resistance. In sharp contrast, barkcloth thermal resistance of 0.034 m^{2}K/W was attributed to the thickness of the samples compared to lower values registered by cotton fabrics. From the experiments conducted the inverse proportional relationship of thermal resistance and thermal conductivity was fulfilled.

Thermal Diffusivity is the measure of the rate at which thermal heat is transferred. Materials with higher thermal diffusivity quickly adjust their base temperature to that of the surroundings. Barkcloth thermal diffusivity was recorded as 0.197x10^{-6} m^{2}s^{-1} slightly higher than the values of cotton single jersey knitted fabrics.

The relative water vapor permeability is the measure of the ability of the material to transfer moisture from the body to the surroundings. Water vapor permeability is an important clothing comfort term because a fabric should be able to serve the double function of transferring internal moisture which may be sweat to the surface and also aide its evaporation to the surroundings. This process can occur through capillary motions of moisture through the fabric fibers or through the pores of the fabric. At higher levels of sweating, the sweat wets the fabric and mass transfer can occur from the previous processes described. The average water vapor permeability of barkcloth was 66% however the measured values were in the range of 60 – 75%. The higher values of water vapor permeability are due to porosity and the nature of barkcloth.

3.3. GREEN EPOXY

Green epoxy CHS-Epoxy G520 is a low molecular weight basic liquid epoxy resin containing no modifiers, certified by International Environmental Product Declaration Consortium (IEC). The green epoxy utilized for the production of biocomposites had not been characterized before, therefore it's behavior was investigated in this section.

3.3.1. Curing behaviour of the bio-epoxy

The curing behaviour curve of the bio-epoxy resin was obtained from DSC and is shown in Figure 3.16. The selected temperature for the curing process of barkcloth biocomposites was 120ºC which is near the temperature peak of the curing curve.

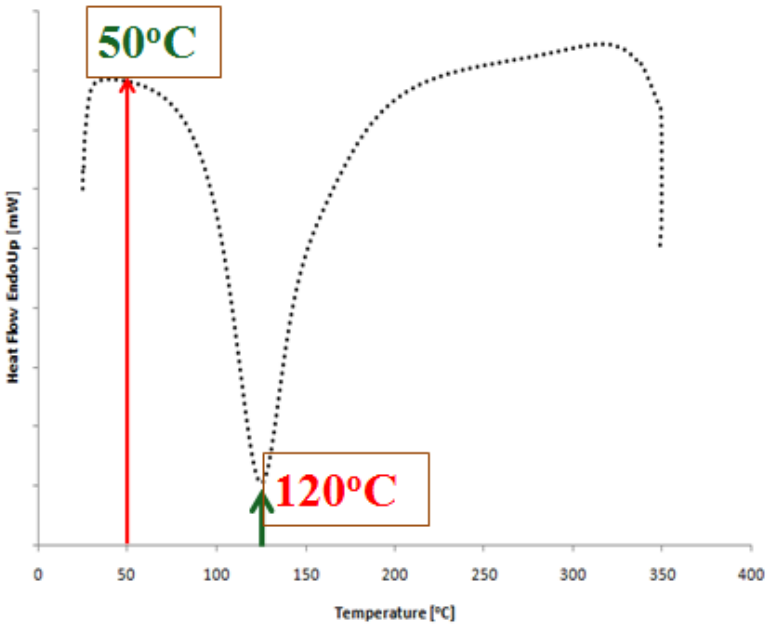

Figure 3.16. Green Epoxy Curing Behaviour

The curve shows only one exothermic peak, which was attributed to the cross-linking reaction between the green epoxy polymer and the hardener. The reaction starts at a temperature of approximately 55^{o}C and ends at about 200^{o}C.

The peak temperature of the curve indicates the maximum cross-linking temperature or fastness of the curing reaction that was obtained at 123^{o}C. For optimization of the curing of the resin, the oven temperature was therefore set at 120^{o}C and the samples baked for 45min. The selected temperature of 120^{o}C ensures maximum cross-linking within a short period of time less than an hour. The 45min was chosen based on the fact that from room temperature to the maximum cross-linking temperature obtained from the curing curve, the virgin resin-hardener mixture took 12 min, therefore introduction of the reinforcing fabric means that baking from 30 to 45 min is sufficient for efficient bond formation and cure of the resin. The exothermic peak at 123^{o}C, released heat of 373 J/g which is higher than the petroleum based epoxy resins exothermicity of 200J/g. This implies that the curing of renewable green epoxy is higher than that of petroleum based epoxy resins at room temperature [137,138].

CHAPTER 4

DESIGN OF COMPOSITES

4.0. PROLOGUE

This chapter is aimed at introducing the steps taken in designing of the Barkcloth Fabric Reinforced Epoxy Laminar Composites (BFRP). The theories and assumptions which dictated the design phase are presented such that the reader is well versed with the topic at hand.

4.1. COMPOSITE MATERIALS DESIGN FUNDAMENTALS

4.1.1. Design Criteria

Design of a structure or component is aimed at avoiding failure of the component during its service life. Currently, the design of fiber reinforced plastic composites uses the same design criteria for metals. In this investigation, since the envisaged barkcloth composites were for interior automotive applications, the designed barkcloth laminar composites must sustain the design ultimate load in static testing [139]. Design Load of Interior automotive components should be >25MPa [140].

4.1.2. Design Allowables

Design allowable properties of laminar composites are based on testing the laminates or using laminate analysis. The latter is utilized for composites obtained for glass and carbon fiber because the material properties do not vary to a larger degree compared to natural fiber composites. Therefore in this investigation, the former i.e. static and dynamic mechanical testing was chosen as a route in this investigation.

4.2. GENERAL DESIGN FUNDAMENTALS

Mallick [139] showed three principal steps followed in designing a composite laminate:

1. Selection of composite material properties (Fiber, Resin and Volume fraction).
2. Selection of the optimum fiber orientation in each ply and the overall stacking sequence of the composite.
3. Selection of the number of plies needed in each orientation and this also determines the thickness of the composite.

4.2.1. Material Selection

Natural nonwoven barkcloth fabrics were utilized in the study. Untreated and surface modified fabrics were utilized for the production of the composites. It was showed in Chapter 4 that the *Ficus natalensis* barkcloth's microfibers bundles are aligned majorly aligned at an angle of ±45° (Figure 3.13 and 3.14); it's this angle that was used as the reference angle so as to come up with the laminar layering sequence for the barkcloth laminar epoxy composites (BFRP).

4.2.2. Fiber-Matrix interface

In order to tailor the fiber-to-matrix interface, surface modification of the fibers was performed. The fabric's surface was treated with the enzyme and plasma for synthetic epoxy composites whereas alkali treatment was preferred for the green composites.

4.2.3. Types of fibers and the reason for the fabric ply arrangement

Layering Sequence I

Figure 4.10 below shows the stacking sequence utilized for the fabrication of the Untreated, Enzyme and Plasma treated Barkcloth Fabric Reinforced Composites; consequently, the direction of the loading of the composites is herewith shown.

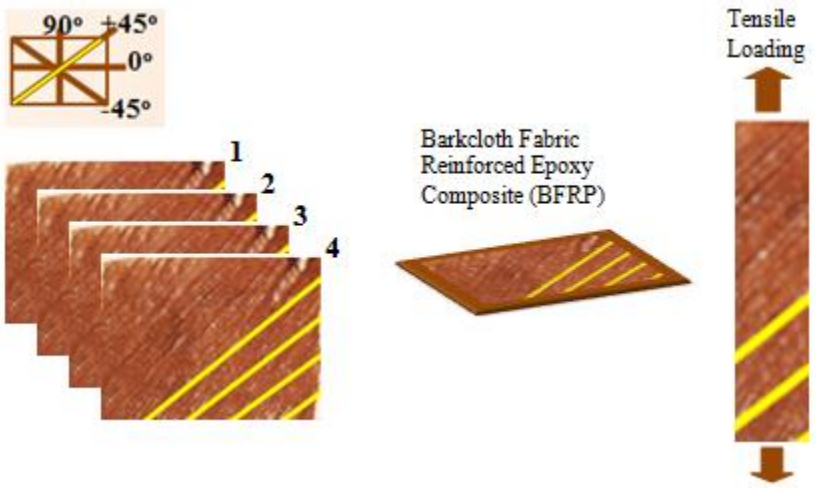

Figure 4.10. Composite Laminate layering sequence I

Layering Sequence II

A second set with advanced hierarchal architecture as shown below was investigated in order to understand if at all the ply angle arrangement has an effect on the thermo-mechanical properties.

Layering Sequence

Composites	Ply arrangement [°]
BFRP I	-45, 45, 0, 90
BFRP II	45, -45, 90, 0
BFRP III	0, 90, 45, -45
BFRP IV	90, 0, -45, 45

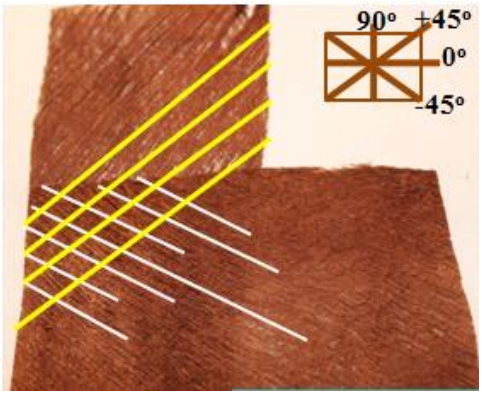

Figure 4.11. Barkcloth Fabric Reinforced Composite (BFRP) Laminate layering sequence

The green epoxy composites (Biocomposites) were fabricated utilizing this layering sequence as well as synthetic epoxy composites with notation BFRP I-IV. Optimization of the fiber properties was achieved through varying the fiber angles through the hierarchal architecture of the barkcloth layers. The layering pattern of the barkcloth fabrics used for the purpose of the study of the effect of layering pattern is shown in Figure 4.11.

A proper selection of laminar stacking sequence eliminates the deleterious free edge effects in a laminar and therefore alternations of +θ and –θ plies should be done so as to achieve positive results. When the stress state in the structure is unknown, a common approach in laminate design is to make it quasi-isotropic and using the layers to determine the total thickness of the laminate [139].

4.2.4. Reinforcement Volume Fraction

The composites produced with VARTM maintained a 40% fiber volume fraction (v_f) whereas the hand lay-up composites reached a volume fraction between 14-18%. The variation of the volume fraction of the composites and laminate thickness is shown in *Appendix B* of this thesis.

Information about the volume fractions of composite components were used for prediction of especially the thermal conductivity of designed composites, as shown in *Appendix C*.

4.2.5. Number of Layers (plies) and thickness

As shown above, in this investigation since the overall loading of the envisaged composites in automotive interior panels should have a minimum of 25MPa, a quasi-isotropic laminate design process was utilized (Figure 4.1). Four barkcloth layers were selected so as to achieve a thickness in the range of 2-4mm which is the range of thickness of most interior automotive components. The green composites (biocomposites) utilized only one layering sequence (BFRP IV) reason being that after the investigation

of the effect of the stacking sequence on the mechanical properties, BFRP IV and BFRP II emerged as the best fabric layering sequence obtained.

4.2.6. Types of Matrix

Two sets of matrices were utilized, synthetic and green epoxy matrices. The synthetic epoxy polymer was utilized with untreated, enzyme and plasma treated composites and also composites investigating the effect of layering/stacking sequence.

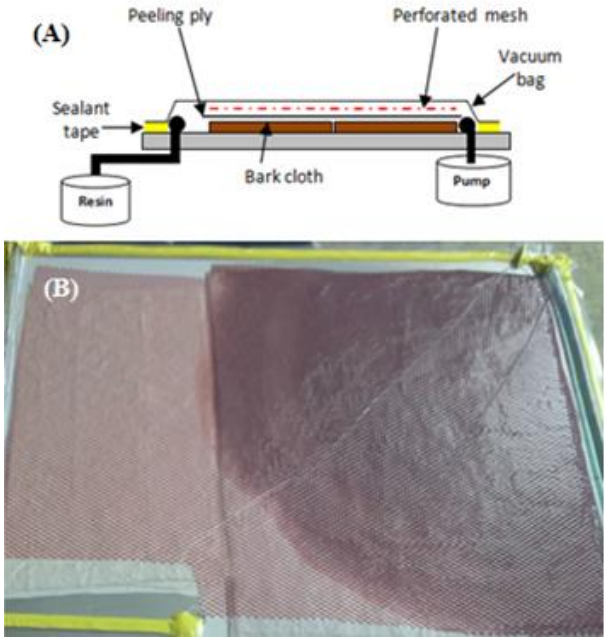

Figure 4.12. Experimental set up of Vacuum Assisted Resign Transfer Molding (VARTM)

4.2.7. Manufacturing Process

Synthetic Epoxy Composite

Vacuum Assisted Resin Transfer Molding (VARTM) was used to prepare the composites (Figure 4.12). The resin to hardener ratio was 100:40 as per the manufacturer's specifications. VARTM ensured that the composites produced had a 40% fiber volume fraction. Four barkcloth plies were used for the composite sample preparation for each set of composites. Synthetic epoxy was utilized for the production of Barkcloth Reinforced Plastic Composite (BFRP). After the resin infusion, the composite was left to cure at room temperature for 72 hours.

Green Epoxy Composite

The biocomposite specimens were prepared using the hand lay-up method due to the fact that the viscosity of the green epoxy polymer was high. The mould was treated with a mould release agent and thereafter Teflon sheets were applied to aid the fast removal of cured composite specimens.

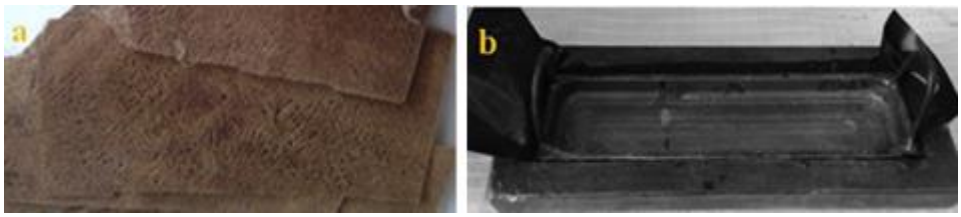

Figure 4.13. Biocomposites processing: (a) Barkcloth fabrics. (b) Fabricated composite mould.

Alkali treated barkcloth fabrics (Figure 4.12a) were impregnated with green epoxy resin and placed in the fabricated mould (Figure 4.12b). The resin to hardener ratio was maintained at 100:32 as per the manufacturer's specifications. Curing of the composites was done using a hot air oven for 45 min. For each set of composites, four barkcloth plies with ply angles 90^{o}, 0^{o}, 45^{o}, 45^{o} were utilized for biopolymer reinforcement.

CHAPTER 5

EXPERIMENTAL

5.0. PROLOGUE

The methods used to characterize the materials are herewith presented putting particular emphasis on the produced samples characterization methods.

5.1. CHARACTERIZATION AND MEASUREMENTS

5.1.1 Fabric thickness

The fabric thickness was obtained using Uni Thickness Meter. The measurement was done at different positions, the probe with a disc delivers a pressure of 1kPa over an area of 25cm^2 for 30s, then the thickness is obtained in mm. Ten readings were obtained and an average statistically computed.

5.1.2. Morphology

The surface morphologies of the fabric and composite fracture surfaces were investigated using a TS5130 Vega-Tescan Scanning Electron Microscope with accelerating voltage of 20kV. The samples (fabrics, fractured composites) were sputter coated with gold so as to increase the surface conductivity.

5.1.3. Surface functional groups

The Nicolet iN10 MX Scanning FTIR Microscope was used for the investigation of the surface functional groups of the barkcloth and epoxy composite samples. The infrared absorbance spectrum of each sample was obtained in the range of 4000-700cm^{-1}.

Further analysis using the X'Pert^3 X-ray powder diffractometer (PANalytical, USA) with Cu-Ka radiation (1.54056˚A) was used in obtaining diffraction patterns for alkali treated and untreated barkcloth. A Circular cut sample was directly mounted on the sample holder and analyzed from 8 to 70^o with 0.017^o incremental step.

5.1.4. Thermal behaviour

Thermogravimetric analysis of fiber samples weighing approximately 7-8mg was carried out using a Mettler Toledo TGA/SDTA851^e under a dynamic nitrogen atmosphere heating from room temperature (25^{o}C) to 500^{o}C at a heating rate of 10^{o}C/min. The Perkin Elmer Differential Scanning Calorimeter DSC6 was used. Samples weighing approximately 10mg were placed in aluminum pans and sealed. The specimens were heated in an inert nitrogen atmosphere from room temperature (25^{o}C) to 450^{o}C at a heating rate of 10^{o}C/min.

5.1.5. Mechanical properties

The fabric strength was quantified through measurements of samples for the bursting strength of the non-woven felt. Samples measuring 5cm by 15cm were tested using a Larbotech fabric tensile testing machine at room temperature.

Tensile properties of barkcloth reinforced epoxy composite samples with dimensions 150x25x2.5mm (Figure 5.1) were characterized in accordance with ASTM D3039. Tensile tests were carried out using a Testometric (M500-25kN) universal mechanical testing machine operating at a crosshead speed of 4mm/min until fracture. Four specimens with tabs were tested to obtain average tensile properties of the composite. The flexural test was conducted as per ASTM D790 using a Tiratest 2300 universal testing apparatus. The samples were tested using three point bending with a recommended speed of testing of 2mm/min. The span length to thickness ratio was 32:1.

The flexure strength was calculated using the formula:

$$f_s = \frac{3PL}{2bd^2} \tag{31}$$

Where P = Load at failure, L = Span length, b = Specimen width, d = Sample thickness.

Figure 5.1. BFRPs samples

5.1.6. Dynamic Mechanical Analysis (DMA)

The dynamic mechanical properties were analyzed using a DMA 40XT machine. The samples with dimensions 56x13x2.5mm were tested using three point bending mode at a frequency of 1Hz from room temperature to 150ºC at a heating rate of 3ºC/min.

5.1.7. Fabric Surface Modification

Alkali

Barkcloth fabrics were subjected to alkali treatment of 5% NaOH solution. The barkcloth fabrics were soaked in an alkaline solution at room temperature for one hour thereafter thoroughly cleaned using distilled water to remove the alkali together with other impurities and then dried in an oven at 80^{o}C.

Enzymes

DLG enzyme was used together with BFE to form a mixture. The enzyme solution and fabric weight ratio was all throughout maintained at 1:30. 0.3g of DLG and 0.6g of BFE were were added in 900ml of distilled water. 0.2g/l of Texawet DAF which is an anti-foaming agent was added and the mixture was conditioned at 55oC ensuring a neutral pH for 90 minutes. Another bath was prepared using BFE enzyme with the same bath ratio above of 1:30. 0.6g of the enzyme was mixed with the anti foaming agent and the bath maintained at 55oC with for 90 minutes. An alkali was added so as to set the pH of 9. Caution was taken such that both enzymes are not heated with a direct heat source.

Plasma

Bark cloth fabrics were treated with Dielectric Barrier Discharge (DBD) plasma using a laboratory device (Universal Plasma Reactor, model FB-460, Class 2.5 from Czech Republic). The sample fabrics were placed in the reactor for the duration of 30s and 60s respectively at power of 150W.

Figure 5.11. Universal plasma reactor with barkcloth samples

5.1.8. Chemical Composition

The lignin, hallocellulose, cellulose and hemicelluloses content was obtained by the method described by Bledzki et al., 2008 [141].

Lignin content

2g grams of the chopped barkcloth sample were placed in a beaker and 15 ml of 72% sulfuric acid was added. The mixture was agitated at 100rpm using a magnetic stirrer for two and half hours at 25°C. 200 ml of distilled water was added to the mixture, then the mixture was boiled for two hours and left to cool for 24 hours. After 24 hours, the mixture containing lignin was filtered and washed with hot water until the pH was neutral. The collected lignin was dried in the crucible at 105°C and cooled down. The lignin residue was weighed until constant weight was obtained.

Hallocellulose content

3g of chopped barkcloth sample were placed in a beaker, and then 160ml of distilled water, 0.5ml of glacial acetic acid and 1.5g of sodium chloride were added. The mixture was agitated and maintained at 75^{o}C for an hour. Additional 0.5ml of glacial acetic acid and 1.5g of sodium chloride was added repeatedly after each passing hour for two hours. The mixture was cooled in an ice bath; the hallocellulose was filtered and washed with acetone, ethanol and water respectively. The same was then dried in the oven set at 105^{o}C and weighed until constant weight was obtained.

α-cellulose content

2g of holocellulose were placed in a beaker and 10 ml of 17.5% solution of sodium hydroxide was added. The barkcloth fabric samples were magnetically stirred so as to be bathed in the alkaline solution. After every five minutes, 10ml of sodium hydroxide was added up to 30minutes. The mixture was kept at 20^{o}C, then 33ml of distilled water was added and the mixture was kept for an hour. The hallocellulose residue was with 100ml of 8.3% solution of sodium hydroxide, 200ml of distilled water, and 15ml of 10% acetic acid and washed again with water. The residue was transferred to a crucible and dried at 105^{o}C until constant weight was obtained.

Hemicellulose content

The content of hemicelluloses of barkcloth was calculated shown below:

$$\text{Hemicellulose} = \text{Hallocellulose} - \alpha\text{-cellulose} \quad (32)$$

5.1.9. Thermo-physiological properties

The thermo-physiological properties were evaluated using ISO 11092 (EN 31092) standard with laboratory room temperature at 24°C and at a relative humidity of 40%. The Alambeta instrument [142] was used to measure the thermal conductivity, thermal diffusivity, thermal absorptivity, thermal

resistance, sample thickness and peak heat flow density. The principle of operation of Alambeta applies a heat flow sensor attached to a metal block with constant temperature which differs from the sample temperature. When the measurement starts, the measuring head with the heat flow sensor drops down and touches the sample placed on the instrument base directly under the measuring head. A photoelectric sensor is used to measure the sample thickness. In order to simulate the real conditions of warm–cool feeling evaluation, the instrument measuring head is heated to 32°C which corresponds to the average human skin temperature, while the fabric is kept at the room temperature.

The samples used an area density of 123g/m^2. The through plane thermal conductivity of the composites was investigated using the Alambeta device. The Permetest instrument [142] was used to measure the relative water vapor permeability and evaporation resistance. Measuring head of the device is covered by a resistant semi-permeable foil, which avoids wetting the sample.

Alambeta thermal conductivity measuring device also measures thermal conductivity of laminar composite specimens up to 8mm. The composites (Figure 5.12) were grinded using sandpaper so as to achieve a uniform smooth surface for thermal conductivity tests. Chemical silicon paste was used to condition the samples such that it aides as both a lubricant to prevent damage to the device's measuring probes and also aide in the fastening of the device heating plate to the samples.

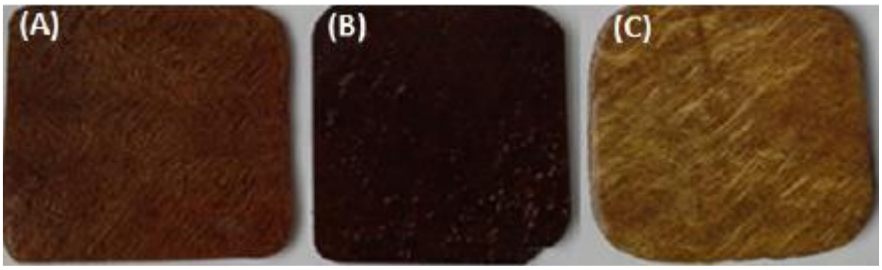

Figure 5.12. Thermal Conductivity Samples: (A) *Ficus brachypoda*; (B) *Ficus natalensis* and (C) *Antiaris toxicaria*

5.1.10. Bio-epoxy resin characterization

The bio-epoxy resin curing behaviour was characterized by thermal analysis using the Perkin Elmer Differential Scanning Calorimeter DSC6. A small drop of resin: hardener (100:32 weight%) weighing approximately 7mg was placed in aluminium crucible and subjected to a heating rate of 10^{o}C/min from 25^{o}C to 400^{o}C.

5.1.11. Acoustic properties

The barkcloth and its composite acoustic properties were investigated using a type 4206 Brüel&Kjær impedance tube according to ISO10534-2 standard using two quarter-inch condenser microphones type 4187 (Figure 5.13). The principle of measurement works in such a way that the sound source is generated by a loudspeaker at the end of the impedance tube; the sound waves are transmitted to the surface of the material sample (Figure 2.41).

When a sound wave strikes the bark cloth materials, it would cause vibration of the particles causing friction, thereby generating heat, which is absorbed by the barkcloth and some sound energy is reflected and picked up by sensors. Barkcloth being a non-woven material, its ability to absorb sound is influenced by the fiber network that dissipates the sound energy and also absorbs the heat generated as the sound energy is being dissipated. The tube measures the physical sound absorption coefficient (the fraction of acoustic energy not reflected by the material surface), which is a quotient of acoustic energy absorbed by the material to the energy of the incident wave.

Species	Layers [mm]				Four layer samples [mm]	Composites samples [mm]
	1	2	3	4		
Antiaris toxicaria	1.07	1.25	0.98	1.33	4.63	2.50
Ficus brachypoda	1.33	1.12	1.23	1.38	5.06	2.12
Ficus natalensis	1.02	1.42	0.72	1.03	4.19	2.93

Figure 5.13. Sound Absorption Measurement procedure: (A) Brüel&Kjær impedance tube set up; (B) Sample of the barkcloth layers utilized.

The material samples had a diameter of 29 mm and were studied in the frequency range of 500–6400 Hz. The composite and multi-layer samples were cut to the above diameter according to the standard. Measurements were measured for composites, single layer, double layers, triple layers and finally quadruple layers. Since the fabricated BFRPs specimens had four plies, acoustic behaviour had to be

characterized for the respective barkcloth layers and their effects on sound absorption. Table 2.1 shows the thickness of the fabric non-woven felts used.

The airflow resistivity was measured utilizing the air resistance meter and the value of airflow resistivity was calculated utilizing the equation below:

$$\sigma = \frac{\Delta P}{\mathrm{Ud}} \tag{33}$$

Where ΔP is the set pressure difference between the surfaces; U is the air flow velocity and d is the thickness of the sample.

CHAPTER 6

Results and Discussion

6.1. MORPHOLOGY OF SURFACE MODIFIED BARKCLOTH

Treatment of barkcloth with commercial enzyme BFE led to ridges and grooves along the microfibers (Figure 6.1). DLG enzyme is a textile auxiliary agent, it catalyzes the decomposition of hemicelluloses and partially lignin in the binder layers of bast fibers. Whereas BFE catalyzes pectin layer decomposition, therefore it is the right enzyme for elementarization of natural fibers. The combination of DLG and BFE treatment led to change in mass of the substrates by 31% whereas BFE alone led to 30% change in mass of the substrates. The change in mass of the weighed substrates shows that the enzymes used dissolved a considerable amount of plant material in the form of waxes, pectins, and other impurities. Because the main function of BFE enzyme is to dissolve impurities, it is observed that its performance was better than DLG and the surfaces are fairly cleaner compared to DLG. The loss in weight of the substrates was more with the DLG enzyme, due to the fact that the nature of DLG affects cellulose, unlike BFE.

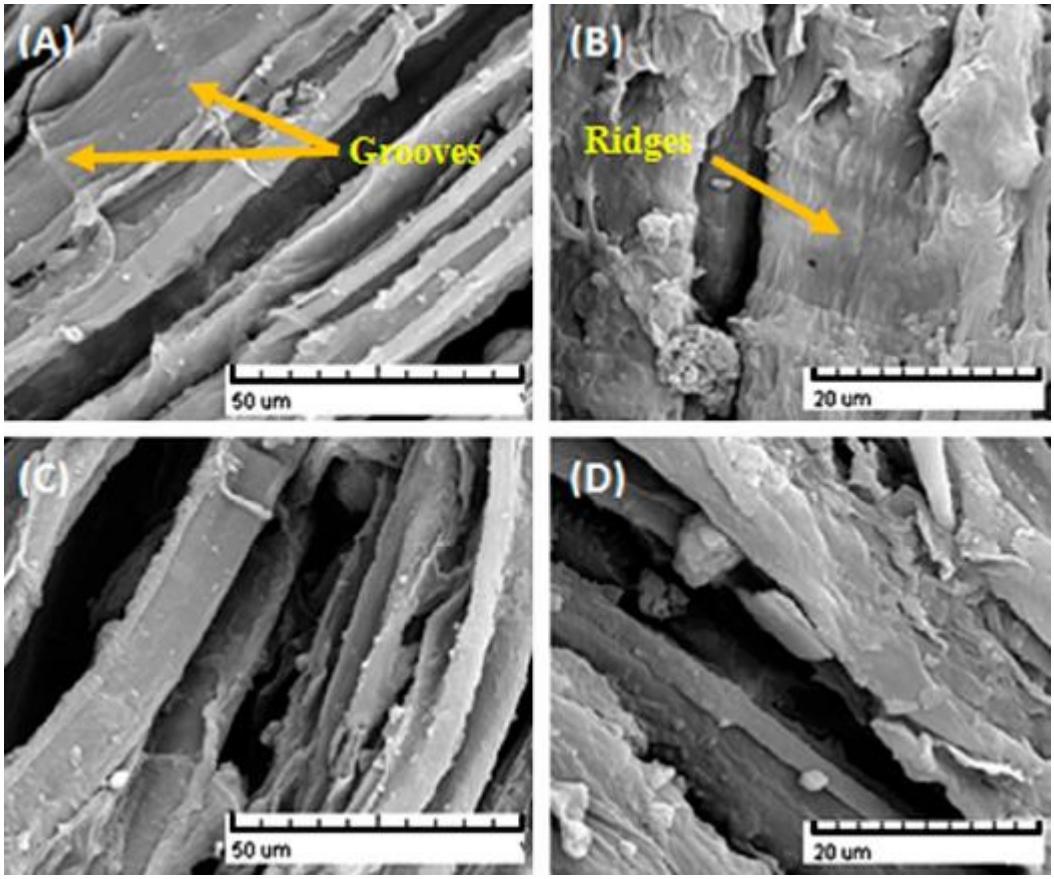

Figure 6.1. Enzyme-treated barkcloth: (A) and (B) BFE enzyme; (C) and (D) DLG enzyme.

Plasmas are used to modify lignocellulosic fibers, therefore, it aids in surface activation of the fiber network [143]. Barkcloth fabric is made up of cellulose; therefore, the only reactive functional group is the hydroxyl group. Treatment with atmospheric plasma leads to oxidation of the cellulose.

The morphology of oxygen plasma-treated fabrics is shown in Figure 6.11. In comparision to untreated fabrics (Figure 4.12), there was no striking visible difference on the surface. This was due to the fact that the treatment times were too short and the plasma generator device had no option of changing the power rating and the intensity of the plasma. The effect of plasma treated fabrics was observed when the fabrics were utilized in the production of the fiber reinforced composites as explained in the proceeding section on composites.

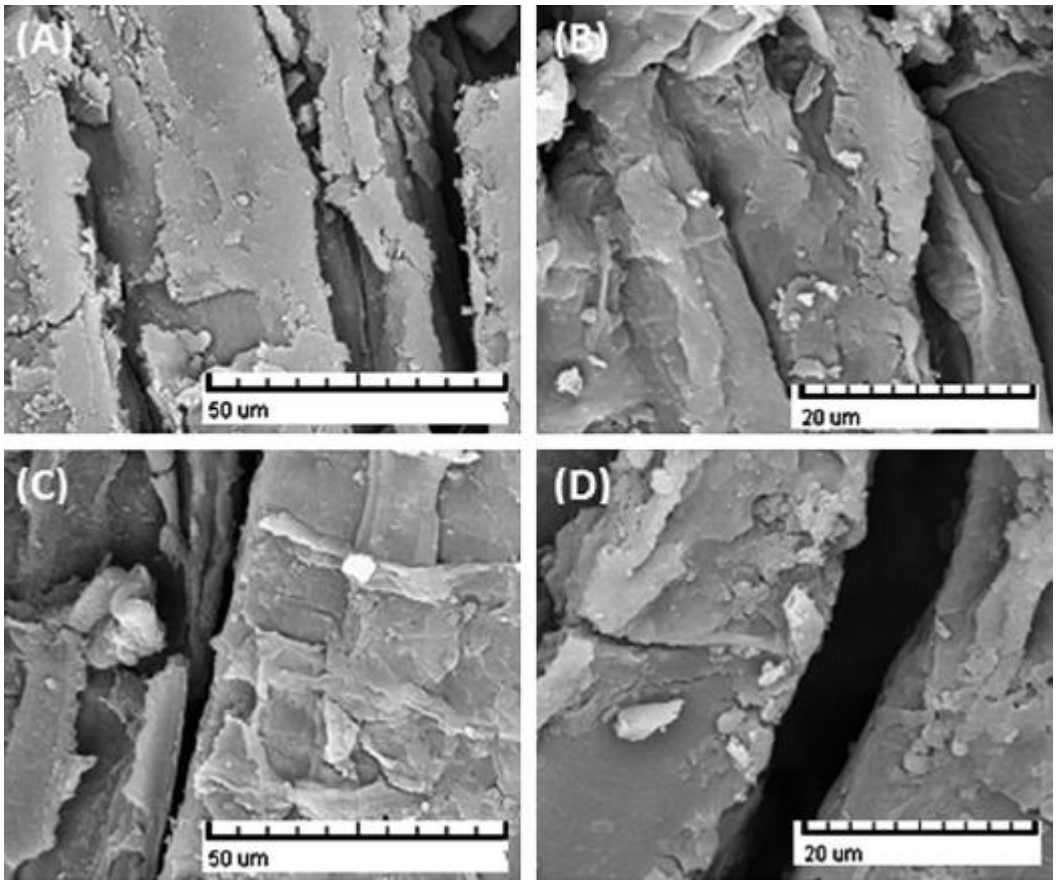

Figure 6.11. Plasma-treated barkcloth: (A) and (B) 30 s; (C) and (D) 60 s.

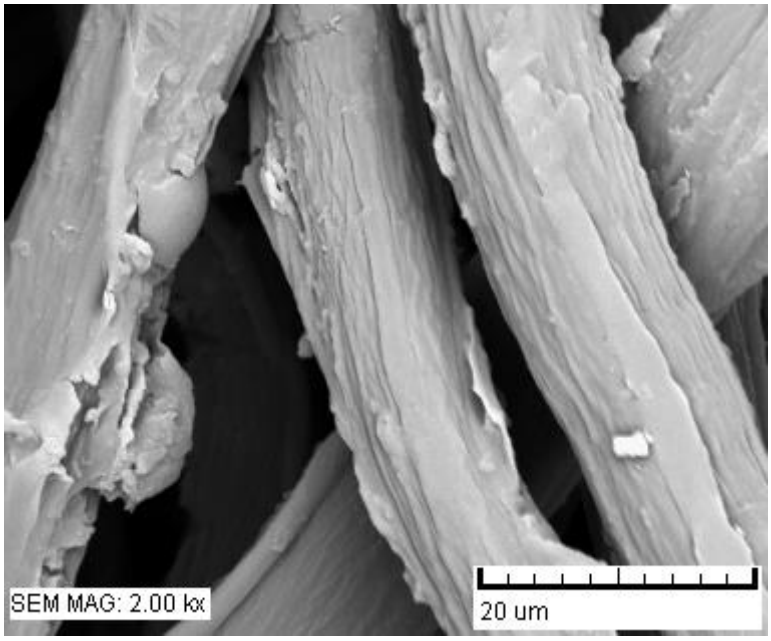

Figure 6.12. Alkali-treated (5wt% NaOH) barkcloth

Alkali treatment is one of the leading most common vegetable fiber surface modification methods. Treatment with alkali aids in the fiber to matrix adhesion and also helps to dissolve the lignin, wax and impurities. Figure 6.12 shows the morphology of alkali treated fabric. Elementarization of the barkcloth cellulose microfibers measuring 12-14µm was observed. The microfibers appear pronounced and cleaner due to the dissolving of plant impurities.

6.2. SURFACE FUNCTIONAL GROUPS OF BARKCLOTH

Functional groups assignments and their respective bonding interactions of barkcloth can be deduced using Fourier Transform Infrared Spectroscopy (Figure 6.13). Natural fibrous specific bands and their corresponding bonding interactions have been studied by numerous researchers [144–150].

6.2.1. Fourier Transfor Infra-red (FTIR)

6.2.1.1. Untreated Barkcloth

There's a variation in the reported bands from one researcher to another, however the difference is not too significant because most natural fibrous materials are made up of celluloses, hemicelluloses and lignin. A broad absorption band in the range of 3300 - 3500cm^{-1} is due to O-H stretching vibrations of cellulose and hemicelluloses. The band at 2900 -2940cm^{-1} corresponds to CH_2 and CH_3 stretching vibrations [149]. The band at 1740cm^{-1} is due to carbonyl groups (C=O) stretching and vibration of acetyl groups of hemicelluloses [149]. After this peak, the sudden leveling off shows that the hemicelluloses are removed from the fiber. The aromatic vibration of the benzene ring in lignin may be at 1615cm^{-1}.

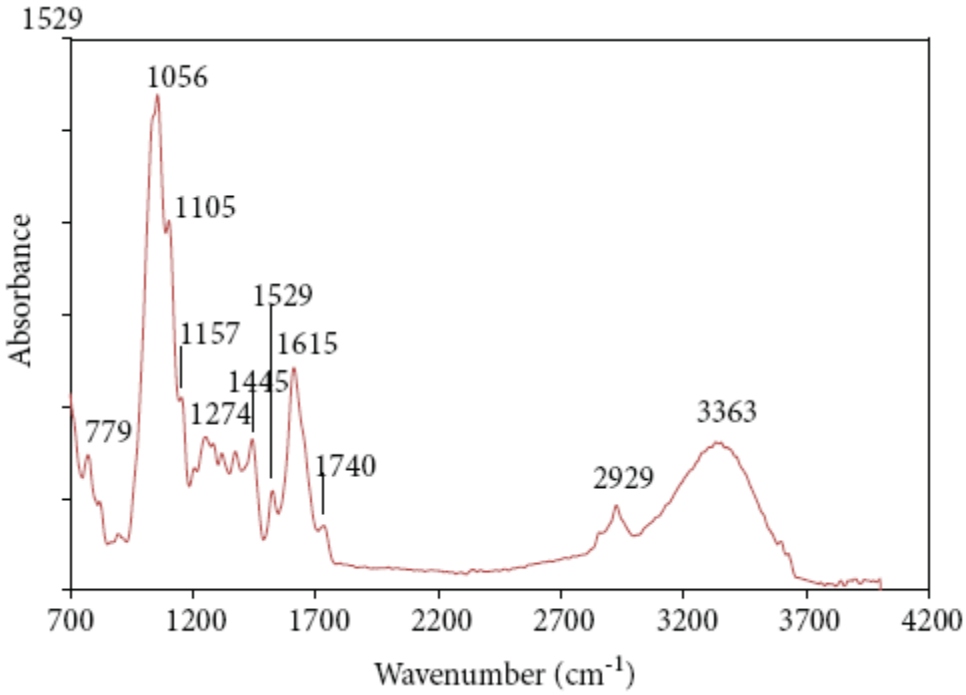

Figure 6.13. FTIR spectra of untreated barkcloth.

The absorption band at 1529cm^{-1} was owing to CH_2 bending in lignin whereas the peak at 1445cm^{-1} was due to O-H in-plane bending [147]. The peak at 1380cm^{-1} was assigned to CH symmetric bending. The band at 1274cm^{-1} may correspond to C-O stretching of acetyl group of lignin [149]. The band at 1157cm^{-1} may be due to C-O-C asymmetrical stretching in cellulose. The broad peak at 1056 cm−1 is due to –C–O–C– pyranose ring skeletal vibration [151]. The band at 779 cm−1 represents glycosidic –C–H deformation, with a ring vibration contribution and –O–H bending which are the characteristics of β-glycosidic linkages between the anhydroglucose units in cellulose [144,151].

6.2.1.2. Enzyme and Plasma Treated Barkcloth

Broad absorption bands at 3353cm^{-1}, 3403cm^{-1} are due to hydrogen bonding (O-H) stretching vibrations of cellulose and hemicelluloses (Figure 6.14 and 6.15). The BFE enzyme absorbance intensity at the above band was less than DLG enzyme meaning that more hemicelluloses were effectively dissolved by the enzymes. Plasma treatment excited the OH reactive bonds of cellulose, therefore, increasing the absorption peak intensity. The band at 2933cm^{-1}, 2938cm^{-1} corresponds to CH_2 and CH_3 stretching vibrations.

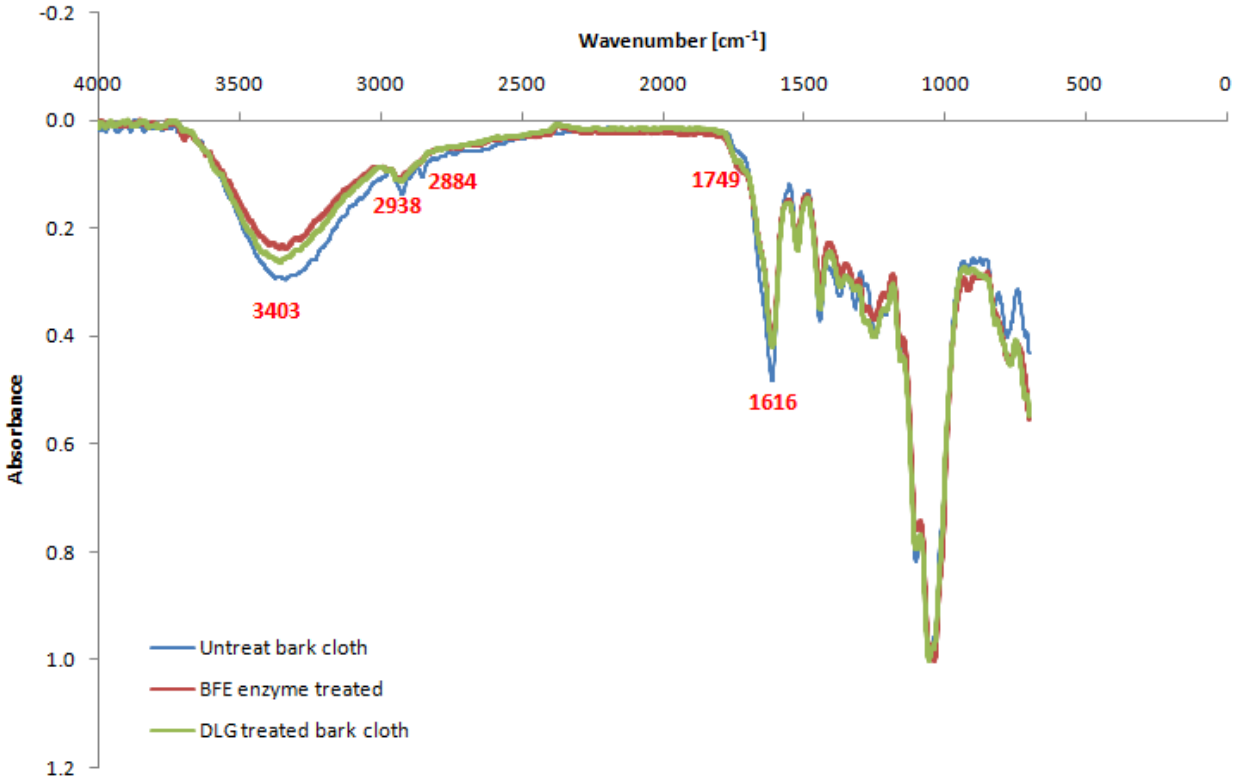

Figure 6.14. Enzyme treated barkcloth surface functional groups

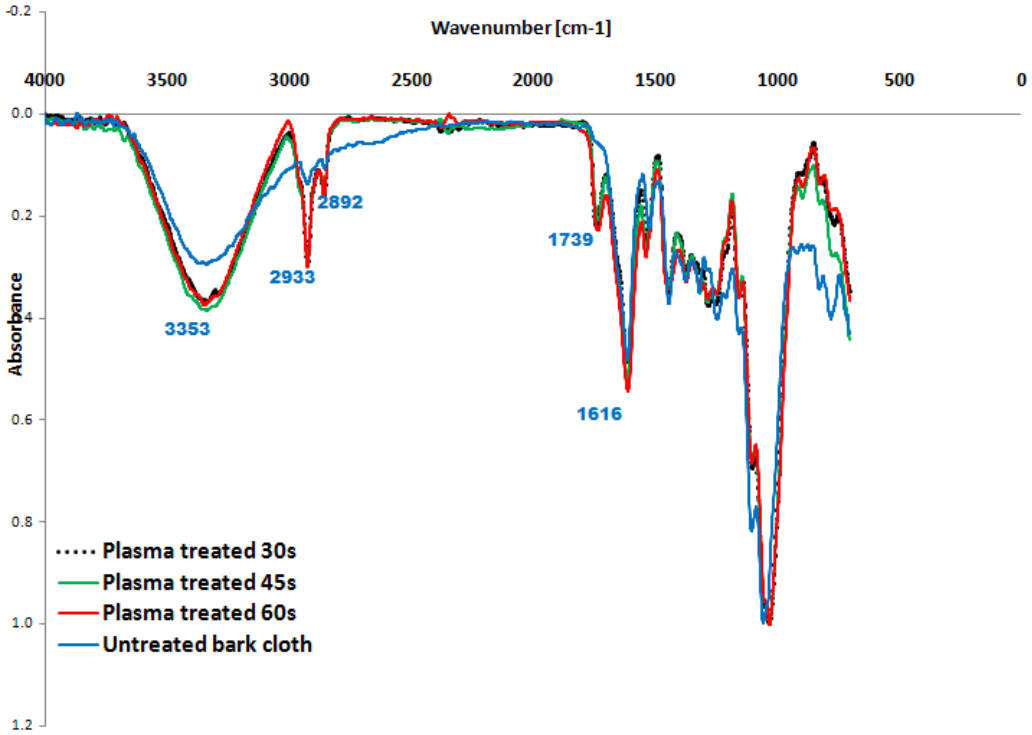

Figure 6.15. Plasma treated barkcloth surface functional groups

The decrease in the absorption band of enzyme treated fabrics is attributed to the lower content of hemicelluloses of the fabric structure which is further confirmed by the band at 1749cm^{-1} that is decreased and is due to carbonyl groups (C=O) stretching and vibration of acetyl groups of hemicelluloses. After this peak, the sudden leveling off shows that the hemicelluloses are removed from the fiber. The aromatic vibration of the benzene ring in lignin may be at 1615cm^{-1}. The absorption band at 1529cm^{-1} was owing to CH_2 bending in lignin.

6.2.1.3. Barkcloth Reinforced Composites

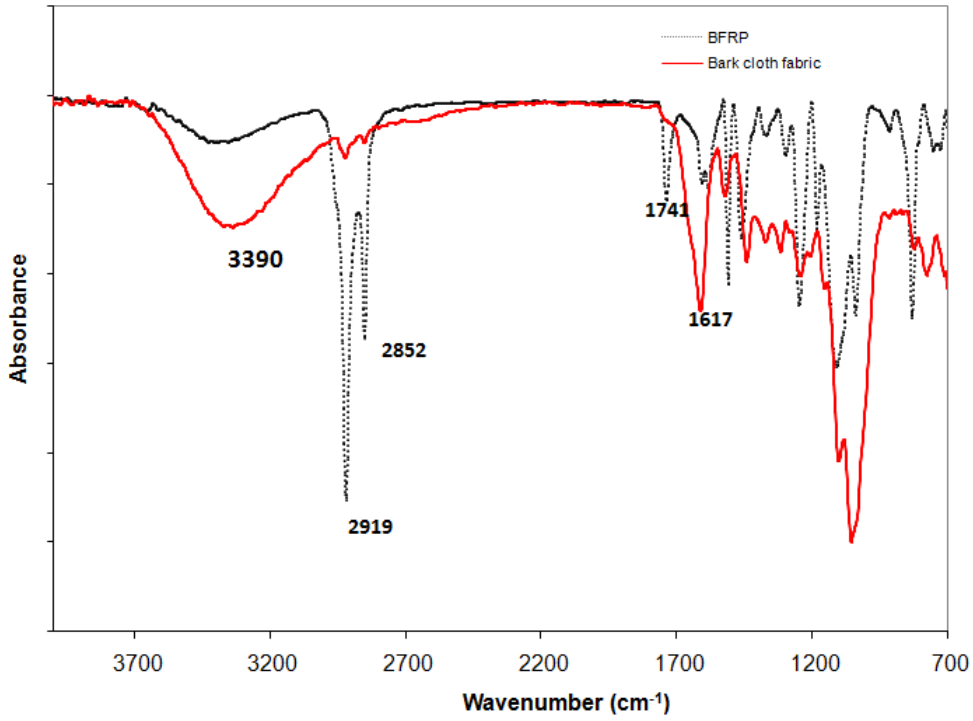

Figure 6.16. BFRPs surface functional groups

The peak at 3419cm^{-1} and 3390cm^{-1} is due to the hydroxyl (OH) stretching vibration of free and hydrogen bonded –OH groups of barkcloth fabric and epoxy respectively (Figure 6.16). The epoxy polymer peak at 3419cm^{-1} is shifted to the left which shows that for epoxy polymers, the peak shifts to the left when there's hydrogen bonding between the epoxy polymer and the reinforcing fibers [152]. The increase in the absorption peak of the composites above that of the fabric at 2919cm^{-1} and 2852cm^{-1} is due to the combination of the asymmetric and symmetric CH_2 and CH_3 of the synthetic epoxy resin. Still at the same bands, the CH and CH_2 groups of cellulose and hemicelluloses in the fabric are observed [153]. The increase in the absorbance band at 1741cm^{-1} of the epoxy polymer is attributed to the presence of carbonyl groups [154] whereas the peak at 1617cm^{-1} correspond to the vibration of the benzene ring in epoxy [152].

6.2.1.4. Alkaline Treated Barkcloth and Biocomposites

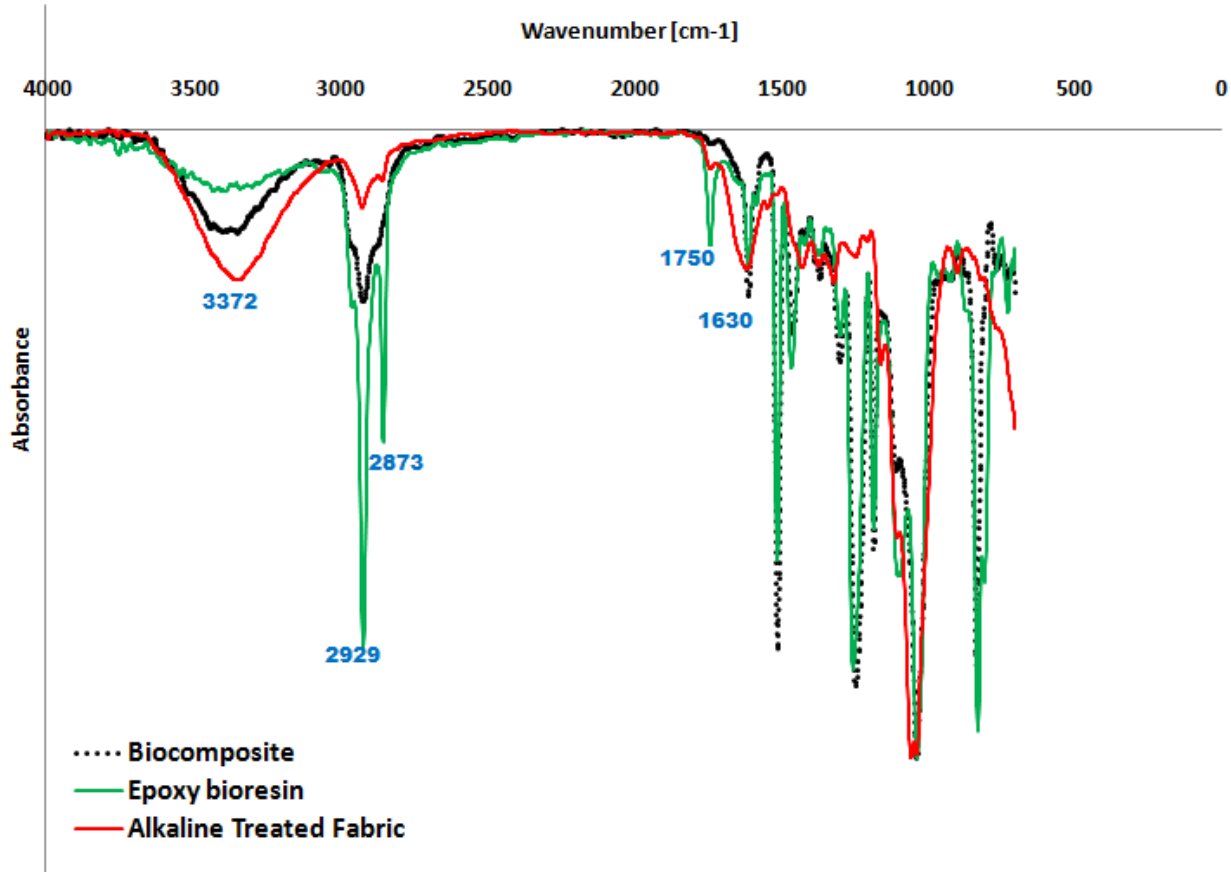

Figure 6.17. Barkcloth biocomposites surface functional groups

Figure 6.17 shows the FTIR of alkaline treated fabrics and corresponding composites. The broad peak at 3372cm^{-1} is attributed to OH-stretching vibration which gives information concerning the hydrogen bonds [149]. The treated fabric had a sharper peak at this intensity compared to the resin and biocomposite. The reduction in the absorbance peak of the biocomposite at 3372 cm^{-1} and 2900cm^{-1} show that the green epoxy polymer effectively cross-linked with the OH-cellulose chains which are activated through alkali treatment of the barkcloth fabric. The peaks at 2929 cm^{-1} and 2873 cm^{-1} correspond to symmetric and asymmetric stretching vibrations of CH and CH2 groups. The increase in the absorption peak of the biocomposites above that of the fabric is due to the combination of the CH and CH2 groups in the green epoxy polymer and the cellulose and hemicelluloses in the fabric [155]. The increase in the absorbance band at 1750 cm^{-1} of the green epoxy polymer is attributed to the presence of carbonyl groups while benzene ring stretching of Lignin is at 1630cm^{-1}.

Alkali treatment has been proven to remove hemicelluloses, lignin and other plant materials leaving a rough surface topography thus increasing fiber to matrix adhesion due to efficient wetting of the fibers and the rough texture positively influencing the bonding [146].

6.2.2. X-Ray Diffraction

Figure 6.18 shows the X-ray diffraction pattern of the barkcloth. Untreated and alkali barkcloth exhibits main 2θ diffraction peaks between 22.8º and 23.2º which correspond (002) crystallographic planes of cellulose I. The peak at 15.3º is due to 001 crystallographic plane of cellulose I.

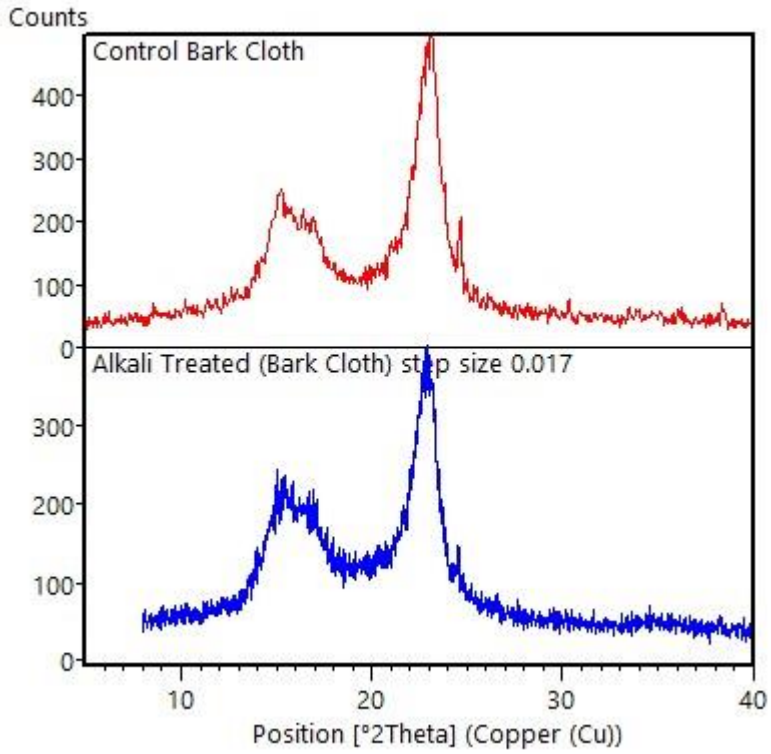

Figure 6.18. X-ray Diffraction of Treated and Untreated Barkcloth

The Segal crystalline index was calculated using the expression [156]

$$CI = \frac{H_{22.55} - H_{18.5}}{H_{22.55}} \quad (34)$$

Where $H_{22.55}$ is the height of the XRD peak at $2\theta = 22.55^{o}$ which is responsible for both amorphous and the crystalline fractions whereas the small peak at at $2\theta = 18.5^{o}$ correspons to the amorphous fraction. The calculated crystallinity index was 79% higher than sisal (71%), jute (71%), Sansevieria cylindria leaf fibers (60%) [28]. A higher value of CI shows that barkcloth crystallites are orderly in nature.

6.3. THERMAL BEHAVIOR OF BARKCLOTH

One of the drawbacks for natural fibers is their limited thermal stability. Therefore, a study of their thermal behavior is of utmost importance for material engineers. For natural fibers, the thermogravimetric behavior is directly proportional to the chemical constituents of the fibers [29,53].

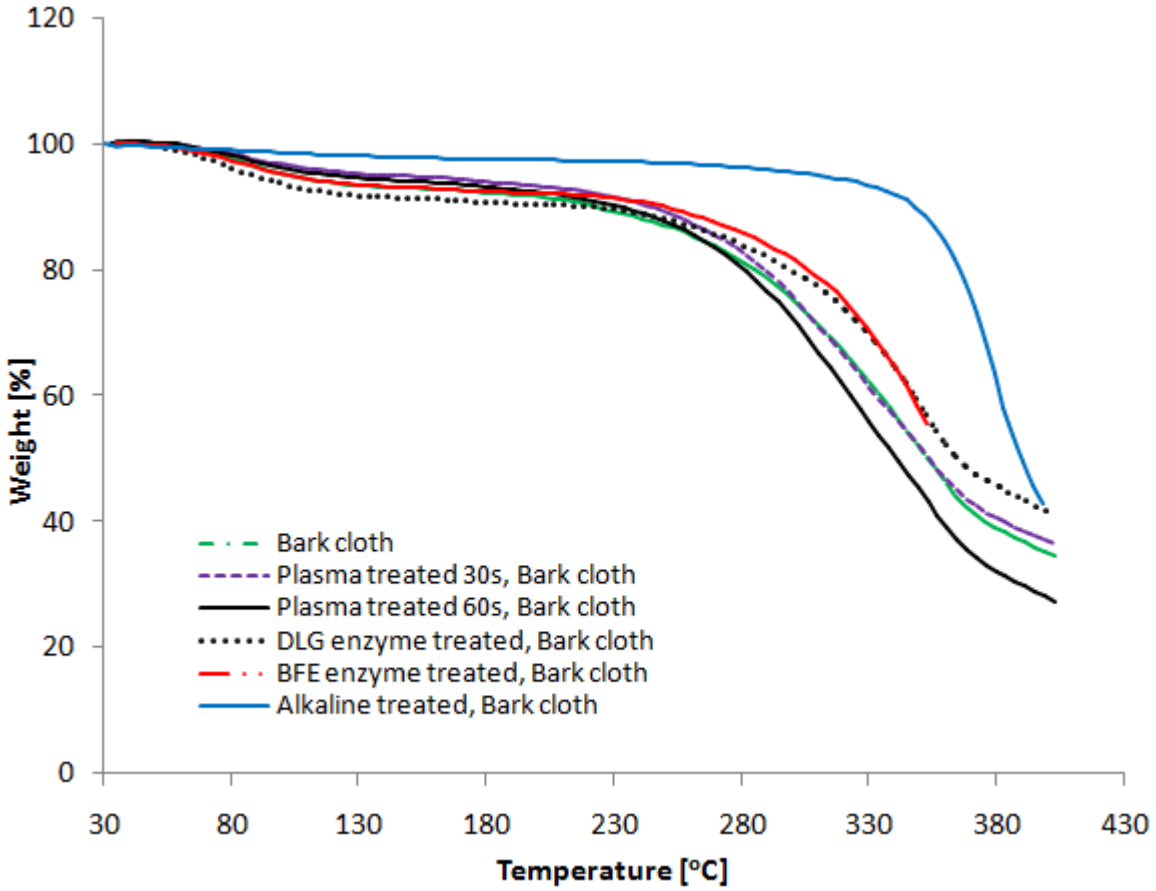

Figure 6.19. Thermogravimetric behavior of treated barkcloth

Figure 6.19 shows the thermogram of untreated barkcloth and surface modified fabrics. The first stage from 25°C - 100°C is attributed to evaporation of water accounting for about 5-10% loss in weight.
The weight loss is higher in enzyme-treated fabrics than plasma due to the fact that the enzymes degraded the plant material in the form of waxes and impurities however this led to thermal stabilization of the fabrics.

Untreated and plasma-treated fabrics were less thermally stable compared to enzyme-treated fabrics. In terms of moisture evaporation, it was observed that plasma treated fabrics had less moisture followed by BFE enzyme-treated fabrics. This is attributed to the fact that plasma made the surface hydrophobic, whereas the BFE enzyme did not degrade the fabric compared to the action by DLG enzyme.

The second stage accounting to about 70% weight loss starts from about 220°C- 370°C with a maximum decomposition temperature corresponding to around 325°C. The temperature range 200°C-315°C corresponds to the cleavage of glycosidic linkages of cellulose which leads to the formation of H_2O, CO_2, alkanes and other hydrocarbon derivatives [151]. The last stage of decomposition starting from around 370°C corresponds to 20% loss in weight is due to char or other decomposition reactions [157].

Barkcloth thermograms show that the fabric is stable below 200°C; therefore alternatives of composite fiber reinforcement can be explored provided the working and production temperature of composites is kept under this temperature. Alkaline treated fabrics showed a stable thermal behavior among the fabrics which tested and, therefore, alkaline treatment was preferred for biocomposite reinforcement processing.

6.4. MECHANICAL PROPERTIES OF BARKCLOTH LAMINAR EPOXY COMPOSITES

6.4.1. Static Mechanical Properties

Figure 6.20 illustrates the typical load-strain behaviour of the tested tensile samples. The behavior was partially linear due to the highly anisotropic structure of barkcloth fabrics. The tensile strength and modulus of a composite material is dependent on the matrix, fiber to matrix adhesion and the reinforcing fiber properties. [158].

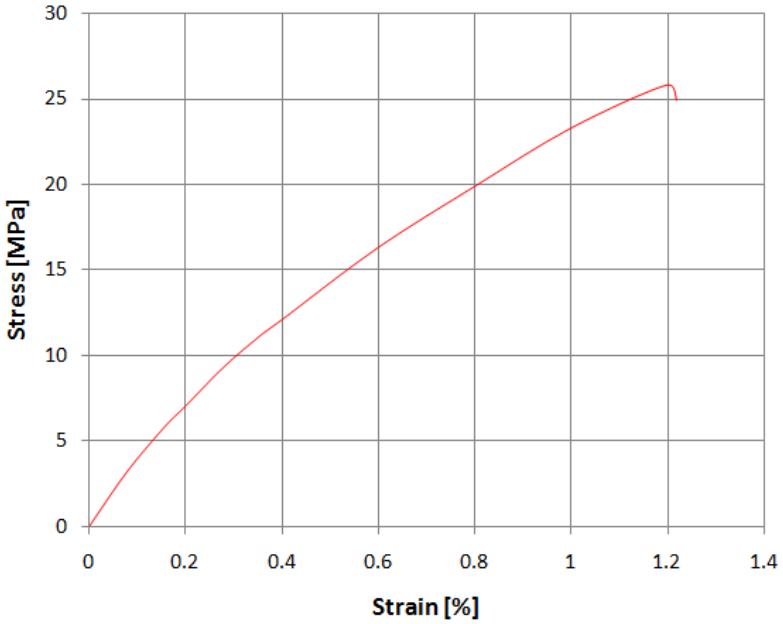

Figure 6.20. Representation of typical stress-strain behavior of the tensile samples

Barkcloth is a naturally occurring non-woven fabric, therefore, the climatic conditions, types of soils; the part from which the bark is extracted and the processing conditions are all variables that affect the strength of the fabric. The Stress - Strain behavior of the tested fabric reinforced composites showed a partially linear behavior (Figure 6.20). This behavior is due to the high anisotropy of barkcloth.

6.4.1.1. Enzyme and Plasma Fabric Treated Composites

The tensile strength and modulus of the developed composites is shown in Figure 6.21 and Figure 6.22 respectively. The strength and modulus of a composite material is dependent on the reinforcing fiber properties, and the matrix properties [56].

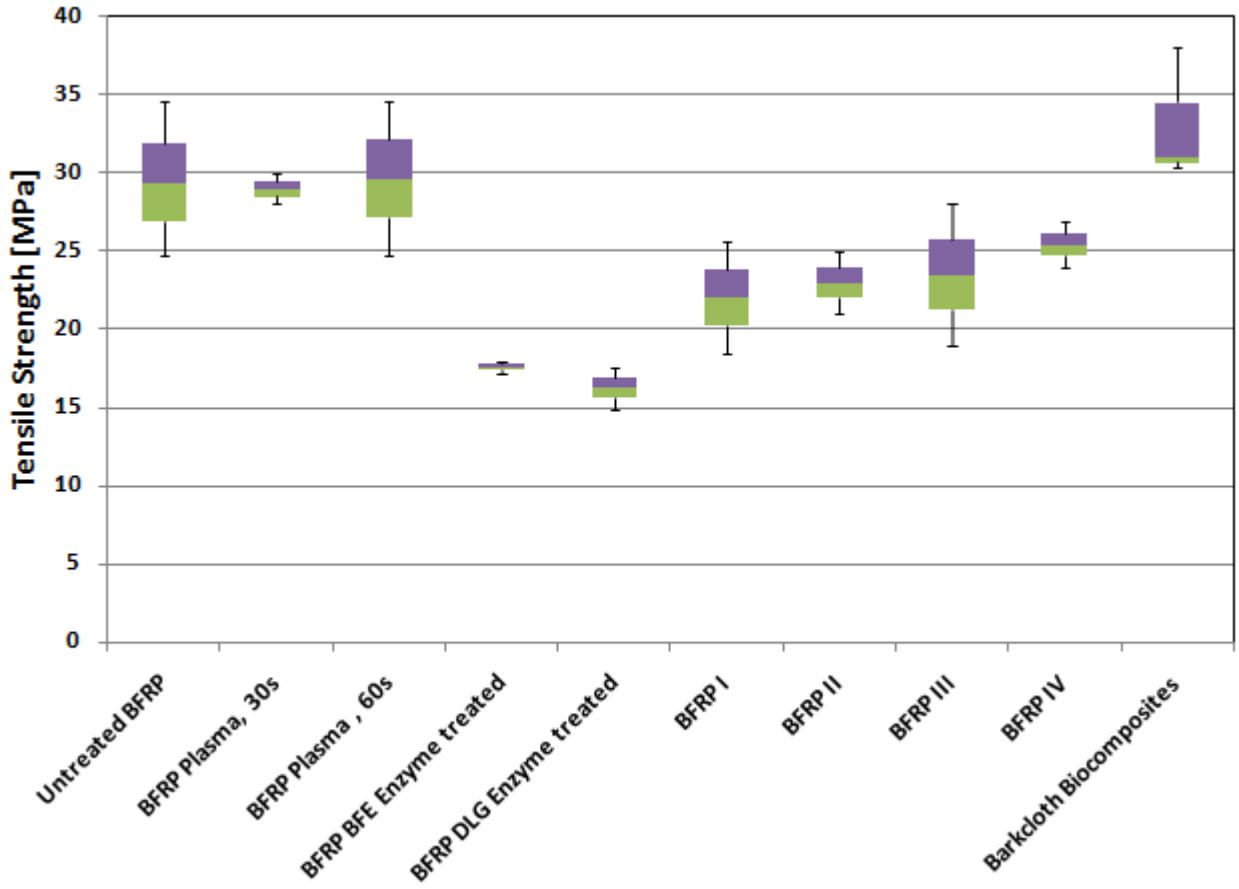

Figure 6.21. Tensile Strength of Barkcloth Fabric Reinforced Plastic Composites

Treatment with atmospheric plasma for 60s slightly enhanced the strength to an average of approximately 30MPa and average modulus ranging from 3.3GPa to 4.5GPa (Figure 6.22). High modulus of the plasma treated composites compared to enzyme treated composites is attributed to the fact that plasma opened up the reactive sites of cellulose, therefore, offering effective fiber-to-epoxy polymer bonding. Enzyme

treated composites exhibited the lowest strength and modulus due to the fact that the natural bonding that binds the barkcloth microfibers together was dissolved and it led to weaker fabrics that was thereafter transferred to the composites. The percentage elongation of enzyme treated composites was the lowest compared to untreated and plasma treated composites (Figure 6.23); this is attributed to reduced strength of the fabrics which are the load bearing materials. According to Sapuan et al. [140] in their investigation on material selection for natural fiber reinforced dashboard composites for automotive, a tensile strength of at least 25MPa is required. In comparison to the engineered barkcloth composites in this investigation, it's evident that barkcloth is a promising material for automotive applications such as door claddings, overhead and instrument panels.

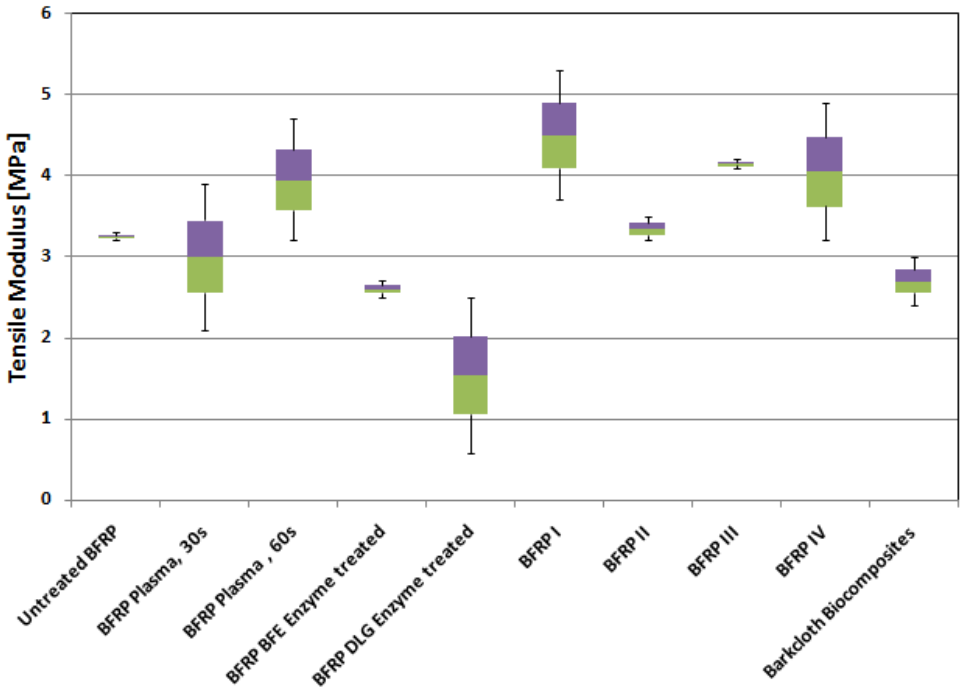

Figure 6.22. Tensile Modulus of Barkcloth Fabric Reinforced Plastic Composites

6.4.1.2. Effect of Fabric layering

It is observed that the stacking sequence BFRP IV had the highest tensile strength, whereas BFRP I had the highest tensile modulus and second lowest percentage of elongation at break. The strength and modulus of a composite material is dependent on the reinforcing fiber properties, fiber-to-matrix adhesion. Because barkcloth fabric has microfibers that are aligned at an angle, it is important to have a stacking sequence that will be beneficial for composite applications. Tensile failure was through matrix failure and the disintegration of the nonwoven structure through the tensile forces.

It is observed that BFRP II exhibited the highest average flexural rigidity followed by BFRP IV, BFRP III, and BFRP I. The flexural modulus shows that composites with stacking sequences II and IV are more rigid than composites with stacking sequences I and II. This rigidity is due to the presence of plies with 45° alignment at the surface.

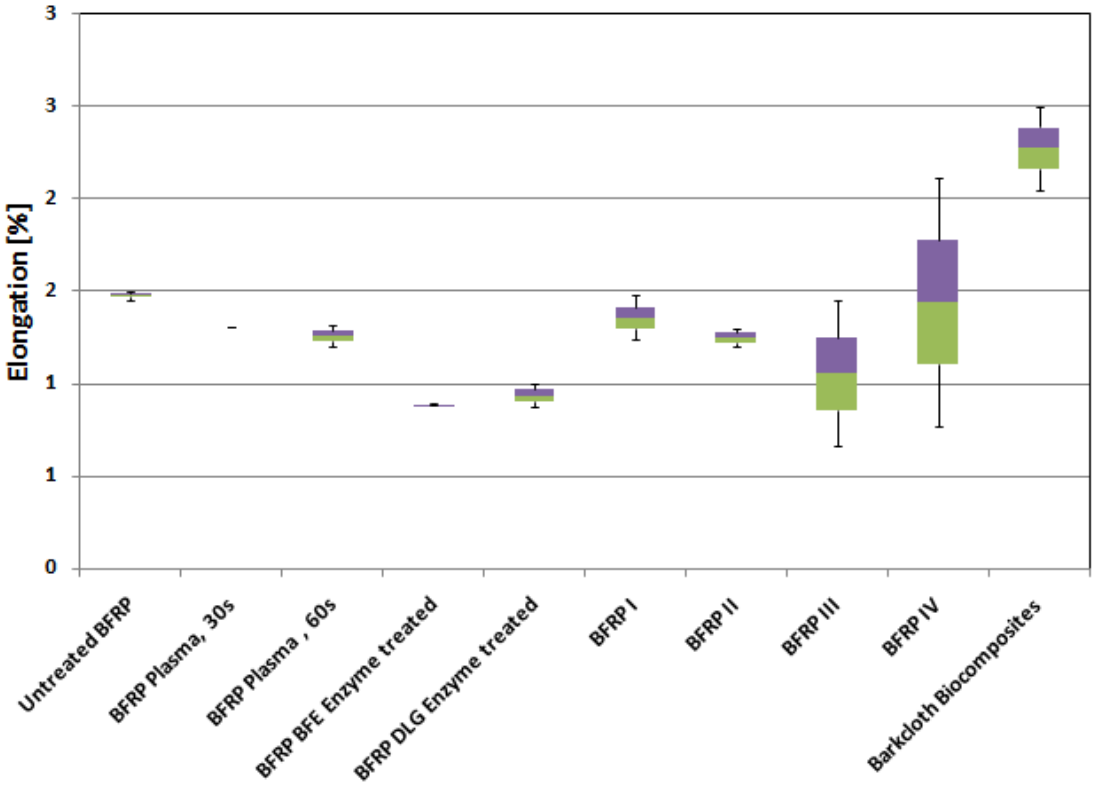

Figure 6.23. Percentage Elongation of Barkcloth Fabric Reinforced Plastic Composites

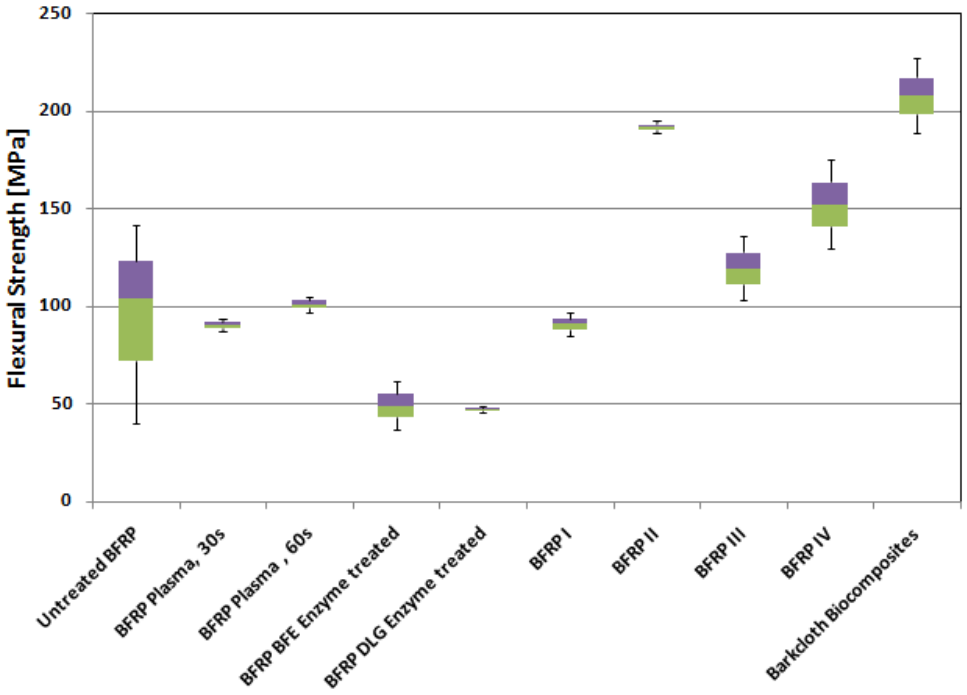

Figure 6.24. Flexural Strength of Barkcloth Fabric Reinforced Plastic Composites

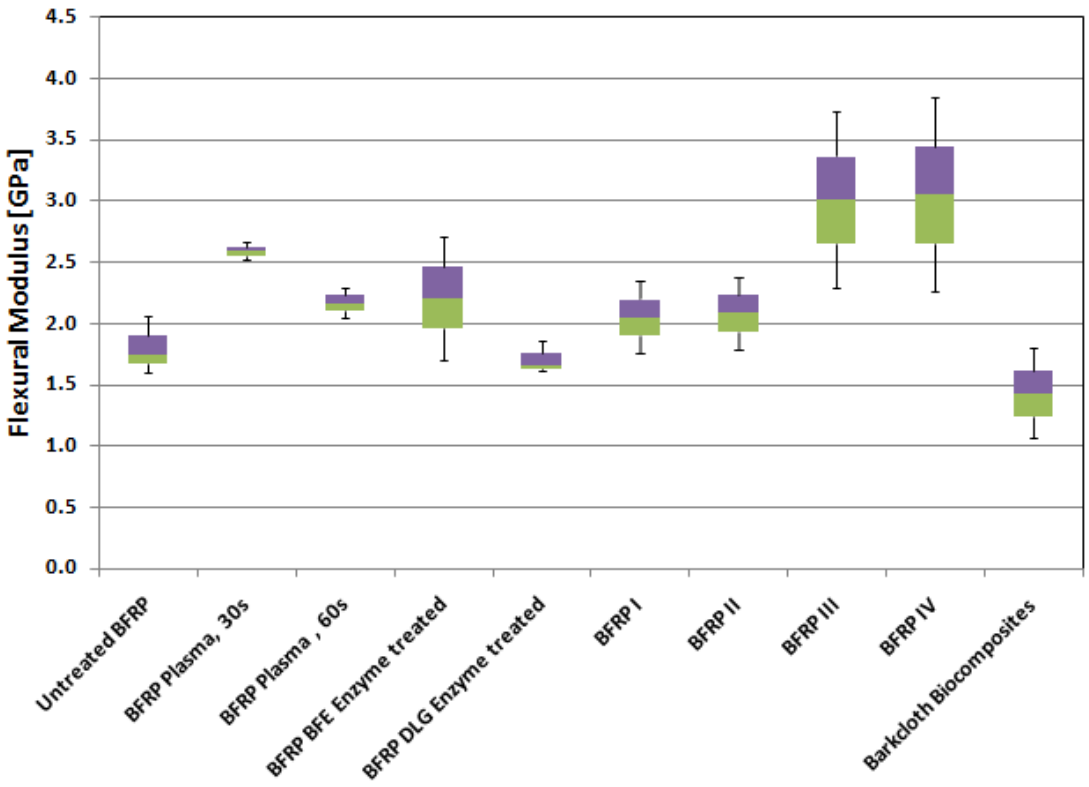

Figure 6.25. Flexural Modulus of Barkcloth Fabric Reinforced Plastic Composites

6.4.1.3. Biocomposites

The composites had ply orientations of 90º,0º,45º, 45º due to the fact that in the investigation of the effect of layering pattern of barkcloth composites using a synthetic epoxy polymer, it was shown that the stacking sequence of barkcloth with orientation 90º,0º,45º, 45º (BFRP IV) was ideal and had higher and consistent favorable mechanical properties [159].

The developed biocomposites had an average strength of 33MPa higher than the strength obtained using synthetic epoxy. The percentage elongation of the biocomposites was higher than the synthetic composites. This is attributed to the green epoxy polymer properties, however, the variability of the reinforcing material is observed with the low modulus of the biocomposites owed to the treatment with alkali that dissolved impurities.

The average flexural strength of the developed green epoxy biocomposites was 207MPa higher than the untreated and synthetic composites. This was due to the effective fiber to matrix adhesion owed to the alkali treatment. During the three points bending, the upper and lower laminate surfaces are loaded with tension and compression forces respectively, whereas the axisymmetric plane is subjected to shear. Therefore, failure during flexure is achieved when the flexural and shear stress reach a critical value [160].

6.4.2. Failure of Composites

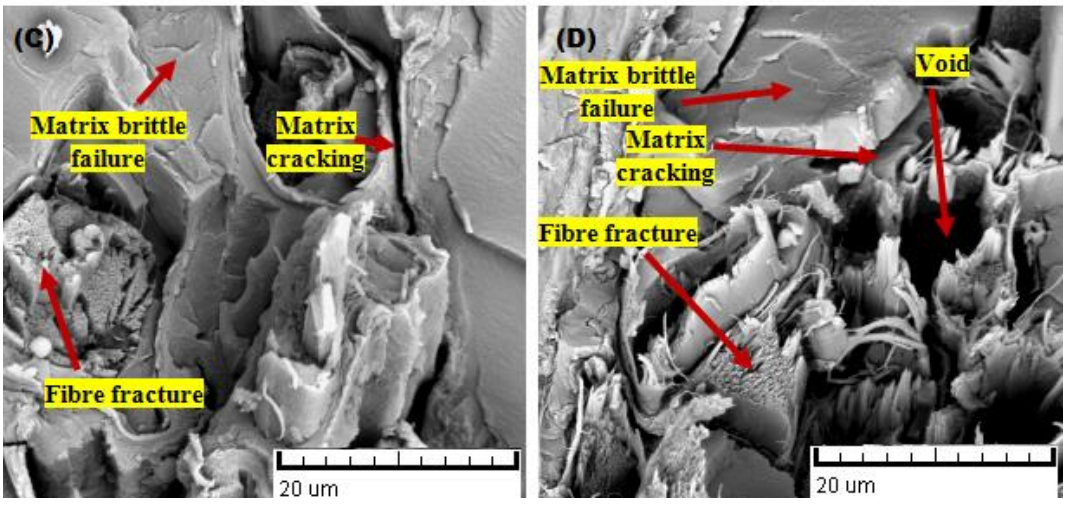

Figure 6.26. Morphology of barkcloth fabric and biocomposites

Failure by tensile was through matrix failure and the disintegration of the non-woven structure through the tensile forces. The entangled microfiber web of the fabric has natural bonds holding the microfibers

together. Generally, BFRP composites experienced three modes of failure: the brittle failure of the epoxy polymer matrix; matrix cracking and fiber fracture (Figure 6.26). Damage of the non-woven structure is triggered by the inter-fiber bond structure; re-arrangement of the fiber network and reloading and finally fiber fracture [161].

According to Sapuan and Abdalla [96] in their investigation on material selection for natural fiber reinforced dashboard composites for automotive, a tensile strength of at least 25MPa is required. In comparison to the engineered barkcloth composites in this investigation (Figure 6.21), it's evident that barkcloth is a promising material for automotive car dashboard, door claddings, instrument panels and laminate panels for building and civil engineering applications.

The barkcloth epoxy composites exhibit an average flexural strength ranging from 47 to 192MPa. The variation in the flexural properties is due to the nature of natural fibers and varying strength along its structure.

6.4.3. Dynamic Mechanical Properties

In order to assess the performance of structural applications, the dynamic mechanical properties help in material evaluation so as to understand the viscoeslastic behavior of the material against temperature, time and frequency. Three parameters storage modulus (E'), loss modulus (E'') and damping factor (tan δ) were obtained over the temperature range from 28^{o}C to 80^{o}C for synthetic epoxy composites and 25^{o}C to 250^{o}C for bioepoxy composites. The storage modulus indicates the viscoelastic rigidity of the composites and is proportional to the energy stored after every deformation cycle. A weak material has a low storage modulus, whereas a strong material exhibits a higher storage modulus. As the composite approaches the glass transition temperature, there's a sudden decrease in the storage modulus attributed to the free molecular movement of the polymer chains.

A low mechanical damping factor indicates closer packing of the composites and elasticity of the material and a higher damping factor indicates a weaker material under loading, which could be due to weak fiber-to-matrix adhesion.

6.4.3.1. Dynamic Mechanical Properties: Enzyme and Plasma Fabric Treated Composites

Figure 6.27 shows the variation of the storage modulus (E') of the barkcloth composites. The storage modulus in the plastic region varies with treatment. It's observed that plasma treatment had a slight effect on the storage modulus compared to the significant effect observed with enzyme treated composites. The increased strength observed with the plasma treated composites is attributed to the strength of the plasma treated fabrics. Plasma treatment positively aided the effective cross-linking between the fabric and epoxy

polymer. The enzyme treated composites, especially BFE had low storage modulus that is attributed to the enzymes that partially dissolved the microfiber natural binders leaving a very light non-woven fleece with reduced strength. The loss modulus (E'') shows the viscous response of the material. The loss modulus of the composites increased significantly in the plastic region and then decreased with increase in temperature in the rubbery region. It's observed that in the plastic region, the plasma composites treated up to 30s showed the highest loss modulus whereas BFE enzyme treated composites exhibited the lowest loss modulus.

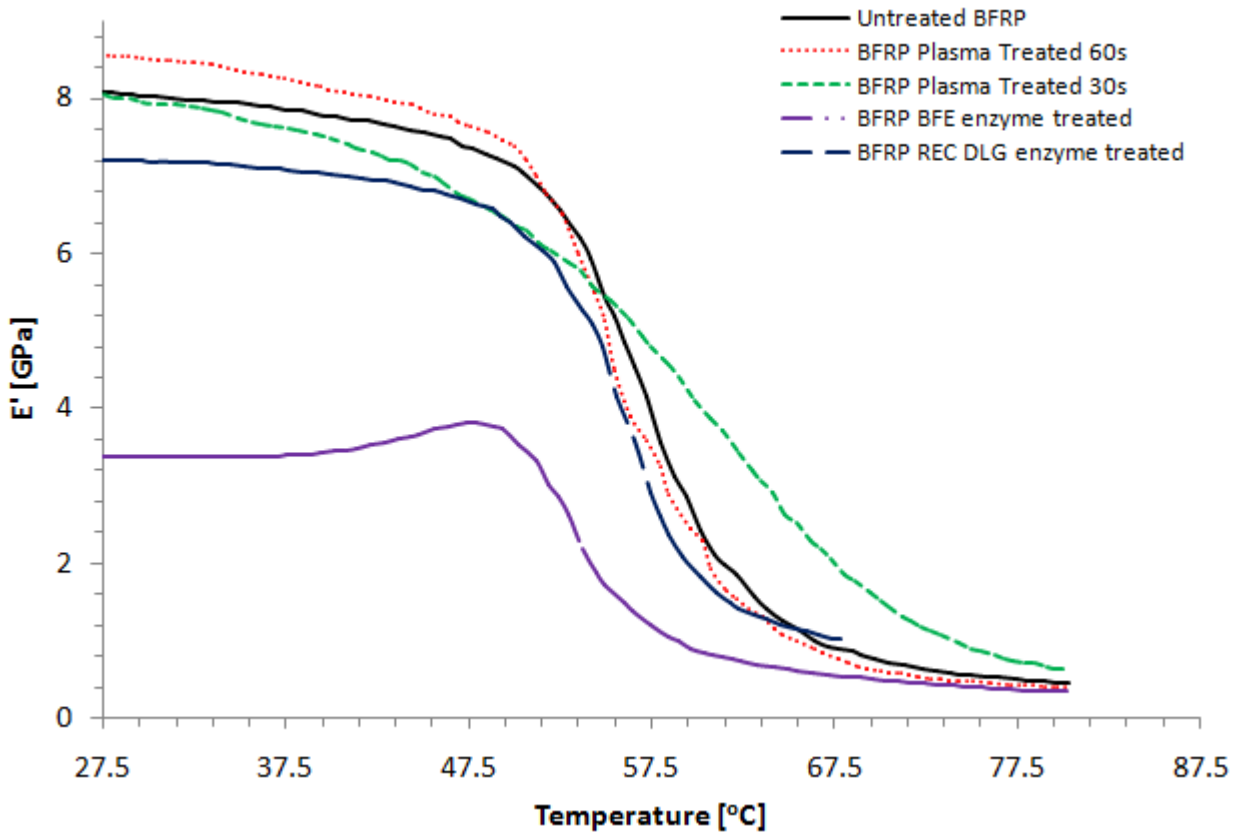

Figure 6.27. Storage modulus behaviour of enzyme and plasma treated barkcloth composites

The mechanical damping factor (Tan δ) shows the strength of the material and helps in evaluating the effect of the efficiency of the filler-matrix adhesion. A high damping factor indicates a weak filler-matrix adhesion, whereas a low damping factor indicates good filler-matrix adhesion that doesn't allow free movement of polymer molecules. It's therefore observed that plasma treated composites for 60s and enzyme treated composites had the best fiber-to-matrix adhesion as can be observed by the lower Tan δ (Figure 6.28). The glass transition temperature is obtained at the level at which the damping factor and loss modulus attain maximum damping values [162]. The glass transition obtained using tan δ is usually

higher; therefore, a more conservative glass transition temperature obtained by the loss modulus is usually taken into consideration. The glass transition temperature of the composites was between 52.9ºC to 59.4ºC.

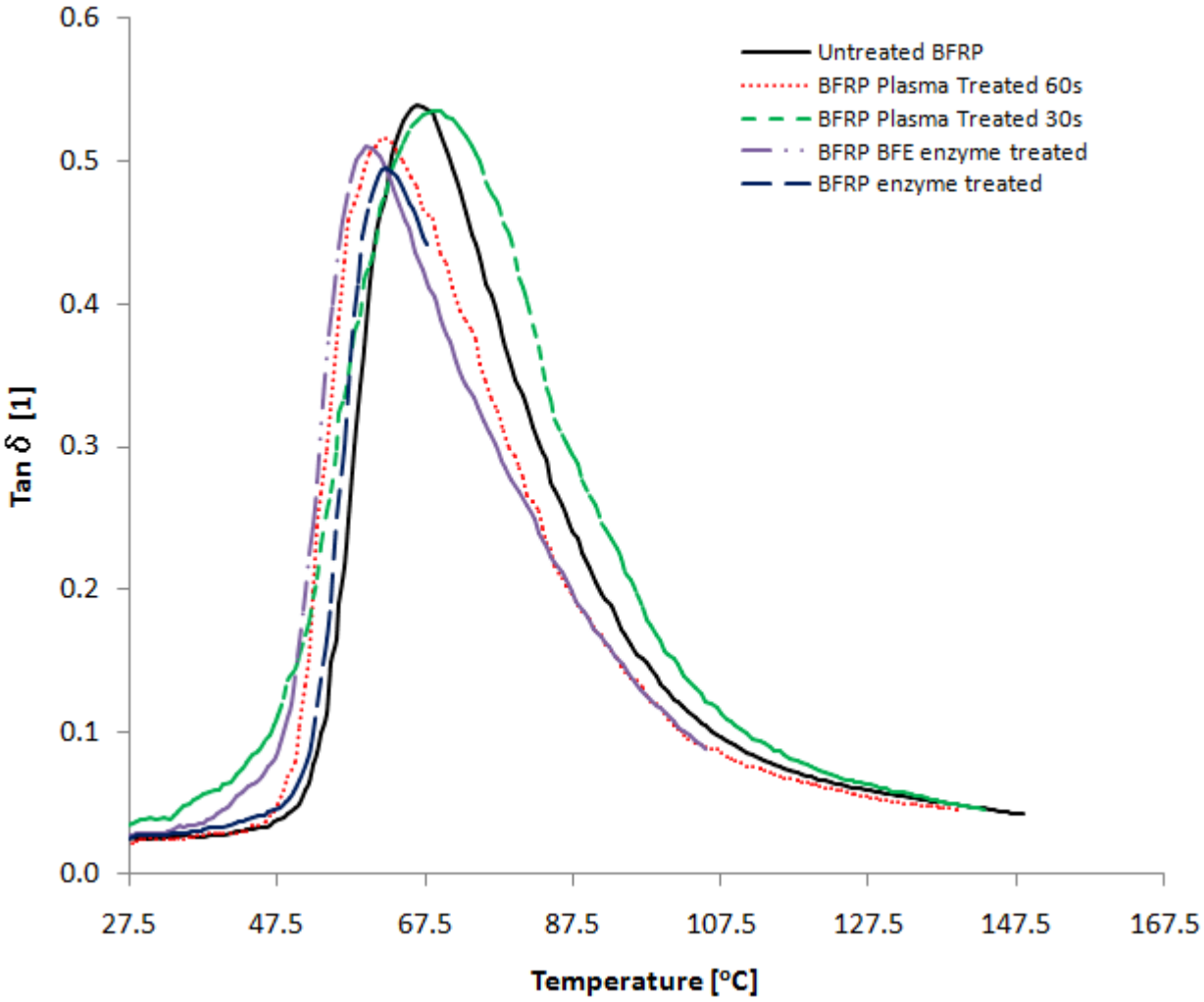

Figure 6.28. Mechanical damping factor of enzyme and plasma treated barkcloth composites

The variation of tan δ against temperature (Figure 6.28) aids in obtaining the glass transition temperature. The T_g obtained from the tan δ curve is slightly higher than that obtained from the loss modulus curve. Beyond the glass transition temperature, the material transitions from glass to rubbery state due to the mobility of polymer chains.

6.4.3.2. Dynamic Mechanical Properties: Effect of Fabric Layering

As the temperature increases, the storage modulus falls sharply in the temperature range 50° to 70°C, which is the glass transition temperature range (Figure 6.29). This fall in the storage modulus is attributed to the mobility of the macromolecular polymer chains, which distorts the initial close packing [163]. The composites from the highest storage modulus to the lowest were those with stacking sequences II, III, I, and IV, which is confirmed by the flexural modulus obtained from the flexural tests in Table III.

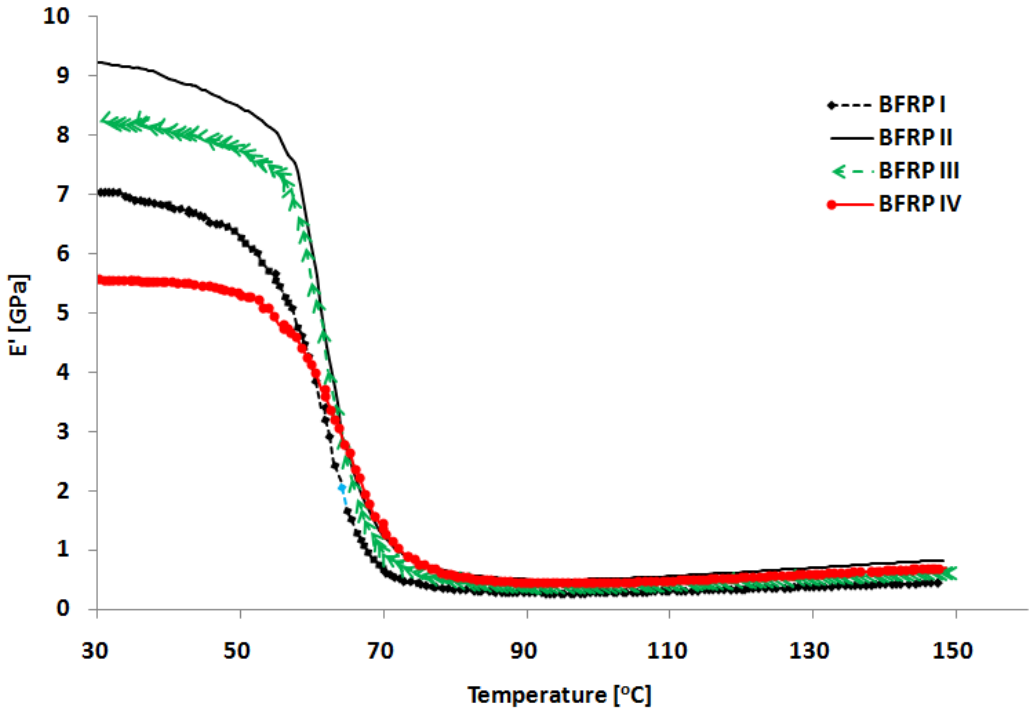

Figure 6.29. Storage modulus of layered BFRPs

The loss modulus (E'') indicates the energy loss of the composites. The polymer chain mobility increases with temperature until the glass transition region, where the loss modulus rapidly falls. Past the glass transition, the composite's elasticity, and viscous behavior greatly reduce because of the mobility of polymer molecules. The peak of the curves shows the glass transition temperature of the developed composites. It is observed that the glass transition temperature as obtained from the loss modulus curves is between 63° and 65°C. Figure 6.30 shows the mechanical damping factor of the composites. The mechanical damping factor is the ratio of the energy stored to the energy lost. The glass transition temperature is approximately 70°C

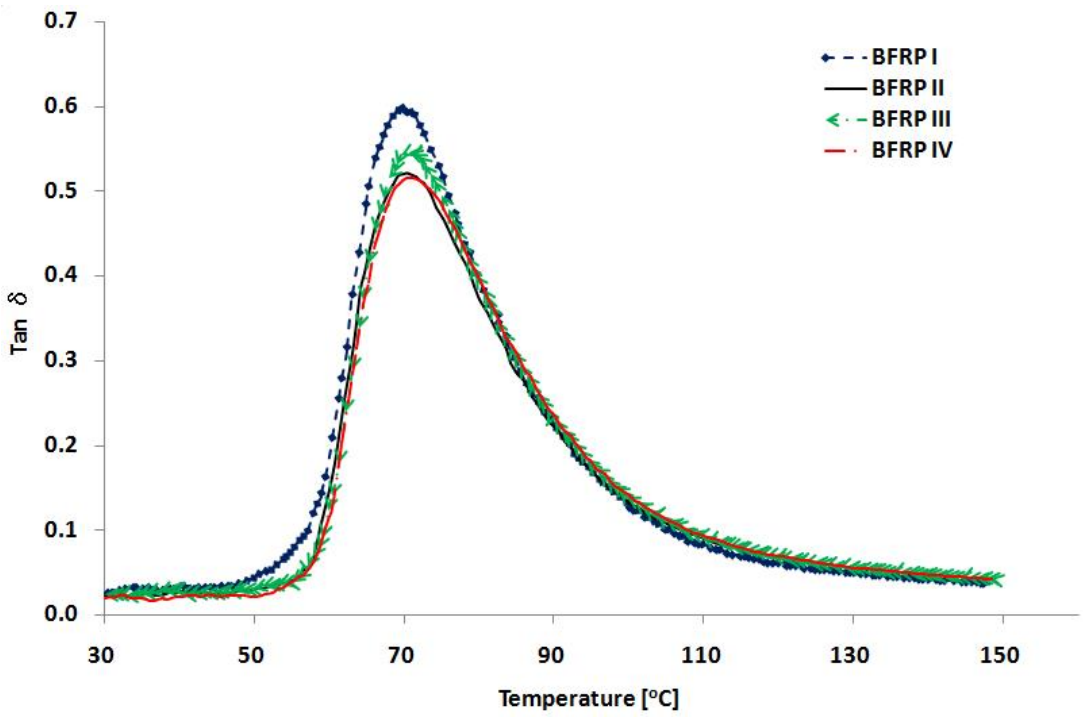

Figure 6.30. Mechanical damping factor of layered composites.

6.4.3.3. Dynamic Mechanical Properties: Biocomposites

Figure 6.31 shows the variation of the storage modulus with the temperature at three scan frequencies of 0.1, 1 and 10 Hz. The storage modulus shows the stiffness of the composites against temperature. It's observed that the storage modulus generally decreases with increasing temperature. The addition of reinforcement to the epoxy polymer greatly enhanced the dynamic mechanical properties increasing the storage modulus from 2.6 GPa of virgin resin to 5.1 GPa of biocomposites at 30°C. The high value of storage modulus of biocomposites is attributed to the reinforcement. Under loading, the polymer chains move about and are re-arranged, with the addition of the barkcloth, the mobility of the polymer chains is greatly reduced. A sudden fall of the modulus of the composites was observed at 130°C which is marked by a sharp decrease in the storage modulus until to around 450MPa at 225°C. As the composite approaches the glass transition temperature, there's a sudden decrease in the storage modulus attributed to the free molecular movement of the polymer chains. Polymer viscoelastic behaviour is a function of time, frequency and temperature. A frequency scan showed that the storage modulus increases with increase in the frequency. So the modulus at 10 Hz (Short time) is higher than the modulus at 0.1Hz (long time). The variation of tanδ against temperature, (Figure 6.32) aids in obtaining the glass transition temperature. It's observed that the Tg obtained by the damping factor curve was 163°C, 170°C and 185°C for 0.1 Hz, 1 Hz and 10 Hz respectively. The Tg increases to a higher temperature as the analysis frequency increases

[164]. Beyond the glass transition temperature, the biocomposite transitions from glass to rubbery state due to the high mobility of the polymer molecular chains.

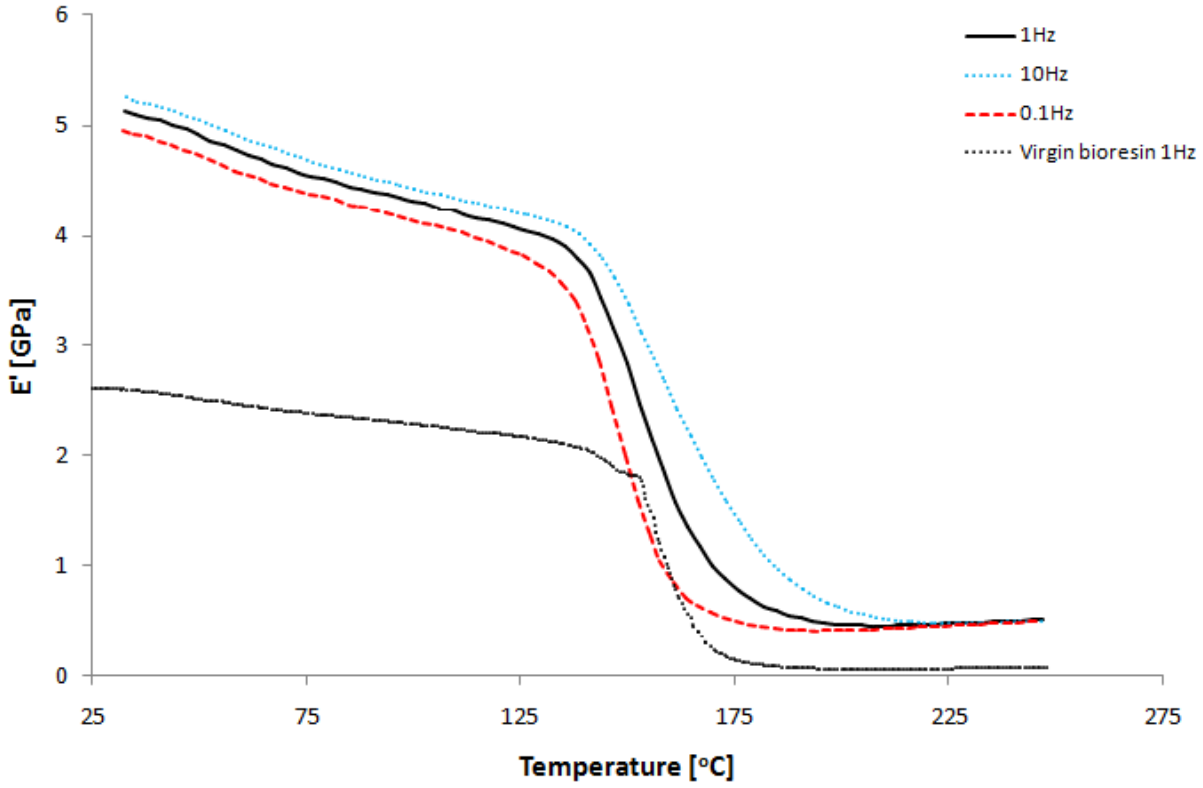

Figure 6.31. Storage modulus of biocomposites with BFRP IV architecture

The virgin epoxy polymer exhibited a sharp and intense peak centered at 175ºC because there is no restriction to the polymer molecular chains at the glass transition temperature. The source of crack initiation is usually weak fiber to matrix bond interface; therefore higher energy is dissipated than strong interfaces. The high tanδ peak, therefore, shows green epoxy polymer is viscous when loaded compared to the reinforced composites [165,166]. The dynamical mechanical properties have therefore shown that from 30ºC, the optimum temperature range of application of biocomposites is up to130ºC. Beyond 130ºC, the composites enter into a rubbery state and the performance is diminished.

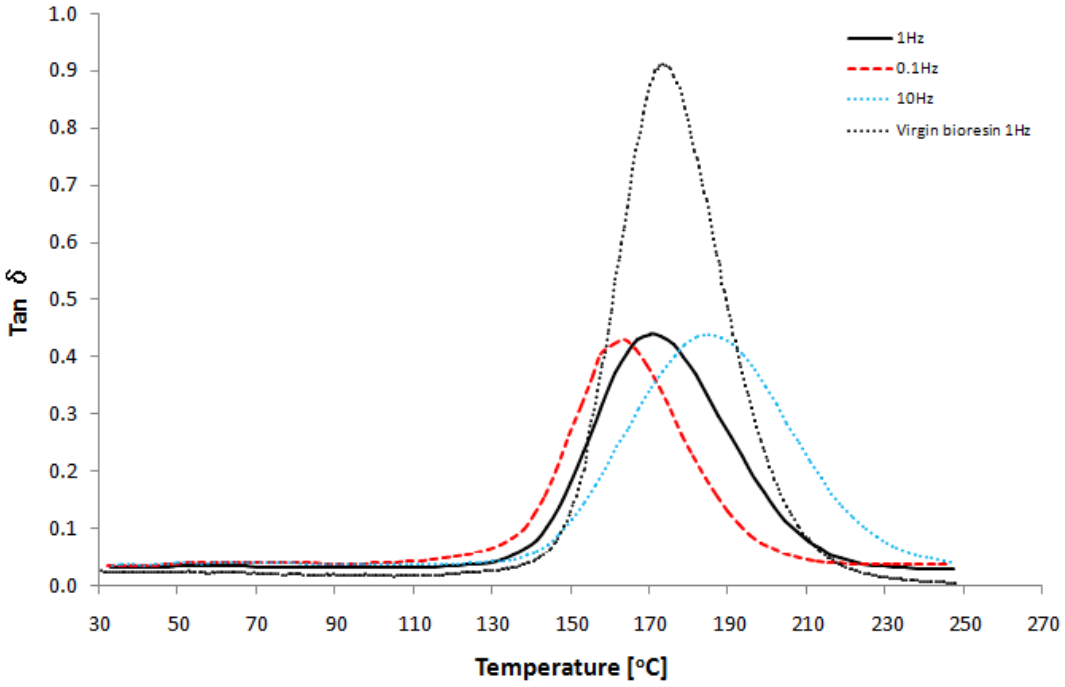

Figure 6.32. Tanδ of biocomposites with BFRP IV architecture

6.5. THERMAL BEHAVIOUR OF BARKCLOTH LAMINAR EPOXY COMPOSITES

6.5.1. Enzyme and Plasma Treated Fabric Composites

The composites thermal behavior as characterized by DSC is shown in Figure 6.33. Incorporation of barkcloth into the epoxy polymer has an effect on the crystallization behavior of semicrystalline synthetic epoxy polymer. The barkcloth reinforced epoxy laminar composites experienced endothermic and exothermic phase transformation. The first endothermic peak at around 55–61°C corresponds to the glass transition temperature (T_g).

Table 6.5. DSC of Enzyme and Plasma Treated Composites

Composites	T_g [°C]	T_c [°C]	T_m [°C]
Untreated	59	141	220
Virgin epoxy	56	133	200
BFE Composites	55	140	210
DLG Composites	56	137	206
Plasma 30s Composites	61	146	213
Plasma 60s Composites	61	150	215

The exothermic peak at around 133-150°C represents the cold crystallization temperature (T_c) of the epoxy polymer chains. As the temperature is increased, a second endothermic peak is observed at around

200-220°C. This peak signifies the melting temperature (T_m) of Epoxy polymer. Table 6.5 shows the effect of surface modification of barkcloth on the T_g, T_c and T_m. Addition of reinforcement generally increased the glass transition temperature, crystallization temperature as well as the melting temperature of the composites because addition of reinforcement limits the mobility of the polymer chains and therefore, a positive effect on the glass transition temperature.

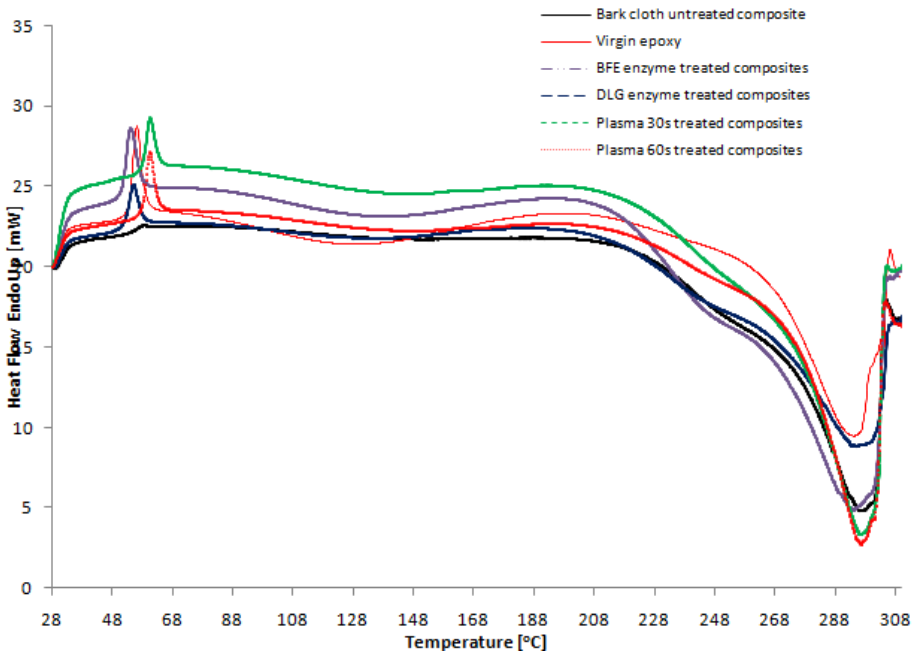

Figure 6.33. DSC of enzyme and plasma treated composites.

4.6.2. Thermal behavior of Biocomposites

Thermal degradation of natural fiber components is dictated by the supramolecular structure of the cellulosic materials [167]. The composites and fabric behavior as characterized by DSC (Figure 6.34), shows an endothermic peak starting from 20°C to 120°C centered at around 52°C. This peak is characterized by the removal of adsorbed moisture from the fabric. As seen from Table 1, barkcloth is majorly made up of cellulose, therefore; its affinity to moisture is high since cellulose is hydrophilic in nature. Studies with NMR have shown that moisture is concentrated in the amorphous or non-crystalline regions of cellulose [168]. Therefore, the endotherm at 52°C corresponds to the amorphous component of cellulose in barkcloth. The peak at 140°C is attributed to the decomposition of paracrystalline molecules of pectin and hemicelluloses in the barkcloth [53]. The leveled behavior of biocomposite confirms that the selected curing temperature of 120°C for 45 min was sufficient for cure. TGA is a useful technique for the study of the thermal behavior of composite materials. Thermal stability of the polymer and reinforcing

materials is an important parameter because manufacturing of composites in most cases requires curing; therefore, the degradation behavior of the reinforcing fibers helps in selecting the processing temperature and also the working temperature of the developed composite materials.

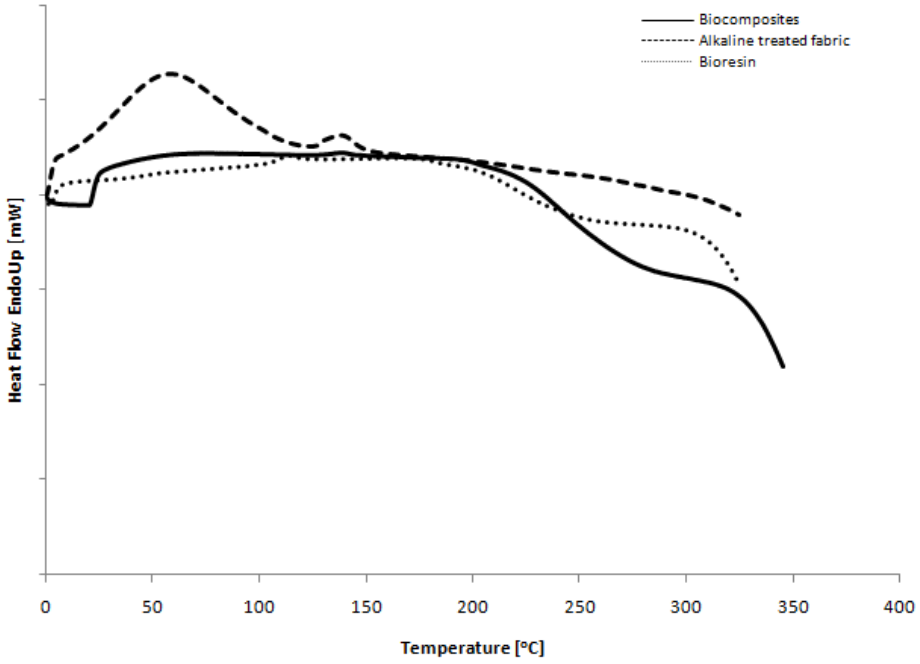

Figure 6.34. DSC of green composites

Thermal stabilization of alkali treated fabrics led to stable biocomposites which had a higher temperature of degradation than synthetic based composites. The onset of degradation was observed at 270°C whereas cellulose decomposition occurred at 350°C, (Figure 6.35).

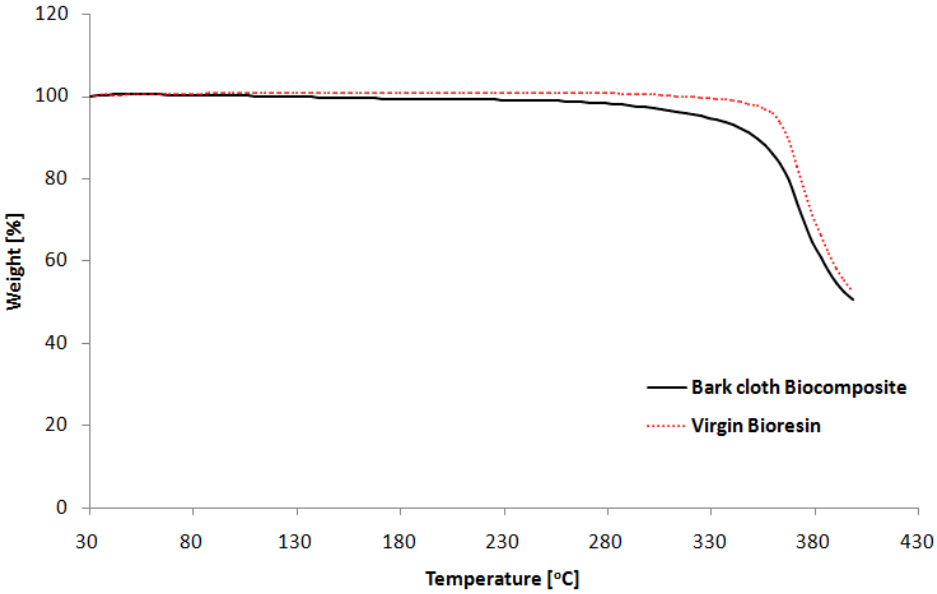

Figure 6.35. TGA of green composites

6.6. OVERVIEW OF BARKCLOTH FABRIC REINFORCED COMPOSITE MATERIAL PROPERTIES

Table 6.6. Summary of the Barkcloth Composite Materials Properties

Laminar Composites/ Property	Ultimate Tensile Strength [MPa]	Tensile Modulus [GPa]	Flexure [MPa]	Flexural Modulus [GPa]	Elongation [%]	Onset of Degradation [ºC]	Tan δ @1Hz [-]	Glass Transition Temp [ºC]
Untreated	25-31	3.2-3.3	40-142	1.6-2.1	1.5	266	0.54	67.2
Plasma Treated 30s	28-30	2.1-3.9	87-94	2.5-2.7	1.31	262	0.54	69.7
Plasma Treated 60s	25-35	3.2-4.7	97-105	2.0-2.3	1.2-1.3	262	0.51	63.1
Enzyme Treated (DLG)	15-18	0.58 -2.5	37-49	1.6-1.9	0.9	285	0.50	62.3
Enzyme Treated (BFE)	17-18	2.5-2.7	49-62	2.2-2.7	0.9	285	0.51	59.7
BFRP I*	18-26	3.7-5.3	85-87	1.8-2.3	1.2-1.5	-	0.60	70.4
BFRP II**	21-25	3.2-3.5	189-195	1.8-2.4	1.3	-	0.52	70.4
BFRP III***	19-28	4.1-4.2	103-136	2.3-3.7	0.6-1.5	-	0.54	70.4
BFRP IV****	24-27	3.2-4.9	130-175	2.3-3.5	0.8-2.1	-	0.52	70.4
Green Composites	30-38	2.4-3	189-227	1.1-1.8	2.1-2.5	345	0.44	170

*****BFRPI layering sequence

******BFRPII layering sequence

*******BFRPIII layering sequence

********BFRPIV layering sequence

6.7. THERMO-ACOUSTIC PROPERTIES

The amount of heat transmitted through a unit area of the material was measured as the thermal conductivity coefficient (k). There is dependence between the thermal conductivity of a material and its sound absorption. When a sound wave strikes a porous fiber network like barkcloth; the sound waves cause vibration in the fiber network. The vibration causes minute heat buildup in the fibers due to friction. Therefore a good absorbing material absorbs the thermal energy of the sound waves and less heat is generated. The case is somewhat different with solid composite materials. The compaction of the barkcloth nonwoven felt results in reduced porosity, therefore increasing flow resistivity and reduced vibration of the fiber network therefore a reduced sound absorption coefficient and higher thermal conductivity. The combination of several nonwoven fabric layers allows the realization of different absorption degrees in one composite structure, which can then absorb sound in wide range of frequencies. High values of thickness and fabric density facilitate sound insulation. Microstructure parameters such as fiber orientation, tortuosity, pore structure, influence the sound absorption efficiency [169].

6.7.1. Thermal insulation behavior of BFRPs

The ficus species had a higher thermal conductivity among the measured specimens whereas Antiaris had the lowest thermal conductivity (Figure 6.36). The high thermal conductivity coefficient is attributed to the epoxy polymer used whose thermal conductivity is approximately 0.2W/mK.

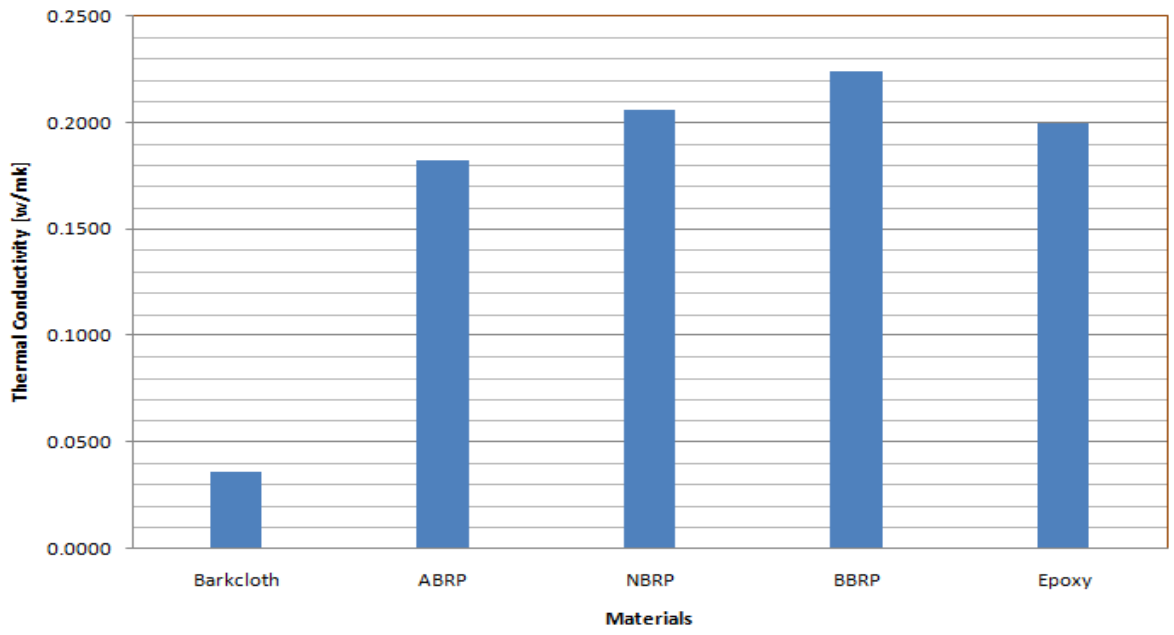

Figure 6.36. Thermal conductivity of composites: *Antiaris* Composites (ABRP); *Ficus natalensis* Composites (NBRP); *Ficus Brachypoda* Composites (BFRP) (Measurements were based one sample)

A lower value of k is characterized as a better thermal insulation material due to the fact that it helps in resisting outside heat transmitted through the fibrous network.

6.7.2. Acoustic Properties

6.7.2.1. Barkcloth Fabrics

The acoustic properties of layered fabrics of the three species are shown in Figure 6.37. The sound absorption properties depend on the thickness since the thickness of one layer was an average of 1.14mm, it's observed that the sound absorption performance of the barkcloth fabrics generally increases with the increase of frequency. The one layer barkcloth fabrics between the frequency range of 1000-3200Hz have an average sound absorption coefficient of 0.05 whereas beyond 5000Hz the fabric's sound absorption is tending to 0.1 and the properties being favorable for Antiaris and F. *natalensis* barkcloth.

The effect of layer thickness was investigated and Figure 6.38 shows the sound absorption properties barkcloth fabrics with one, two, three and four layers.

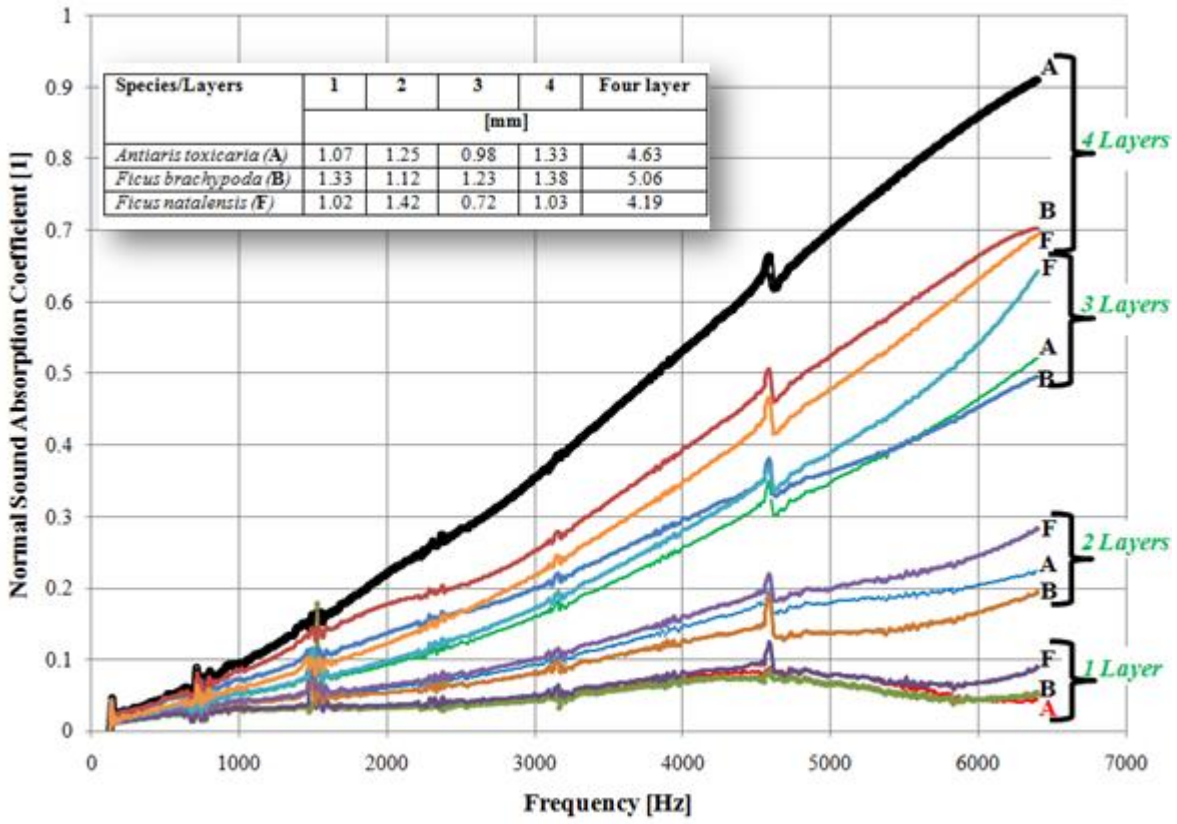

Figure 6.37. Sound Absorption Behavior of Barkcloth

The sound absorption properties increase with an increase in sample thickness. All the fabrics studied had a gradual increase of sound absorption coefficient. *Ficus natalensis*' four layer fabrics had a sound absorption coefficient of 0.7 at 6400Hz.

The two layer samples showed a sound absorption coefficient of 0.1 at 3000Hz; 0.15 at 4000Hz; 0.2 at 5000Hz and 0.25 at 6000Hz. The addition of another layer almost doubled the sound absorption performance of the fabrics as can be seen in the behavior of the samples with three layers.

Ficus brachypoda fabrics showed the same behavior as *Ficus natalensis* fabrics (Figure 6.37). It's observed that the three layer fabrics of f.natalensis were better than for f. brachypoda as can be seen from the graphs. F. brachypoda had a sound absorption coefficient of 0.71 at 6400Hz.

The sound absorption performance of *Antiaris toxicaria* fabrics at 6400Hz was overall best having a sound absorption coefficient of 0.92 compared to the average of 0.7 obtained by the Ficus barkcloth species. Krucinska et al. [170] showed that cotton/PLA composites of 5.8mm thickness with microfibers had a sound absorption coefficient of 0.93 at 6400Hz. The barkcloth fabrics showed an irregular dependence of sound absorption coefficient of like other nonwovens over a wide frequency range, this behavior was also confirmed elsewhere [171].

The comparable excellent acoustic properties of barkcloth fabrics at high frequencies is attributed to the fiber entanglement of the fabrics and porosity. Antiaris barkcloth with four layers showed better sound absorption properties compared to other types of barkcloth. The increase of the thickness of the fabrics will definitely increase the sound absorption coefficients.

6.7.2.2. Fabric Reinforced Composites

The sound absorption properties were investigated further whereby the four layers of barkcloth were utilized in the production of composites. Two surfaces were investigated in order to understand whether the perturbations on the composite surface have an effect on the sound absorption properties. The molded composites' sound absorption properties of smooth surfaces are shown in Figure 6.38.

The ficus barkcloth composites have a sound absorption coefficient below 0.1 for the frequency of upto 3700Hz and thereafter, f. brachypoda sound absorption properties increased with increase in frequency reaching its peak of 0.35 at 6400Hz. Antiaris BFRC sound absorption increased for frequency of 5000Hz and then decreased, showing the same trend with F. natalensis BFRC.

Effect of Composite Surface Roughness

The effect of surface perturbations on the sound absorption properties is shown in Figure 6.38 and Figure 6.39 which showed a marked increase in the sound absorption properties with rough surface. It's observed that the perturbations increased the sound absorption properties of Antiaris BFRC having an average sound absorption coefficient of 0.15 between frequency ranges of 2500-5000Hz.

The low performance of the composites with sound absorption is due to the effective packing of the method used for the production of the composites. VARTM is an efficient method of production of composites with fewer voids and with smooth, even packing which showed insignificant sound absorption properties compared to the fabrics which were used to reinforce the epoxy resin.

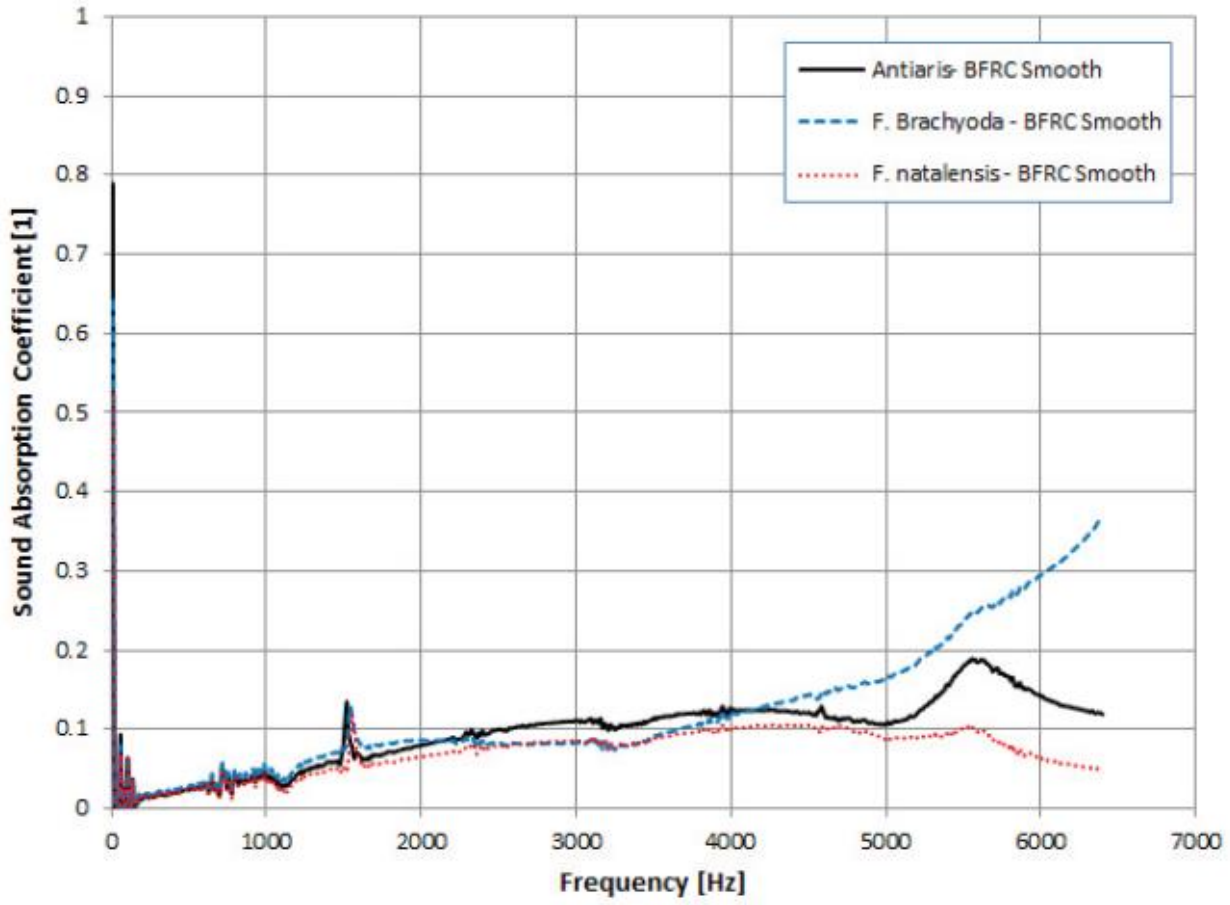

Figure 6.38. Barkcloth epoxy laminar composite sound absorption properties with smooth surfaces

When a sound wave strikes a porous fiber network like barkcloth; the sound waves cause vibration in the fiber network. The vibration causes minute heat buildup in the fibers due to friction. Therefore, a good absorbing material absorbs the thermal energy of the sound waves and less heat is generated. However, in

composites, the compaction of the barkcloth nonwoven felt results in reduced porosity, therefore increasing flow resistivity and reduced vibration of the fiber network therefore a reduced sound absorption coefficient and higher thermal conductivity[50].

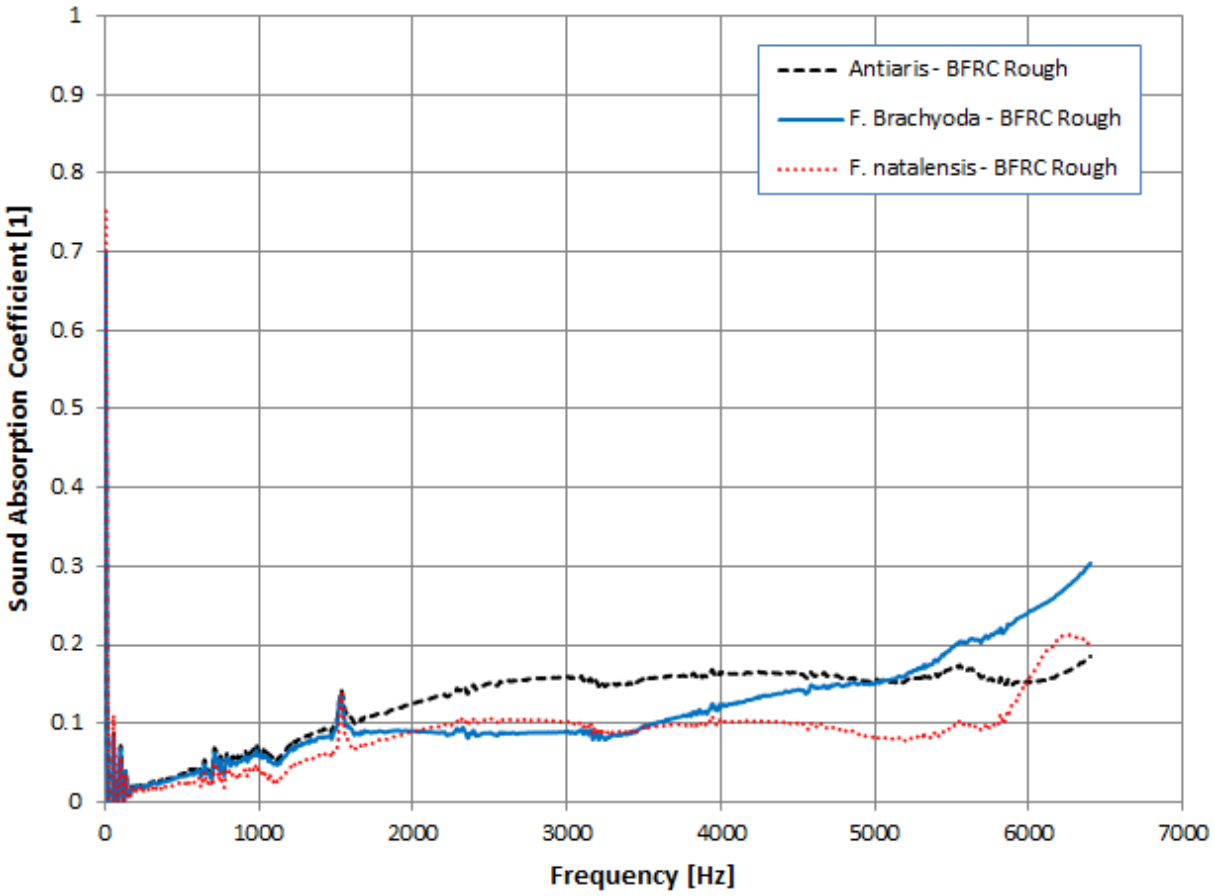

Figure 6.39. Barkcloth epoxy laminar composite sound absorption properties with surface perturbations

6.7.3. Modeling of Acoustic Properties

The ability to predict a material behavior using models offers a fast time-saving economical design of structures without prototype production and the rigorous experimental series needed to refine a material. Figure 6.41 shows the Delany – Bazley model as applied to the one layer AT Barkcloth fabrics, it is observed that the model is in agreement at least for the frequency below 3000Hz, however, beyond this frequency, the Delany – Bazley model is incapable of modeling sound absorption behavior of one layer AT barkcloth fabrics. This phenomenon is typical for the Delany – Bazley model as reported elsewhere showing that the model is inadequate for very low and very high frequencies [172].

Four other empirical models (Figure 6.41) were employed with four layers AT fabrics so as to compare the behavior of the predicted models, it was observed that the models are in agreement with experimental data up to the frequency of 3500Hz and thereafter the models' under predicted the sound absorption

behavior. The underprediction of the models could be due to the fact that barkcloth is a highly anisotropic material with not uniform fiber distribution network that rendered the underprediction at higher frequencies.

Table 6.7. Airflow resistivity of samples

Samples	Sample Thickness [mm]	Air permeability [mms^{-1}]	Airflow resistivity [$Pa.s.m^{-2}$]
S1	1.47	720	94482.24
S2	1.17	571	149684.91
S3	1.50	566	117785.63
S4	0.91	736	149307.21

6.7.3.1. Effect of Air gap on the Acoustic Properties

Since barkcloth is a new material and with prospects of sound absorption applications, another material design parameter was implemented in the model whereby an air gap was incorporated between the two material layers.

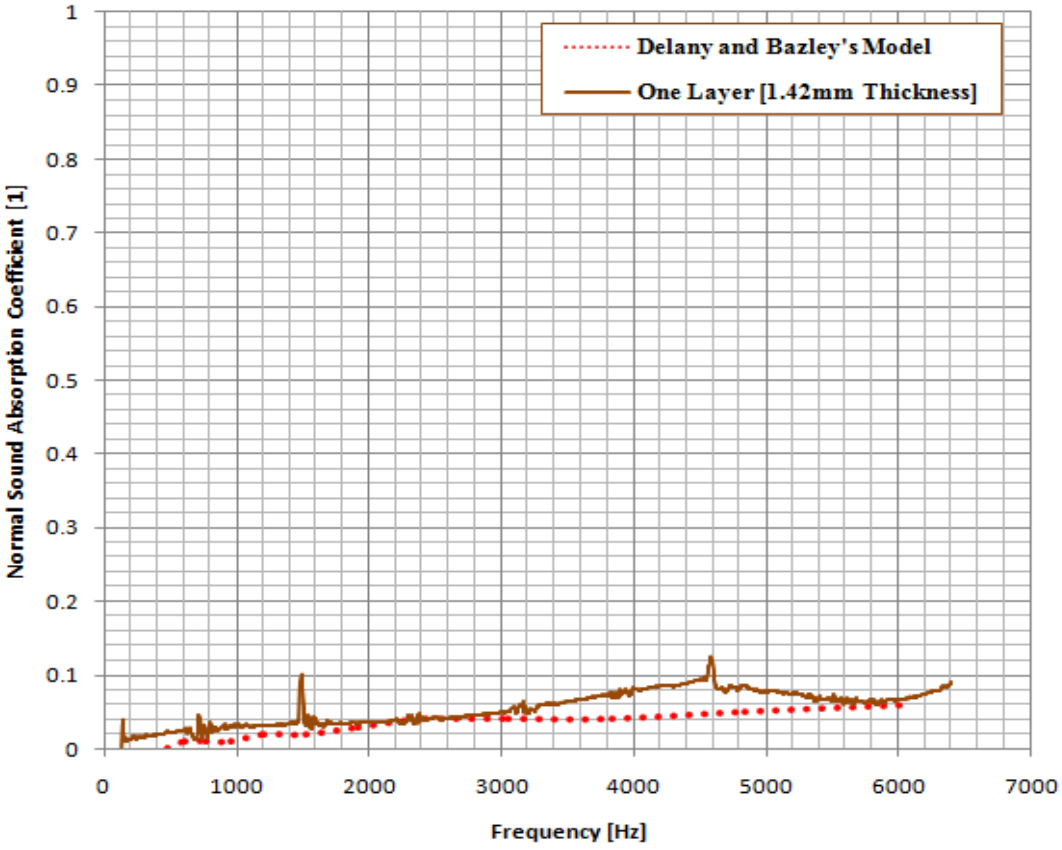

Figure 6.40 Delany – Bazley model with one layer Antiaris toxicaria fabrics

The Allard – Champoux model was utilized for prediction of the behavior of two layers AT fabrics. It's observed that the model is in good agreement with the experimental data.

Incorporation of an air gap between the two AT fabrics was observed to have positive effects on the sound absorption properties. The larger the distance between the airgap, the higher the absorption at lower frequencies and reduction in the absorption at higher frequencies (Figure 6.42).

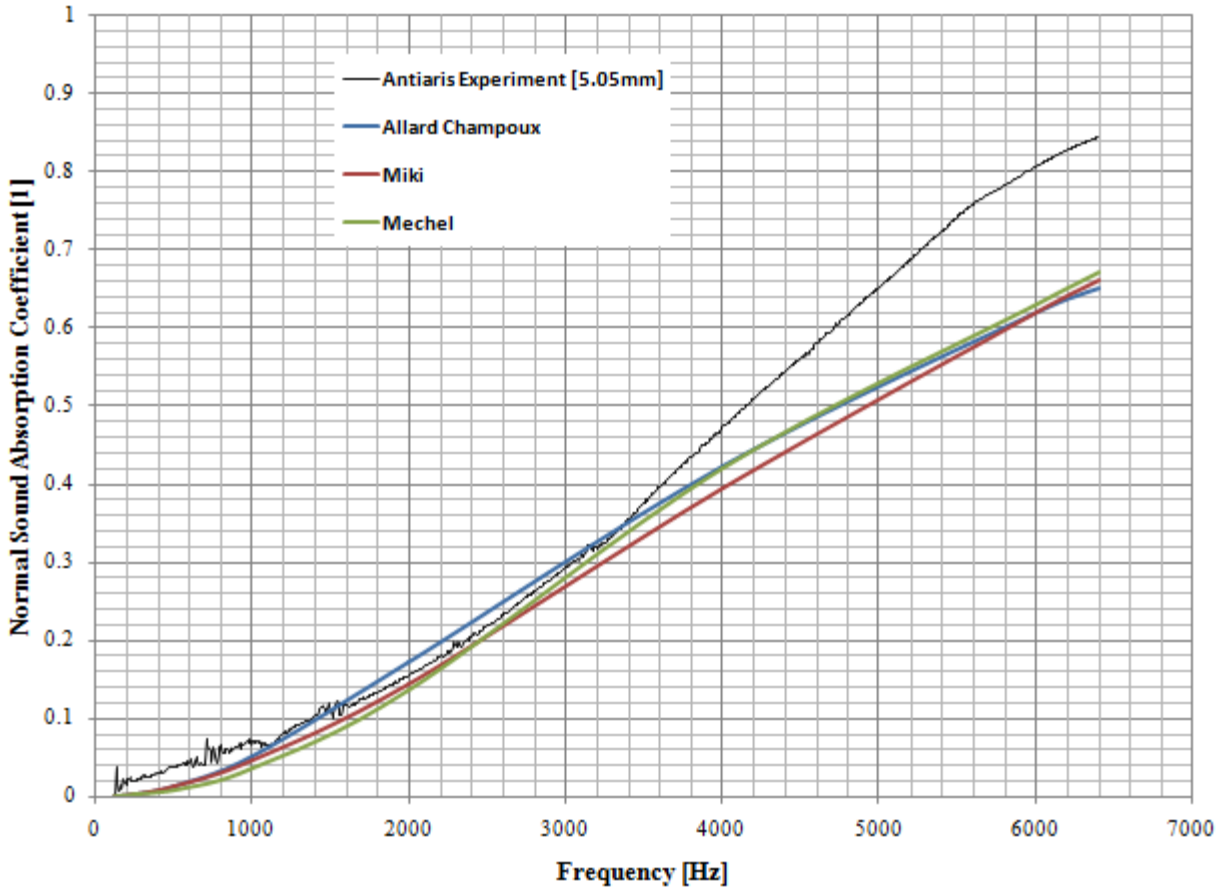

Figure 6.41. Sound Absorption Models of Antiaris toxicaria 4-layer fabrics.

In the long run, the introduction of a small air gap between the layers would gradually increase the sound absorption of two layers AT fabrics reaching a sound absorption coefficient of 0.78 at frequencies of above 4000Hz.

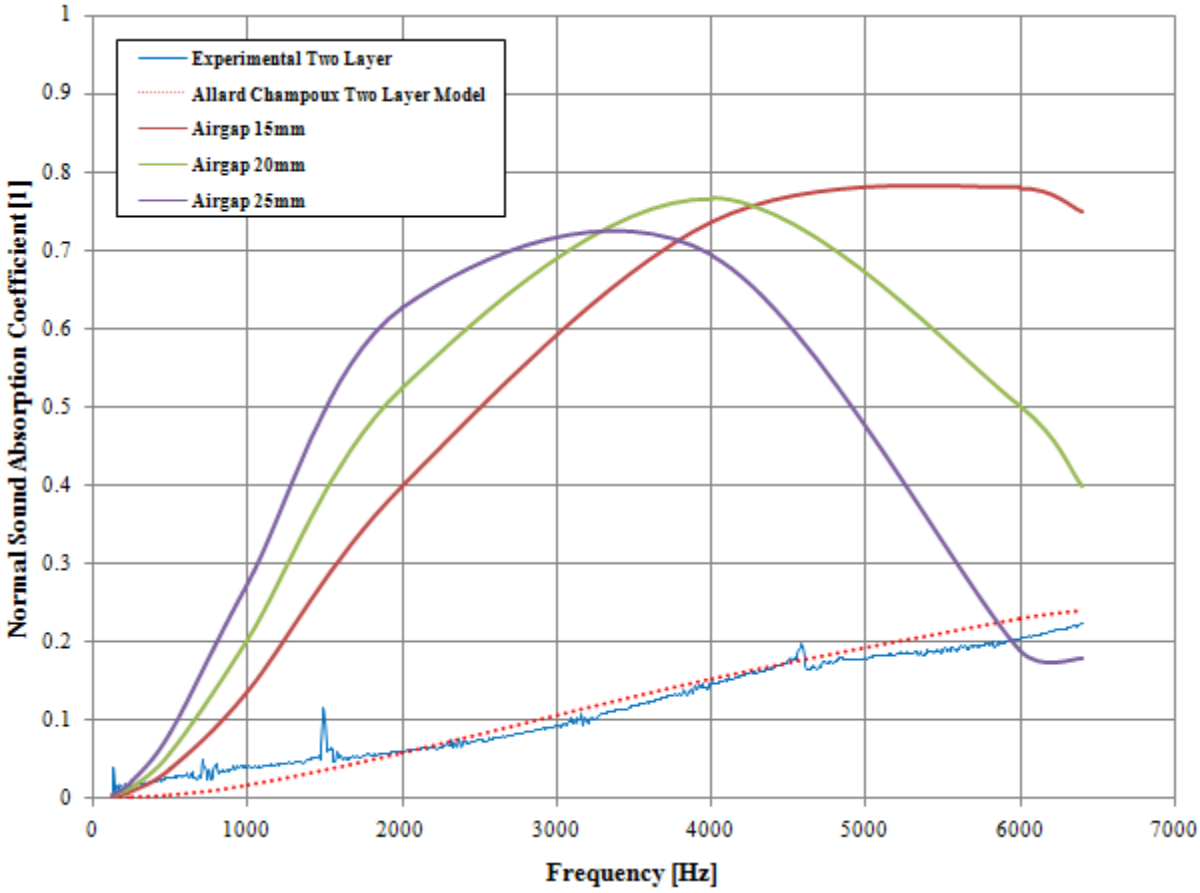

Figure 6.42. Prediction Model of behavior of fabrics wih incorporation of an air gap in between.

CHAPTER 7

CONCLUSIONS

7.0. PROLOGUE

This chapter summarizes the major findings of the investigation and presents the new knowledge that has been contributed by the study.

7.1. MORPHOLOGY AND THERMO-PHYSIOLOGICAL PROPERTIES

The fabric morphology is made up of a dense network of micro-fibers that are naturally bonded and aligned at angles. The inter-fiber bond gives the strength of the load bearing microfibers and damage is initiated through separation of the individual fibers through the failure of the inter-fiber bond and thence fracture. The transverse section of the fabric is characterized by air cavities and microfibers surrounded by plant material.

Barkcloth is majorly composed of Cellulose (69%); based on the Crystallinity Index, barkcloth has highly ordered crystallites (79%) higher than jute (71%) and sisal (71%). Treatment with alkaline solution aided the fiber to matrix adhesion and also helped to dissolve the lignin, wax and other plant impurities.

Enzyme treatment eroded the strength of the fabric, whereas treatment with plasma had a slight effect on the reinforced laminar composites.

The thermal conductivity of barkcloth is comparable to cotton rendering the barkcloth from *F. natalensis*, a comfortable fabric. The lower value of thermal absorptivity of barkcloth, compared to the value of cotton, shows that the fabric has a warm feeling when in contact with the skin. Barkcloth had a higher water vapor permeability compared to cotton and other fabrics meaning its clothing comfort properties are reasonable. In terms of clothing comfort, the fabric fulfills all the requirements for thermal clothing comfort.

7.2. THERMAL BEHAVIOR

The biocomposites exhibited a high glass transition temperature in the range of 163-185^{o}C depending on the frequency. The thermal analysis illustrated that bark cloth biocomposites are stable until 290^{o}C, a crucial intrinsic temperature that is important if other serial production techniques such as compression moulding are to be used with thermoplastic resins. Synthetic epoxy composites had a low glass transition temperature ranging from 60-70^{o}C.

7.3. MECHANICAL PROPERTIES

For the first time, biodegradable barkcloth reinforced green epoxy biocomposites have been developed for the possible application in interior automotive panels. Production of barkcloth composites through the hierarchal architecture of the plies yields varying mechanical properties. Comparative evaluation of the effect layering pattern showed that the ply stacking sequence 90^o, 0^o, -45^o, 45^o had one of the best mechanical properties and, therefore, was chosen as the stacking sequence for the investigation of barkcloth reinforced green epoxy biocomposites. The static mechanical properties show that that alkaline treated biocomposites had an average tensile strength 33MPa and modulus of approximately 4GPa. The flexural strength of the composites was 207MPa. The biocomposites exhibited glass transition temperature in the range of 163^oC to 185^oC depending on the frequency. The developed biocomposites with an average strength of 33MPa higher was higher than the 25MPa threshold strength needed for car instrument or dashboard panels, make barkcloth reinforced green epoxy composites an alternative material for interior automotive panels.

The dynamical mechanical properties showed that the optimum temperature range of application of biocomposites was up to130^oC. Beyond this temperature, the composites enter into a rubbery state and the performance is diminished.

7.4. THERMO-ACOUSTIC PROPERTIES

In this investigation, for the first time, barkcloth was presented as a potential sound absorption material. The results show that barkcloth nonwoven fabric had good sound absorption properties and can be used as an alternative replacement for the synthetic commercial fibers which are widely used in the industry. The investigated sound absorption properties showed that *Antiaris toxicaria* barkcloth had higher sound absorption properties at higher frequencies. Increasing the barkcloth fiber layers showed a positive trend towards sound absorption coefficient, therefore giving a prediction of multi-layer products of antiaris barkcloth with potential to provide positive results even at low frequency ranges. Production of composites showed that there's a decrease in the sound absorption properties that's due to the decrease in the porosity and thickness due to the compression of the fabrics under pressure, therefore reducing the vibration of the fibers since they are bonded in the matrix that increases stiffness and thereafter decreasing the overall acoustic properties of the barkcloth reinforced composites. Empirical sound absorption models nearly predicted the sound absorption behavior of barkcloth fabrics, but due to the scope of work, there's need for further modification of existing models and further testing for a perfect model. Nevertheless, the Allard-Champoux model is preferred for predicting the barkcloth sound absorption properties.

CHAPTER 8

APPLICATIONS AND FUTURE WORK

8.0. PROLOGUE

This chapter introduces to the reader the proposed application of barkcloth and some already available concepts of barkcloth.

8.1. AUTOMOTIVE APPLICATIONS

BFRP can be applied in automotive instrument panels. Whereas the layered fabrics can find applications in car headliners.

Figure 8.0. Scheme of flow of barkcloth automotive panel development

8.1.1. Headliners

Headliners are materials installed on the ceilings inside of vehicles and are intended for the purpose of occupant protection through thermal insulation and sound absorption. A good headliner should be able to keep outside heat out of the vehicle and also preserve interior heat for the best comfort of the occupants. Typical car headliners have 200-220g/m^2 [173]. Barkcloth has a low thermal conductivity and yet has high sound absorption properties; therefore, its application in car headliners is a novel concept that will serve the triple purpose of decoration, thermal insulation through restriction of heat migration and sound absorption through reduction of noise inside the vehicle.

Thinsulate™ brand acoustic insulation used in vehicles made by the 3M company is shown in Figure 8.1(B). Sound absorbing properties of Thinsulate acoustical insulation material AU1220, were measured according to ASTM E1050, Dual Microphone Impedance Tube Method measuring Normal Incidence Sound [173]. Barkcloth offers a sustainable green alternative with superior sound insulation properties at higher frequencies which are unpleasant to the human ear.

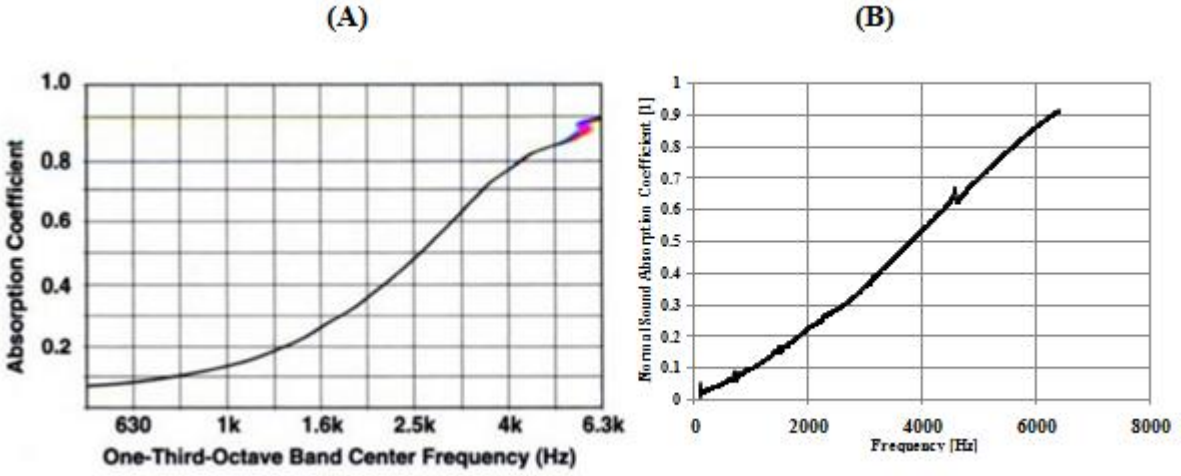

Figure 8.1. Comparision of Acoustical insulation of commercial Thinsulate™ from 3M Company (A); Barkcloth (Antiaris toxicaria) non woven fabric (B)

8.1.2. Gear Lever and Steering Wheel Fabric Cover

Figure 8.2. Barkcloth fabric and reinforced composite automotive applications.
Image courtesy of Barktex

8.2. FOOTWEAR

Just like clothing, closed shoes are supposed to keep the wearer's feet warm. The low thermal conductivity exhibited by barkcloth (0.035m^2.K/W) compared to commercial synthetics such as Thinsulate™ (0.036m^2.K/W) which are widely used for thermal insulation in sleeping bags, shoes and winter jackets, render barkcloth fabric shoes sustainable and an alternative to synthetic canvas.

Figure 8.3. Barkcloth fabric and reinforced footwear applications.
Image courtesy of Barktex

8.3. PANELING AND FURNITURE

Figure 8.4. Barkcloth in wall décor and panels.
Image courtesy of Barktex

8.4. FUTURE WORK

This work has endeavored to introduce barkcloth to the scientific community, a material with a lot of potential and yet minimal research had been done. Due to the scope of the task, the following is recommended for follow-up work.

1. Extraction of barkcloth nanofibrils for reinforcement of films.
2. Coatings of barkcloth for applied applications such as electromagnetic shielding.
3. Investigation of the Creep and Fatigue behavior of Barkcloth Reinforced Composites.
4. Investigation of Durability, Abrasion resistance and Weathering

REFERENCES

[1] J. Rwawiire, Samson, Wandera, No Title, in: Nat. Fibers A Blue Print Ecofriendly Text. Biocomposites, Proceedings of XVth International Scientific and Practical Workshop: Physics of Fibrous Materials, 2012: pp. 67–73.

[2] United Nations Framework Convention on Climate Change, 1992.

[3] G. Koronis, A. Silva, M. Fontul, Green composites: A review of adequate materials for automotive applications, Compos. Part B Eng. 44 (2013) 120–127. doi:http://dx.doi.org/10.1016/j.compositesb.2012.07.004.

[4] D.B. Dittenber, H.V.S. Gangarao, Critical review of recent publications on use of natural composites in infrastructure, Compos. Part A Appl. Sci. Manuf. 43 (2012) 1419–1429. doi:10.1016/j.compositesa.2011.11.019.

[5] A. Mwasha, Designing bio-based geotextiles for reinforcing an embankment erected on the soft soil, Mater. Des. 30 (2009) 2657–2664. doi:10.1016/j.matdes.2008.10.029.

[6] P. Methacanon, U. Weerawatsophon, N. Sumransin, C. Prahsarn, D.T. Bergado, Properties and potential application of the selected natural fibers as limited life geotextiles, Carbohydr. Polym. 82 (2010) 1090–1096. doi:10.1016/j.carbpol.2010.06.036.

[7] S.M. Sapuan, M. a. Maleque, Design and fabrication of natural woven fabric reinforced epoxy composite for household telephone stand, Mater. Des. 26 (2005) 65–71. doi:10.1016/j.matdes.2004.03.015.

[8] J. Summerscales, N.P.J. Dissanayake, A.S. Virk, W. Hall, A review of bast fibres and their composites. Part 1 – Fibres as reinforcements, Compos. Part A Appl. Sci. Manuf. 41 (2010) 1329–1335. doi:10.1016/j.compositesa.2010.06.001.

[9] F.P. La Mantia, M. Morreale, Green composites: A brief review, Compos. Part A Appl. Sci. Manuf. 42 (2011) 579–588. doi:10.1016/j.compositesa.2011.01.017.

[10] F.M. AL-Oqla, S.M. Sapuan, Natural fiber reinforced polymer composites in industrial applications: feasibility of date palm fibers for sustainable automotive industry, J. Clean. Prod. 66 (2014) 347–354. doi:10.1016/j.jclepro.2013.10.050.

[11] E.D.H. Favoino, The potential role of compost in reducing greenhouse gases, Waste Manag. Res. 26 (2008) 61–69.

[12] Directive 2000/53/EC of the European Parliament and The Council For End-of-life Vehicles, Off. J. Eur. Communities. ABl.EG Nr. (2000).

[13] C. Alves, P.M.C. Ferrão, A.J. Silva, L.G. Reis, M. Freitas, L.B. Rodrigues, et al., Ecodesign of automotive components making use of natural jute fiber composites, J. Clean. Prod. 18 (2010) 313–327. doi:http://dx.doi.org/10.1016/j.jclepro.2009.10.022.

[14] M. Karus, M. Kaup, S. Ortmann, Use of Natural Fibres in Composites in the German and Austrian Automotive Industry—Market Survey 2002, J. Ind. Hemp. 8 (2003) 73–78. doi:10.1300/J237v08n02_05.

[15] M.M. Farag, Quantitative methods of materials substitution: Application to automotive components, Mater. Des. 29 (2008) 374–380. doi:http://dx.doi.org/10.1016/j.matdes.2007.01.028.

[16] J. Njuguna, P. Wambua, K. Pielichowski, K. Kayvantash, Natural Fibre-Reinforced Polymer Composites and Nanocomposites for Automotive Applications, in: S. Kalia, B.S. Kaith, I. Kaur (Eds.), Cellul. Fibers Bio- Nano-Polymer Compos. SE - 23, Springer Berlin Heidelberg, 2011: pp. 661–700. doi:10.1007/978-3-642-17370-7_23.

[17] A.M. Cunha, A.R. Campos, C. Cristovão, C. Vila, V. Santos, J.C. Parajó, Sustainable materials in

automotive applications, Plast. Rubber Compos. 35 (2006) 233–241. doi:10.1179/174328906X146487.

[18] N. Ayrilmis, S. Jarusombuti, V. Fueangvivat, P. Bauchongkol, R. White, Coir fiber reinforced polypropylene composite panel for automotive interior applications, Fibers Polym. 12 (2011) 919–926. doi:10.1007/s12221-011-0919-1.

[19] G. Mougin, M. Magnani, N. Eikelenberg, Natural-fibres composites for the automotive industry: challenges, solutions and applications, Int. J. Mater. Prod. Technol. 36 (2009) 176–188. doi:10.1504/IJMPT.2009.027829.

[20] K. Wötzel, R. Wirth, M. Flake, Life cycle studies on hemp fibre reinforced components and ABS for automotive parts, Die Angew. Makromol. Chemie. 272 (1999) 121–127. doi:10.1002/(SICI)1522-9505(19991201)272:1<121::AID-APMC121>3.0.CO;2-T.

[21] M. Karus, M. Kaup, Natural Fibres in the European Automotive Industry, J. Ind. Hemp. 7 (2002) 119–131. doi:10.1300/J237v07n01_10.

[22] D. Puglia, J. Biagiotti, J.M. Kenny, A Review on Natural Fibre-Based Composites—Part II, J. Nat. Fibers. 1 (2005) 23–65. doi:10.1300/J395v01n03_03.

[23] C. Baillie, ed., Green Composites: Polymer Composites and the Environment, illustrate, CRC Press, 2005.

[24] T.D. Hapuarachchi, Development and characterisation of flame retardant nanoparticulate bio-based polymer composites, Queen Mary University of London, 2010.

[25] A.K. Mohanty, M. Misra, L.T. Drzal, Natural fibers, biopolymers, and biocomposites, CRC Press, 2005.

[26] S. Rwawiire, B. Tomkova, Morphological, Thermal, and Mechanical Characterization of *Sansevieria trifasciata* Fibers, J. Nat. Fibers. 12 (2015) 201–210. doi:10.1080/15440478.2014.914006.

[27] K. Ramanaiah, A. V Ratna Prasad, K. Hema Chandra Reddy, Mechanical, thermophysical and fire properties of sansevieria fiber-reinforced polyester composites, Mater. Des. 49 (2013) 986–991. doi:http://dx.doi.org/10.1016/j.matdes.2013.02.056.

[28] V.S. Sreenivasan, S. Somasundaram, D. Ravindran, V. Manikandan, R. Narayanasamy, Microstructural, physico-chemical and mechanical characterisation of Sansevieria cylindrica fibres – An exploratory investigation, Mater. Des. 32 (2011) 453–461. doi:http://dx.doi.org/10.1016/j.matdes.2010.06.004.

[29] D.C.O. Nascimento, A.S. Ferreira, S.N. Monteiro, R.C.M.P. Aquino, S.G. Kestur, Studies on the characterization of piassava fibers and their epoxy composites, Compos. Part A Appl. Sci. Manuf. 43 (2012) 353–362. doi:http://dx.doi.org/10.1016/j.compositesa.2011.12.004.

[30] I.M. De Rosa, J.M. Kenny, M. Maniruzzaman, M. Moniruzzaman, M. Monti, D. Puglia, et al., Effect of chemical treatments on the mechanical and thermal behaviour of okra (Abelmoschus esculentus) fibres, Compos. Sci. Technol. 71 (2011) 246–254. doi:http://dx.doi.org/10.1016/j.compscitech.2010.11.023.

[31] M.A. Norul Izani, M.T. Paridah, U.M.K. Anwar, M.Y. Mohd Nor, P.S. H'ng, Effects of fiber treatment on morphology, tensile and thermogravimetric analysis of oil palm empty fruit bunches fibers, Compos. Part B Eng. 45 (2013) 1251–1257. doi:http://dx.doi.org/10.1016/j.compositesb.2012.07.027.

[32] J.D.D. Melo, L.F.M. Carvalho, A.M. Medeiros, C.R.O. Souto, C.A. Paskocimas, A biodegradable composite material based on polyhydroxybutyrate (PHB) and carnauba fibers, Compos. Part B Eng. 43 (2012) 2827–2835. doi:http://dx.doi.org/10.1016/j.compositesb.2012.04.046.

[33] S. Rwawiire, G.W. Luggya, B. Tomkova, Morphology , Thermal , and Mechanical Characterization of Bark Cloth from Ficus natalensis, 2013 (2013).

[34] P. Wambua, J. Ivens, I. Verpoest, Natural fibres: can they replace glass in fibre reinforced plastics?, Compos. Sci. Technol. 63 (2003) 1259–1264. doi:http://dx.doi.org/10.1016/S0266-3538(03)00096-4.

[35] Global Natural Fibre Composites Market 2014-2019: Trends, Forecast and Opportunity Analysis, (n.d.). 26. http://www.researchandmarkets.com/reports/2881528/global-natural-fiber-composites-market-2014-2019.

[36] J. HOBSON, M. CARUS, Targets for bio-based composites and natural fibres, JEC Compos. (n.d.) 31–32. http://cat.inist.fr/?aModele=afficheN&cpsidt=23939041 (accessed October 11, 2015).

[37] A. Hodzic, R. Shanks, Natural fibre composites: Materials, processes and properties, Woodhead Publishing, 2014.

[38] L. Herrera-estrada, S. Pillay, U. Vaidya, BANANA FIBER COMPOSITES FOR AUTOMOTIVE AND TRANSPORTATION APPLICATIONS Lina Herrera-Estrada , Selvum Pillay and Uday Vaidya, (n.d.).

[39] G. Siqueira, J. Bras, A. Dufresne, Cellulosic Bionanocomposites: A Review of Preparation, Properties and Applications, (2010) 728–765. doi:10.3390/polym2040728.

[40] X. Li, Æ.L.G. Tabil, Æ.S. Panigrahi, Chemical Treatments of Natural Fiber for Use in Natural Fiber-Reinforced Composites : A Review, (2007) 25–33. doi:10.1007/s10924-006-0042-3.

[41] M.J. John, R.D. Anandjiwala, Recent Developments in Chemical Modification and Characterization of Natural Fiber-Reinforced Composites, (2008). doi:10.1002/pc.

[42] S. Kalia, B.S. Kaith, I. Kaur, Pretreatments of natural fibers and their application as reinforcing material in polymer composites—a review, Polym. Eng. Sci. 49 (2009) 1253–1272.

[43] F. El-Hosseiny, D.H. Page, The mechanical properties of single wood pulp fibres: theories of strength, Fibre Sci. Technol. 8 (1975) 21–31.

[44] A. Dufresne, Polymer nanocomposites from biological sources, Encycl. Nanosci. Nanotechnol. 21 (2010) 219–250.

[45] A.K. Bledzki, J. Gassan, Composites reinforced with cellulose based fibres, Prog. Polym. Sci. 24 (1999) 221–274.

[46] E. Sjostrom, Wood chemistry: fundamentals and applications, Elsevier, 2013.

[47] F. Tanaka, T. Iwata, Estimation of the elastic modulus of cellulose crystal by molecular mechanics simulation, Cellulose. 13 (2006) 509–517.

[48] D. Fengel, G. Wegener, Wood: chemistry, ultrastructure, reactions, Walter de Gruyter, 1983.

[49] A.R. Sena, M.A.M. Araujo, F.V.D. Souza, L.H.C. Mattoso, J.M. Marconcini, Characterization and comparative evaluation of thermal , structural , chemical , mechanical and morphological properties of six pineapple leaf fiber varieties for use in composites, Ind. Crop. Prod. 43 (2013) 529–537. doi:10.1016/j.indcrop.2012.08.001.

[50] H.V. Scheller, P. Ulvskov, Hemicelluloses, Plant Biol. 61 (2010) 263.

[51] D.N.-S. Hon, N. Shiraishi, Wood and cellulosic chemistry, revised, and expanded, CRC Press, 2000.

[52] D. Lopes, S.N. Monteiro, F. Perisse, A.P. Barbosa, A.B. Bevitori, O.A.D.A. Silva, et al., Natural Lignocellulosic Fibers as Engineering Materials — An Overview, 42 (2011) 20–22.

doi:10.1007/s11661-011-0789-6.

[53] S.N. Monteiro, V. Calado, R.J.S. Rodriguez, F.M. Margem, Thermogravimetric behavior of natural fibers reinforced polymer composites-An overview, Mater. Sci. Eng. A. 557 (2012) 17–28. doi:10.1016/j.msea.2012.05.109.

[54] M. Ho, H. Wang, J. Lee, C. Ho, K. Lau, J. Leng, et al., Composites : Part B Critical factors on manufacturing processes of natural fibre composites, Compos. Part B. 43 (2012) 3549–3562. doi:10.1016/j.compositesb.2011.10.001.

[55] A. Célino, S. Fréour, F. Jacquemin, P. Casari, The hygroscopic behavior of plant fibers: A review, Front. Chem. 1 (2013).

[56] D. Nabi Saheb, J.P. Jog, Natural fiber polymer composites: A review, Adv. Polym. Technol. 18 (1999) 351–363. doi:10.1002/(SICI)1098-2329(199924)18:4<351::AID-ADV6>3.0.CO;2-X.

[57] R. Masoodi, K.M. Pillai, Journal of Reinforced Plastics and Composites, (2012). doi:10.1177/0731684411434654.

[58] D. Li, W. Wang, F. Tian, W. Liao, C.J. Bae, The oldest bark cloth beater in southern China (Dingmo, Bubing basin, Guangxi), Quat. Int. 354 (2014) 184–189.

[59] UNESCO, Bark Cloth Making in Uganda, (n.d.). http://www.unesco.org/culture/intangible-heritage/40afr_uk.htm.

[60] L. Robertson, Rethinking Material Culture: Ugandan Bark Cloth, (2014).

[61] G. Marsh, Next step for automotive materials, Mater. Today. 6 (2003) 36–43.

[62] R.E. Drumright, P.R. Gruber, D.E. Henton, Polylactic acid technology, Adv. Mater. 12 (2000) 1841–1846.

[63] G. Mehta, A.K. Mohanty, M. Misra, L.T. Drzal, Biobased resin as a toughening agent for biocomposites, Green Chem. 6 (2004) 254–258.

[64] T. Peijs, Composites turn green, Dep. Mater. Queen Mary, Univ. London. (2002).

[65] S. THOMAS, Biomass grass makes for compostable cars, Mater. World. 9 (2001).

[66] A.M. Thayer, Chasing the innovation wave, Chem. Eng. News. 77 (1999) 17–21.

[67] J. Holbery, D. Houston, Natural-fiber-reinforced polymer composites in automotive applications, Jom. 58 (2006) 80–86.

[68] J. Gassan, A.K. Bledzki, Effect of moisture content on the properties of silanized jute-epoxy composites, Polym. Compos. 18 (1997) 179–184.

[69] V. Mishra, S. Biswas, Physical and mechanical properties of bi-directional jute fiber epoxy composites, Procedia Eng. 51 (2013) 561–566.

[70] P. Ganan, S. Garbizu, R. Llano-Ponte, I. Mondragon, Surface modification of sisal fibers: effects on the mechanical and thermal properties of their epoxy composites, Polym. Compos. 26 (2005) 121–127.

[71] E.T.N. Bisanda, M.P. Ansell, The effect of silane treatment on the mechanical and physical properties of sisal-epoxy composites, Compos. Sci. Technol. 41 (1991) 165–178.

[72] D. Bachtiar, S.M. Sapuan, M.M. Hamdan, The effect of alkaline treatment on tensile properties of sugar palm fibre reinforced epoxy composites, Mater. Des. 29 (2008) 1285–1290.

[73] S.M. Sapuan, A. Leenie, M. Harimi, Y.K. Beng, Mechanical properties of woven banana fibre reinforced epoxy composites, Mater. Des. 27 (2006) 689–693.

[74] J. Gassan, A.K. Bledzki, Possibilities for improving the mechanical properties of jute/epoxy

composites by alkali treatment of fibres, Compos. Sci. Technol. 59 (1999) 1303–1309.

[75] J. Gassan, V.S. Gutowski, Effects of corona discharge and UV treatment on the properties of jute-fibre epoxy composites, Compos. Sci. Technol. 60 (2000) 2857–2863.

[76] P.K. Kushwaha, R. Kumar, Effect of silanes on mechanical properties of bamboo fiber-epoxy composites, J. Reinf. Plast. Compos. 29 (2010) 718–724.

[77] B.F. Yousif, A. Shalwan, C.W. Chin, K.C. Ming, Flexural properties of treated and untreated kenaf/epoxy composites, Mater. Des. 40 (2012) 378–385.

[78] A.V.R. Prasad, K.M. Rao, Mechanical properties of natural fibre reinforced polyester composites: Jowar, sisal and bamboo, Mater. Des. 32 (2011) 4658–4663.

[79] M. Baiardo, E. Zini, M. Scandola, Flax fibre–polyester composites, Compos. Part A Appl. Sci. Manuf. 35 (2004) 703–710.

[80] K.G. Satyanarayana, K. Sukumaran, A.G. Kulkarni, S.G.K. Pillai, P.K. Rohatgi, Fabrication and properties of natural fibre-reinforced polyester composites, Composites. 17 (1986) 329–333.

[81] R. Malkapuram, V. Kumar, Y.S. Negi, Journal of Reinforced Plastics and Recent Development in Natural Fiber, (2009). doi:10.1177/0731684407087759.

[82] R. Malkapuram, V. Kumar, Y.S. Negi, Recent development in natural fiber reinforced polypropylene composites, J. Reinf. Plast. Compos. (2008).

[83] A.K. Mohanty, M. Misra, L.T. Drzal, Surface modifications of natural fibers and performance of the resulting biocomposites: an overview, Compos. Interfaces. 8 (2001) 313–343.

[84] M.M. Kabir, H. Wang, K.T. Lau, F. Cardona, Composites : Part B Chemical treatments on plant-based natural fibre reinforced polymer composites : An overview, Compos. Part B. 43 (2012) 2883–2892. doi:10.1016/j.compositesb.2012.04.053.

[85] R.F. Gibson, Principles of composite material mechanics, CRC press, 2011.

[86] N. Malhotra, K. Sheikh, S. Rani, A review on mechanical characterization of natural fiber reinforced polymer composites, J. Eng. Res. Stud. 3 (2012) 75–80.

[87] K. Pietrak, T.S. Wi, A review of models for e ff ective thermal conductivity of composite materials, 95 (2015) 14–24.

[88] J.-K. Lee, Prediction of thermal conductivity of composites with spherical fillers by successive embedding, Arch. Appl. Mech. 77 (2007) 453–460.

[89] P. Meshgin, Y. Xi, Multi-scale composite models for the effective thermal conductivity of PCM-concrete, Constr. Build. Mater. 48 (2013) 371–378. doi:http://dx.doi.org/10.1016/j.conbuildmat.2013.06.068.

[90] J.C. Maxwell, A treatise on electricity and magnetism, Clarendon Press, 1892.

[91] S.C. Cheng, R.I. Vachon, The prediction of the thermal conductivity of two and three phase solid heterogeneous mixtures, Int. J. Heat Mass Transf. 12 (1969) 249–264.

[92] A. Shalwan, B.F. Yousif, In State of Art : Mechanical and tribological behaviour of polymeric composites based on natural fibres, J. Mater. (2012). doi:10.1016/j.matdes.2012.07.014.

[93] P. Moszynski, WHO warns noise pollution is a growing hazard to health in Europe, BMJ. 342 (2011).

[94] U. Berardi, G. Iannace, Acoustic characterization of natural fibers for sound absorption applications, Build. Environ. (2015). doi:10.1016/j.buildenv.2015.05.029.

[95] M. Arenas, Jorge Crocker, Recent Trends in Porous Sound-Absorbing Materials, Noise Vib.

Control Mag. (2010) 12–17. http://www.sandv.com/downloads/1007croc.pdf.

[96] S.. Sapuan, H.. Abdalla, A prototype knowledge-based system for the material selection of polymeric-based composites for automotive components, Compos. Part A Appl. Sci. Manuf. 29 (1998) 731–742. doi:10.1016/S1359-835X(98)00049-9.

[97] O. Faruk, A.K. Bledzki, H.-P. Fink, M. Sain, Progress Report on Natural Fiber Reinforced Composites, Macromol. Mater. Eng. 299 (2014) 9–26. doi:10.1002/mame.201300008.

[98] F. Asdrubali, Survey on The Acoustical Properties of New Sustainable Materials for Noise Control, Euronoise. (2006) 1–10.

[99] J. Rouquerolt, D. Avnir, C.W. Fairbridge, D.H. Everett, J.H. Haynes, N. Pernicone, et al., Recommendations for the characterization of porous solids, Pure Appl. Chem. 66 (1994) 1739–1758. doi:doi:10.1351/pac199466081739.

[100] C. Wassilieff, Sound absorption of wood-based materials, Appl. Acoust. 48 (1996) 339–356. doi:10.1016/0003-682X(96)00013-8.

[101] D.T. Liu, K.F. Xia, R.D. Yang, J. Li, K.F. Chen, M.M. Nazhad, Manufacturing of a biocomposite with both thermal and acoustic properties, J. Compos. Mater. . 46 (2012) 1011–1020. doi:10.1177/0021998311414069.

[102] J. Mohammad, N. Johari, M. Fouladi, Numerical Investigation on the Sound Absorption Coefficients of Malaysian Wood, Proc. 20th Int. Congr. Acoust. ICA 2010. (2010) 7. http://www.acoustics.asn.au/conference_proceedings/ICA2010/cdrom-ICA2010/papers/p746.pdf.

[103] N. Okuda, M. Sato, Manufacture and mechanical properties of binderless boards from kenaf core, J. Wood Sci. 50 (2004) 53–61. doi:10.1007/s10086-003-0528-8.

[104] J. Zhao, X.-M. Wang, J.M. Chang, Y. Yao, Q. Cui, Sound insulation property of wood–waste tire rubber composite, Compos. Sci. Technol. 70 (2010) 2033–2038. doi:10.1016/j.compscitech.2010.03.015.

[105] Z. Jiang, R. Zhao, B. Fei, Sound absorption property of wood for five eucalypt species, J. For. Res. 15 (2004) 207–210.

[106] S. Fatima, A.R. Mohanty, Acoustical and fire-retardant properties of jute composite materials, Appl. Acoust. 72 (2011) 108–114. doi:10.1016/j.apacoust.2010.10.005.

[107] Y. Na, G. Cho, Sound absorption and viscoelastic property of acoustical automotive nonwovens and their plasma treatment, Fibers Polym. 11 (2010) 782–789. doi:10.1007/s12221-010-0782-5.

[108] G. Thilagavathi, E. Pradeep, T. Kannaian, L. Sasikala, Development of Natural Fiber Nonwovens for Application as Car Interiors for Noise Control, J. Ind. Text. 39 (2010) 267–278. doi:10.1177/1528083709347124.

[109] S. Sengupta, Sound reduction by needle-punched nonwoven fabrics, Indian J. Fibre Text. Res. 35 (2010) 237–242.

[110] W. Yang, Y. Li, Sound absorption performance of natural fibers and their composites, Sci. China Technol. Sci. 55 (2012) 2278–2283. doi:10.1007/s11431-012-4943-1.

[111] L. Ismail, M. Ghazali, Sound Absorption of Arenga Pinnata Natural Fiber, World Acad. Sci. …. 4 (2010) 804–806. http://www.waset.ac.nz/journals/waset/v43/v43-143.pdf.

[112] and M.Z.N. Zulkifh, R., MJ Mohd Nor, MF Mat Tahir, A. R. Ismail, Acoustics Properties of multi-layer coir fibers sound Absorption Panel, J. Appl. Sci. 8 (2008) 3709–3714.

[113] M. Hosseini Fouladi, M. Ayub, M. Jailani Mohd Nor, Analysis of coir fiber acoustical characteristics, Appl. Acoust. 72 (2011) 35–42. doi:http://dx.doi.org/10.1016/j.apacoust.2010.09.007.

[114] S. Mahzan, a M.A. Zaidi, N. Arsat, M.N.M. Hatta, M.I. Ghazali, S.R. Mohideen, Study on Sound Absorption Properties of Coconut Coir Fibre Reinforced Composite with Added Recycled Rubber, Integr. Eng. (2009) 1–6.

[115] H. Xiang, D. Wang, H. Liua, N. Zhao, J. Xu, Investigation on sound absorption properties of kapok fibers, Chinese J. Polym. Sci. 31 (2013) 521–529. doi:10.1007/s10118-013-1241-8.

[116] H.-S. Yang, D.-J. Kim, H.-J. Kim, Rice straw–wood particle composite for sound absorbing wooden construction materials, Bioresour. Technol. 86 (2003) 117–121. doi:http://dx.doi.org/10.1016/S0960-8524(02)00163-3.

[117] H.S. Seddeq, N.M. Aly, a. Marwa A, M. Elshakankery, Investigation on sound absorption properties for recycled fibrous materials, J. Ind. Text. 43 (2012) 56–73. doi:10.1177/1528083712446956.

[118] K. Doost-hoseini, H.R. Taghiyari, A. Elyasi, Correlation between sound absorption coefficients with physical and mechanical properties of insulation boards made from sugar cane bagasse, Compos. Part B Eng. 58 (2014) 10–15. doi:10.1016/j.compositesb.2013.10.011.

[119] S. Ersoy, H. Küçük, Investigation of industrial tea-leaf-fibre waste material for its sound absorption properties, Appl. Acoust. 70 (2009) 215–220. doi:10.1016/j.apacoust.2007.12.005.

[120] M.E. Delany, E.N. Bazley, Acoustical properties of fibrous absorbent materials, Appl. Acoust. 3 (1970) 105–116.

[121] B. East, Acoustical characterisation of porous sound absorbing materials : a review Laith Egab , Xu Wang * and Mohammad Fard, 10 (2014).

[122] Y. Miki, Acoustical properties of porous materials. Modifications of Delany-Bazley models., J. Acoust. Soc. Japan. 11 (1990) 19–24.

[123] F.P. Mechel, I.L. Ver, Sound absorbing materials and sound absorbers, Noise Vib. Control Eng. John Wiley Sons, New York. (1992).

[124] Y. Champoux, J. Allard, Dynamic tortuosity and bulk modulus in air-saturated porous media, J. Appl. Phys. 70 (1991) 1975–1979.

[125] D.A. Bies, C.H. Hansen, Engineering noise control: theory and practice, CRC press, 2009.

[126] M. Harrison, Vehicle refinement: controlling noise and vibration in road vehicles, Elsevier, 2004.

[127] S. Rwawiire, B. Tomkova, J. Militky, A. Jabbar, B.M. Kale, Development of a biocomposite based on green epoxy polymer and natural cellulose fabric (bark cloth) for automotive instrument panel applications, Compos. Part B Eng. 81 (2015) 149–157. doi:http://dx.doi.org/10.1016/j.compositesb.2015.06.021.

[128] E. Ghassemieh, M. Acar, H. Versteeg, Microstructural analysis of non-woven fabrics using scanning electron microscopy and image processing. Part 1: development and verification of the methods, Proc. Inst. Mech. Eng. Part L J. Mater. Des. Appl. 216 (2002) 199–207.

[129] E. Ghassemieh, M. Acar, H.K. Versteeg, Microstructural analysis of non-woven fabrics using scanning electron microscopy and image processing. Part 2: application to hydroentangled fabrics, Proc. Inst. Mech. Eng. Part L J. Mater. Des. Appl. 216 (2002) 211–218.

[130] S.. b Rwawiire, B.. Tomkova, Comparative evaluation of thermal conductivity of bark cloth epoxy composites, in: Fiber Soc. Spring 2014 Tech. Conf. Fibers Prog., 2014. http://www.scopus.com/inward/record.url?eid=2-s2.0-84929538676&partnerID=40&md5=fbc6e4d19de4cdf815a389cb2b08237f.

[131] S. Rwawiire, B. Tomkova, E. Gliscinska, I. Krucinska, INVESTIGATION OF SOUND ABSORPTION PROPERTIES OF BARK CLOTH, 15 (2015). doi:10.1515/aut-2015-0010.

[132] B. Pourdehyhimi, R. Dent, A. Jerbi, S. Tanaka, A. Deshpande, Measuring fiber orientation in nonwovens part V: real webs, Text. Res. J. 69 (1999) 185–192.

[133] A. Porras, A. Maranon, I.A. Ashcroft, Characterization of a novel natural cellulose fabric from Manicaria saccifera palm as possible reinforcement of composite materials, Compos. Part B Eng. 74 (2015) 66–73.

[134] O. Demiryürek, D. Uysaltürk, Thermal comfort properties of Viloft/cotton and Viloft/polyester blended knitted fabrics, Text. Res. J. (2013) 0040517513478458.

[135] N. Oğlakcioğlu, A. Marmarali, Thermal comfort properties of some knitted structures, Fibres Text. East. Eur. 15 (2007) 94–96.

[136] P. Chidambaram, R. Govindan, K.C. Venkatraman, Study of thermal comfort properties of cotton/regenerated bamboo knitted fabrics, African J. Basic Appl. Sci. 4 (2012) 60–66.

[137] V. Fombuena, L. Bernardi, O. Fenollar, T. Boronat, R. Balart, Characterization of green composites from biobased epoxy matrices and bio-fillers derived from seashell wastes, Mater. Des. 57 (2014) 168–174.

[138] D. Bertomeu, D. García-Sanoguera, O. Fenollar, T. Boronat, R. Balart, Use of eco-friendly epoxy resins from renewable resources as potential substitutes of petrochemical epoxy resins for ambient cured composites with flax reinforcements, Polym. Compos. 33 (2012) 683–692.

[139] P.K. Mallick, Fiber-reinforced composites: materials, manufacturing, and design, CRC press, 2007.

[140] S.M. Sapuan, J.Y. Kho, E.S. Zainudin, Z. Leman, B.A.A. Ali, A. Hambali, Materials selection for natural fiber reinforced polymer composites using analytical hierarchy process, Indian J. Eng. Mater. Sci. 18 (2011) 255–267.

[141] A.K. Bledzki, A.A. Mamun, M. Lucka-Gabor, V.S. Gutowski, The effects of acetylation on properties of flax fibre and its polypropylene composites, Express Polym Lett. 2 (2008) 413–422.

[142] L. Hes, I. Dolezal, New method and equipment for measuring thermal properties of textiles, 繊維機械学会誌. 42 (1989) T124–T128.

[143] H. Höcker, Plasma treatment of textile fibers, Pure Appl. Chem. 74 (2002) 423–427.

[144] M. Åkerholm, B. Hinterstoisser, L. Salmén, Characterization of the crystalline structure of cellulose using static and dynamic FT-IR spectroscopy, Carbohydr. Res. 339 (2004) 569–578.

[145] A. Alemdar, M. Sain, Biocomposites from wheat straw nanofibers: Morphology, thermal and mechanical properties, Compos. Sci. Technol. 68 (2008) 557–565.

[146] M.A. AlMaadeed, R. Kahraman, P.N. Khanam, S. Al-Maadeed, Characterization of untreated and treated male and female date palm leaves, Mater. Des. 43 (2013) 526–531.

[147] J. Biagiotti, D. Puglia, L. Torre, J.M. Kenny, A. Arbelaiz, G. Cantero, et al., A systematic investigation on the influence of the chemical treatment of natural fibers on the properties of their polymer matrix composites, Polym. Compos. 25 (2004) 470–479.

[148] W. Liu, A.K. Mohanty, L.T. Drzal, P. Askel, M. Misra, Effects of alkali treatment on the structure, morphology and thermal properties of native grass fibers as reinforcements for polymer matrix composites, J. Mater. Sci. 39 (2004) 1051–1054.

[149] L.Y. Mwaikambo, M.P. Ansell, Chemical modification of hemp, sisal, jute, and kapok fibers by alkalization, J. Appl. Polym. Sci. 84 (2002) 2222–2234. doi:10.1002/app.10460.

[150] A.R.S. Neto, M.A.M. Araujo, F.V.D. Souza, L.H.C. Mattoso, J.M. Marconcini, Characterization and comparative evaluation of thermal, structural, chemical, mechanical and morphological

properties of six pineapple leaf fiber varieties for use in composites, Ind. Crops Prod. 43 (2013) 529–537.

[151] Y. Seki, M. Sarikanat, K. Sever, C. Durmuşkahya, Extraction and properties of Ferula communis (chakshir) fibers as novel reinforcement for composites materials, Compos. Part B Eng. 44 (2013) 517–523.

[152] H. Alamri, I.M. Low, Mechanical properties and water absorption behaviour of recycled cellulose fibre reinforced epoxy composites, Polym. Test. 31 (2012) 620–628. doi:http://dx.doi.org/10.1016/j.polymertesting.2012.04.002.

[153] I.M. De Rosa, J.M. Kenny, D. Puglia, C. Santulli, F. Sarasini, Morphological, thermal and mechanical characterization of okra (Abelmoschus esculentus) fibres as potential reinforcement in polymer composites, Compos. Sci. Technol. 70 (2010) 116–122. doi:10.1016/j.compscitech.2009.09.013.

[154] A. Alawar, A.M. Hamed, K. Al-Kaabi, Characterization of treated date palm tree fiber as composite reinforcement, Compos. Part B Eng. 40 (2009) 601–606.

[155] I.M. De Rosa, J.M. Kenny, D. Puglia, C. Santulli, F. Sarasini, Morphological, thermal and mechanical characterization of okra (Abelmoschus esculentus) fibres as potential reinforcement in polymer composites, Compos. Sci. Technol. 70 (2010) 116–122.

[156] L. Segal, J.J. Creely, A.E. Martin, C.M. Conrad, An empirical method for estimating the degree of crystallinity of native cellulose using the X-ray diffractometer, Text. Res. J. 29 (1959) 786–794.

[157] H. Deka, M. Misra, A. Mohanty, Renewable resource based "all green composites" from kenaf biofiber and poly (furfuryl alcohol) bioresin, Ind. Crops Prod. 41 (2013) 94–101.

[158] D.N. Saheb, J.P. Jog, Natural fiber polymer composites: A review, Adv. Polym. Technol. 18 (1999) 351–363. doi:10.1002/(SICI)1098-2329(199924)18:4<351::AID-ADV6>3.0.CO;2-X.

[159] S. Rwawiire, B. Tomkova, J. Militky, B.M. Kale, P. Prucha, Effect of Layering Pattern on the Mechanical Properties of Bark Cloth (*Ficus natalensis*) Epoxy Composites, Int. J. Polym. Anal. Charact. 20 (2015) 160–171. doi:10.1080/1023666X.2015.988534.

[160] M.Z. Rong, M.Q. Zhang, Y. Liu, G.C. Yang, H.M. Zeng, The effect of fiber treatment on the mechanical properties of unidirectional sisal-reinforced epoxy composites, Compos. Sci. Technol. 61 (2001) 1437–1447.

[161] A. Ridruejo, C. González, J. LLorca, A constitutive model for the in-plane mechanical behavior of nonwoven fabrics, Int. J. Solids Struct. 49 (2012) 2215–2229.

[162] F. Zhou, G. Cheng, B. Jiang, Effect of silane treatment on microstructure of sisal fibers, Appl. Surf. Sci. 292 (2014) 806–812. doi:10.1016/j.apsusc.2013.12.054.

[163] M. Ho, H. Wang, K. Lau, J. Leng, Effect of silk fiber to the mechanical and thermal properties of its biodegradable composites, J. Appl. Polym. Sci. 127 (2013) 2389–2396.

[164] B. Nandan, L.D. Kandpal, G.N. Mathur, Glass transition behaviour of poly (ether ether ketone)/poly (aryl ether sulphone) blends: dynamic mechanical and dielectric relaxation studies, Polymer (Guildf). 44 (2003) 1267–1279.

[165] S.G. Kuzak, A. Shanmugam, Dynamic mechanical analysis of fiber-reinforced phenolics, J. Appl. Polym. Sci. 73 (1999) 649–658.

[166] L.A. Pothan, Z. Oommen, S. Thomas, Dynamic mechanical analysis of banana fiber reinforced polyester composites, Compos. Sci. Technol. 63 (2003) 283–293.

[167] D. Ciolacu, F. Ciolacu, V.I. Popa, Amorphous cellulose—structure and characterization, Cellul. Chem. Technol. 45 (2011) 13.

[168] D.N. Mahato, B.K. Mathur, S. Bhattacherjee, DSC and IR methods for determination of accessibility of cellulosic coir fibre and thermal degradation under mercerization, Indian J. Fibre Text. Res. 38 (2013) 96–100.

[169] C. Cherif, Textile Materials for Lightweight Constructions: Technologies-Methods-Materials-Properties, Springer, 2015.

[170] I. Kruci ska, E. Gli ci ska, M. Michalak, D. Ciecha ska, J. Kazimierczak, a. Bloda, Sound-absorbing green composites based on cellulose ultra-short/ultra-fine fibers, Text. Res. J. 85 (2015) 646–657. doi:10.1177/0040517514553873.

[171] E. Gliścińska, M. Michalak, I. Krucińska, Sound absorption property of nonwoven based composites, Autex Res. J. 13 (n.d.) 150–155.

[172] L. Egab, X. Wang, M. Fard, Acoustical characterisation of porous sound absorbing materials: a review, Int. J. Veh. Noise Vib. 10 (2014) 129–149.

[173] W. Fung, M. Hardcastle, Textiles in automotive engineering, Woodhead Publishing, 2001.

APPENDIX A: MATLAB IMAGE ANALYSIS CODES

The Input Image (Ficus_SEM.tiff)

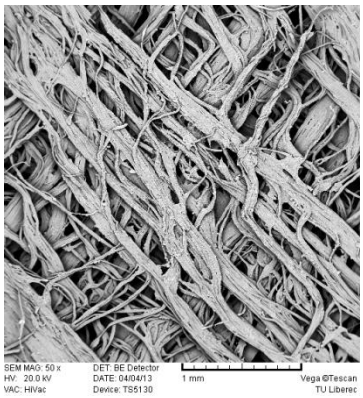

Conversion of SEM image to Binary Image

```
>>  I = imread('C:\Users\sammy\Desktop\HT\Ficus_SEM.tiff');
>> BW = im2bw(I,0.4);
imshow(I), figure, imshow(BW)
```

Computation of the Hough Transform

```
>> [H,theta,rho] = hough(BW);
>> figure, imshow(imadjust(mat2gray(H)),[],'XData',theta,'YData',rho,...
       'InitialMagnification','fit');
xlabel('\theta (degrees)'), ylabel('\rho');
axis on, axis normal, hold on;
colormap(hot)
```

Computation of peaks in the Hough Transform

```
>> P = houghpeaks(H,5,'threshold',ceil(0.3*max(H(:))));
>> x = theta(P(:,2));
y = rho(P(:,1));
plot(x,y,'s','color','black');
```

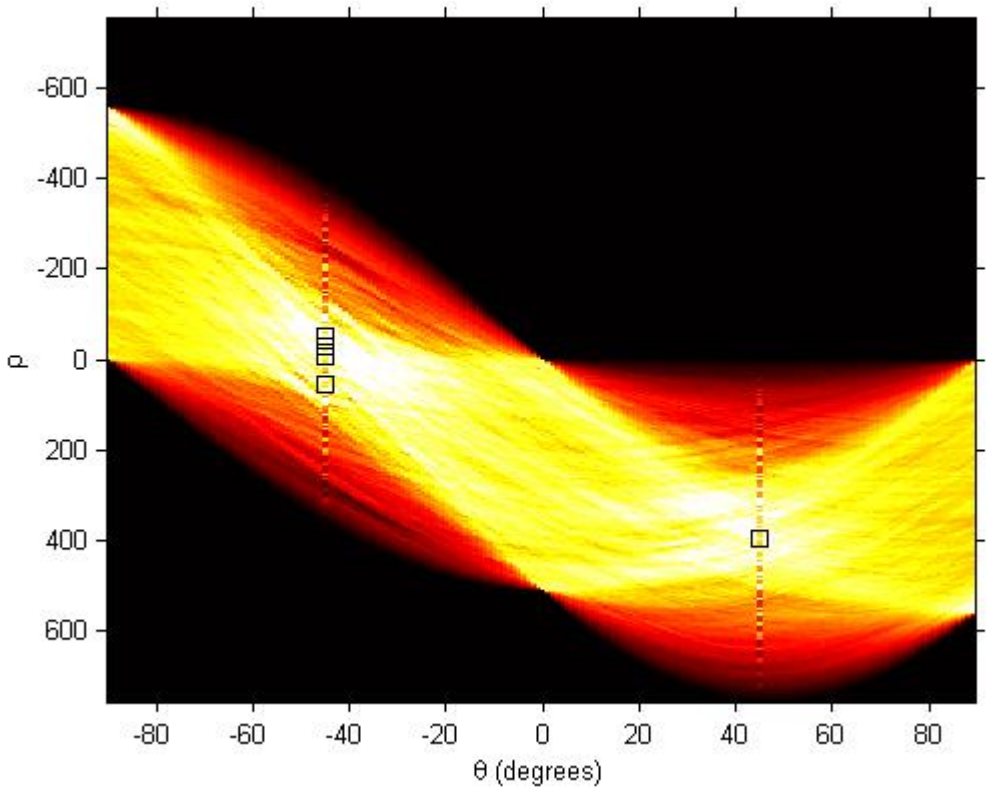

APPENDIX B: FIBER VOLUME FRACTION VARIATION

The thickness of the composite laminate, d is related to the fiber volume fraction, v_f; the areal weight of the barkcloth fabrics, A_w through the following equation and the figure below:

$$d = \frac{n * A_w}{\rho_f * v_f}$$

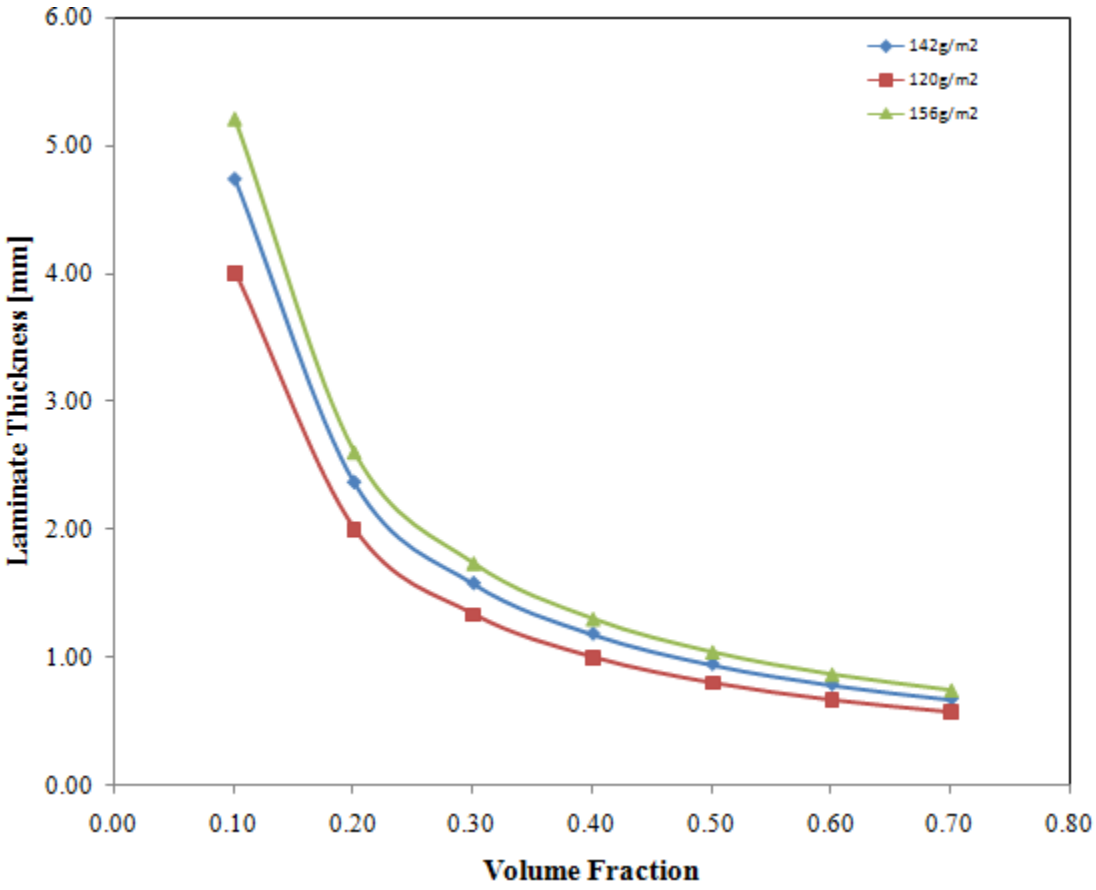

APPENDIX C: MECHANICAL PROPERTIES PREDICTION

Rules of Mixtures

From Equation (2)

$$E_c = v_f E_f + (1 - v_f) E_m$$

$v_f = 0.40$

$E_f = 2.54MPa$

$E_m = 3GPa$

Tensile Modulus

$E_c = 1.80GPa$ (Predicted)

$E_c = 3.2 - 3.3GPa$ (Measured)

Thermal Conductivity of Composite

Using Equations (4) – (8)